RRA-T7206
June 1972

RRA RADIATION RESEARCH ASSOCIATES
Fort Worth, Texas

ANALYSIS OF RADIATION AND METEOROID SATELLITE DATA

B.J. Farmer

Final Report Contract No. NAS9-11903

Sponsored by
NATIONAL AERONAUTICS AND SPACE ADMINISTRATION
MANNED SPACECRAFT CENTER

RRA-T7206
June 1972

ANALYSIS OF RADIATION AND METEOROID SATELLITE DATA

B. J. Farmer

Final Report

Prepared for
NATIONAL AERONAUTICS AND SPACE ADMINISTATION
Manned Spacecraft Center
Houston, Texas
under
Contract NAS9-11903

RADIATION RESEARCH ASSOCIATES, INC.
3550 Hulen Street
Fort Worth, Texas 76107

TABLE OF CONTENTS

FIGURES

FIGURES (Continued)

TABLES

I. INTRODUCTION

This report is submitted in accordance with the terms of Contract NAS9-11903, Contract Schedule, Article XIII, and covered the period from 15 June 1970 through 30 June 1971. During this program, which was primarily one of computerized data analysis, the data obtained in earth orbit by the Radiation and Meteoroid Satellite (RMS) was interpreted and reduced to a form which will be usable by future space experimenters.

The RMS was launched by NASA on 9 November 1970 from Wallops Island, Virginia in conjunction with the Orbiting Frog Otolith satellite. The RMS contained two experiments: (1) a nuclear radiation experiment composed of a radiation spectrometer, a real-time pulse-height spectrum-to-dose convertor and three NASA ionization chambers, and (2) a meteoroid experiment capable of measuring both flux and particle velocity. The spacecraft re-entered the Earth's atmosphere on 7 February 1971. The RMS mission is discussed in detail in Ref. 1.

The required tasks of this contract are detailed in Paragraph II of the Statement of Work. They were accomplished during this program in the manner summarized as follows: Computer programs were written which lifted the raw data and associated ephemeris data from the GFE magnetic tapes. The engineering data was then used to evaluate the performance of the spacecraft and the experiments. The radiation data was used to prepare flux, spectral, and dose maps of the South Atlantic magnetic anomaly where possible. The meteoroid data was used to determine a rough estimate of the meteoroid flux and in general evaluate the performance of the thin-film meteoroid sensors.

The degree of success of the RMS mission was evaluated in light of the separation anomaly which occurred between RMS and OFO during launch.

II. SUMMARY

The initial phases of this program were dominated by the problems associated with the conversion of the raw satellite data into a form compatible with FORTRAN programming. The original RMS data tapes were in the same format as stored in the satellite memory as detailed in Ref. 2. The data were removed from the stacked words, often bit by bit, and arranged in an indexed format. In attempting to obtain an actual time correlation of data events for the radiation data analysis a serious problem was found with the frame header times which were established at the time of data transmission time from the satellite to the ground station. Errors, which were found to be from several sources, both human and electronic, were removed only after a complex and time consuming reference to the station pass summaries which were supplied by Goddard Space Flight Center.

A series of programs was written in which the data were manipulated on the magnetic tapes until a complete record of the RMS mission was contained on only two tapes, one with the meteoroid data and the other with the radiation data. In addition the radiation tape contained the position converted to B and L coordinates for each radiation dose and spectral data point. These final tapes were used to make the memory data correlations for the meteoroid analysis and radiation dose and spectral maps.

In the analysis of the radiation data many intercorrelations were made between the systems on board the satellite and, in addition, correlations were made with the NASA models of the radiation belts (Ref. 3). This resulted in sufficient information to sort the good data from that which was bad or questionable. The final data, which was presented as dose and spectral maps of the radiation in the South Atlantic magnetic anomaly, is believed to be accurate.

This work was by no means an exhaustive study of the radiation data from the satellite. The information was simply tabulated and

presented in a form for direct comparison to the models of the radiation belts, but no interpretation with respect to temporal variations, for example, were provided within the scope of the program. The tapes are available so that the presentation of the data in any form and any level of detail on any portion of the mission will be simple and efficient.

The analysis of the meteoroid data was conducted in great detail, not because of the value of the velocity and flux data, but primarily to establish the areas of usefulness of the thin-film sensors themselves. Rather striking correlations resulted between the orbital mechanics of the vehicle and the number of events which occurred in the sensors. The most important of these being that when the spinning of the satellite ceased, virtually all spurious events also ceased. The final implication being that the sensors must be used in coincidence when rapid sunlight variations occur; however, they may serve as valuable flux monitors if temperature and other stressing effects are eliminated.

A Poisson analysis was made of the meteoroid flux data. This analysis served to point out the precaution which must be taken if reliable data is to be obtained with the sensors.

A brief analysis was made to evaluate the success of the mission in light of the anomaly which occurred during the injection of the RMS/OFO package into orbit. The meteoroid experiment seemed to be unaffected by the problem (except possibly the high loss of front plane sensors); however, malfunctions occurred in the radiation experiment which were attributed to an impact between the vehicles. Even with the malfunctions, some aspects of each of the mission objectives were accomplished, yet in each case the total amount of information anticipated was not obtained. These may be outlined briefly as follows:

(a) Real-time pulse-height spectrum to dose conversion was accomplished; however, no actual comparisons were available due to the malfunction of the unshielded ionization chamber and the error in the high energy proton data.

(b) Spectral and dose maps were obtained for electrons and protons, however, the high energy portion of the proton spectrum was lost.

It is difficult to assign a "figure of merit" to the success of the overall mission without assigning a weighting factor to each item. The concept spectrum-to-dose conversion was shown to operate in a real-time mode in the space environment, yet an accurate analysis of the accuracy of the concept was not possible. Also valuable data from the spectrometer and ionization chamber were lost, yet the data obtained is of significant value relative to the effects of the "Starfish" high altitude nuclear test. The actual figure of merit relating to the mission success must be based on the criterion established for such an evaluation.

III. TRANSLATION OF RMS DATA AND EPHEMERIS TAPES

3.1 RMS Master Digital Data Tape (MDDT) Translation

Two computer programs were written to translate the seven-track RMS MDDT tapes into a single nine-track tape compatible with the data analysis procedures developed for the IBM 360 computer. These programs, designated RRA-118 and RRA-119, produced the G-1 and G-2 output tapes, respectively. The RRA-118 program performed the following functions:

(a) read frame headers and data records from the seven-track MDDT tapes;

(b) selected the good quality real-time data frames and the pertinent minor frames of each RMS memory dump;

(c) converted the header information and binary data from each frame into appropriate single-word output data; and

(d) wrote the converted data on a nine-track output tape (G-1).

The RRA-119 program performed the following functions:

(a) read the nine-track output tape;

(b) printed a descriptive listing of the total record of header and frame data for each frame stored on the G-1 tape; and

(c) wrote the G-2 output tape.

Generalized flow diagrams for these programs are given in Figs. 3-1 and 3-2.

Some difficulties were encountered in translating the RMS stacked data tapes into the G-1 tape file which were due to the imperfect nature of the raw data stacked on the seven-track tapes and the presence of non-systematic errors in the header information supplied for each of the data frames.

These included errors noted in the header information for some of the data frames which were associated with the assignment of orbit numbers and the computation of the GMT which establishes the spacecraft transmission time. In several cases, the orbit number for an entire run of data did not agree with the GMT presented in the GFSC header or the spacecraft clock

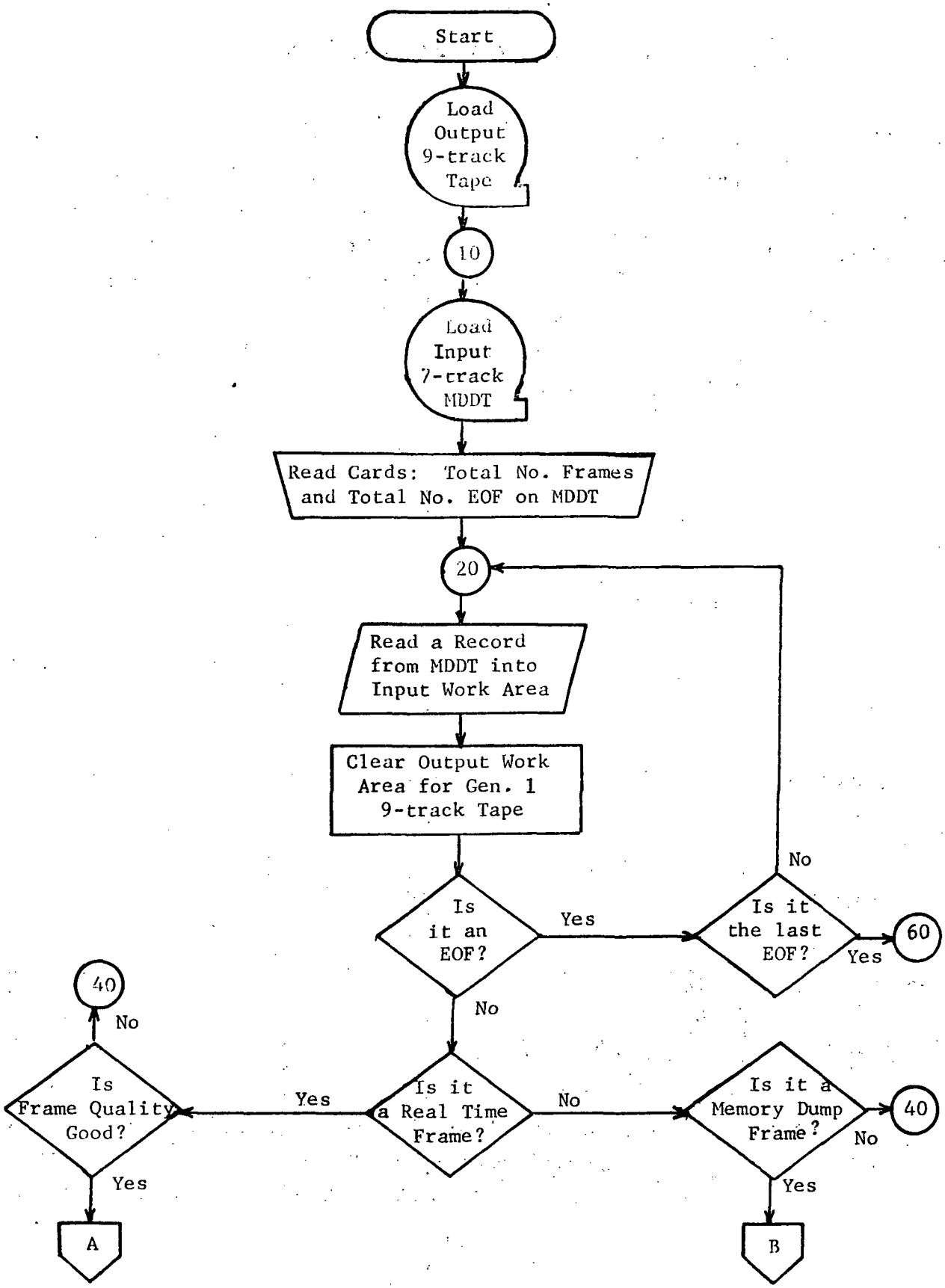

Fig. 3-1. SCHEMATIC FLOW OF RRA-118 TAPE TRANSLATION PROGRAM WHICH PRINTED DESCRIPTIVE LISTING OF THE RMS FRAME HEADER AND DATA INFORMATION AND WROTE THE G-2 TAPE

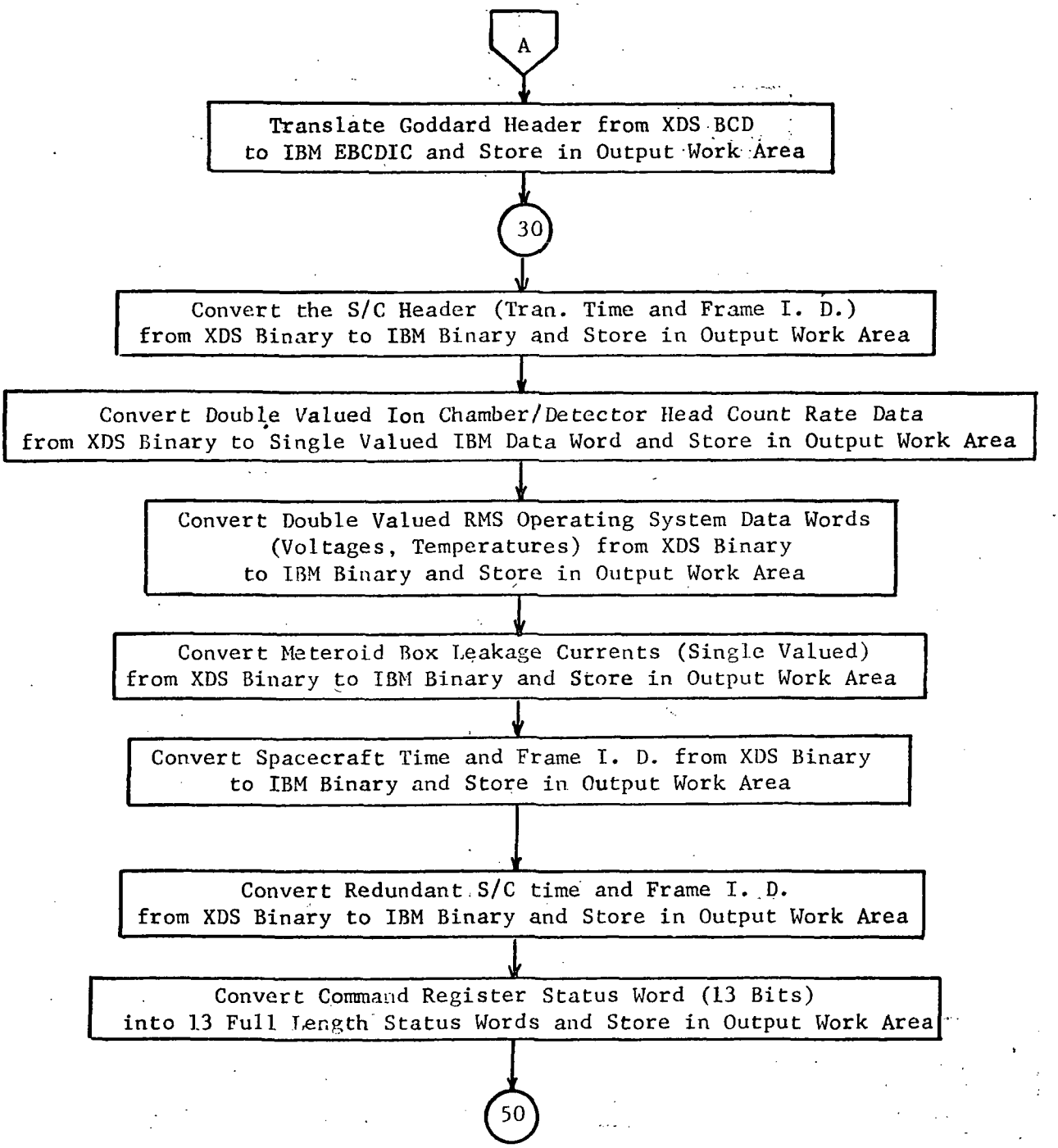

Fig. 3-1. (CONTINUED)

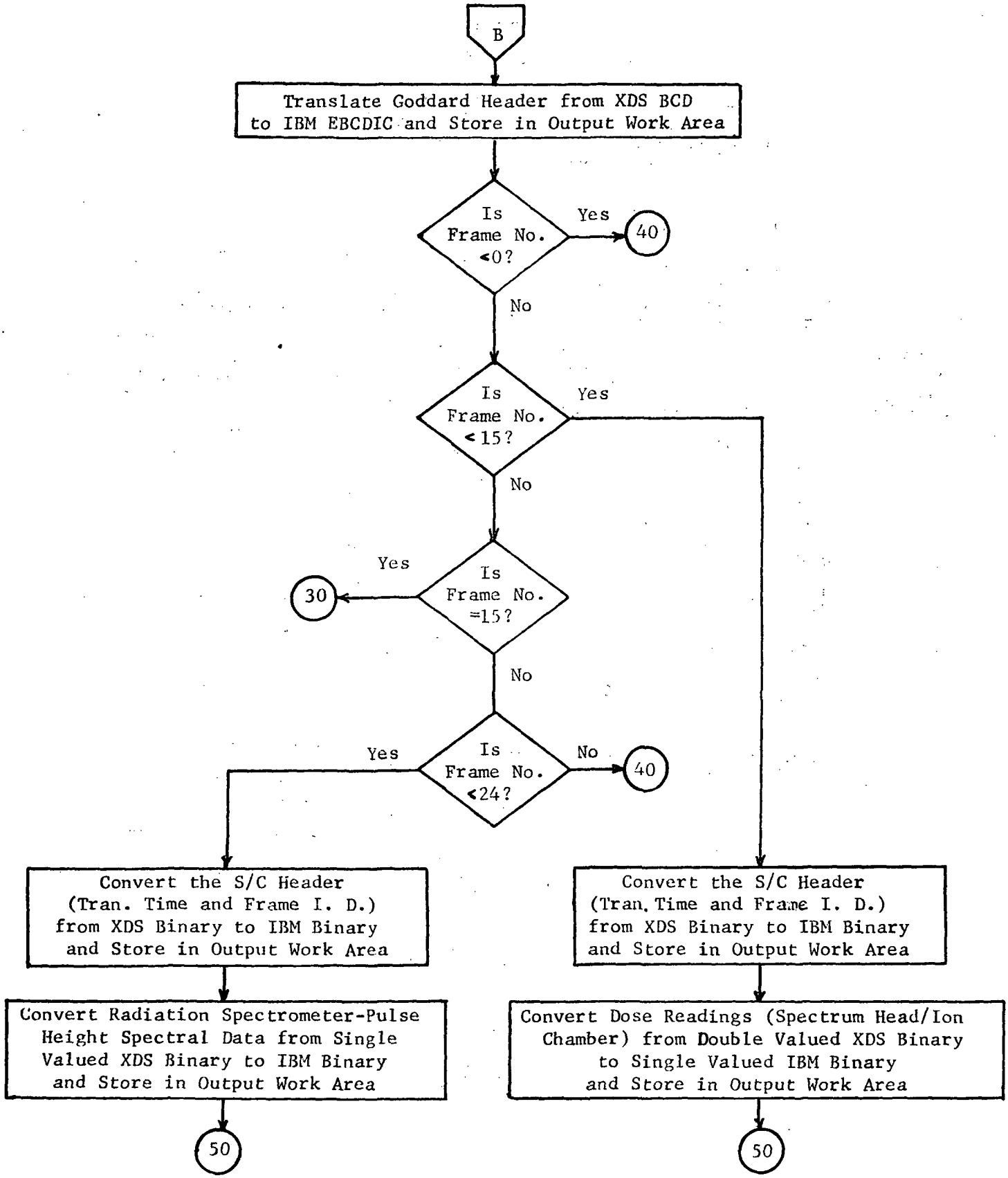

Fig. 3-1. (CONTINUED)

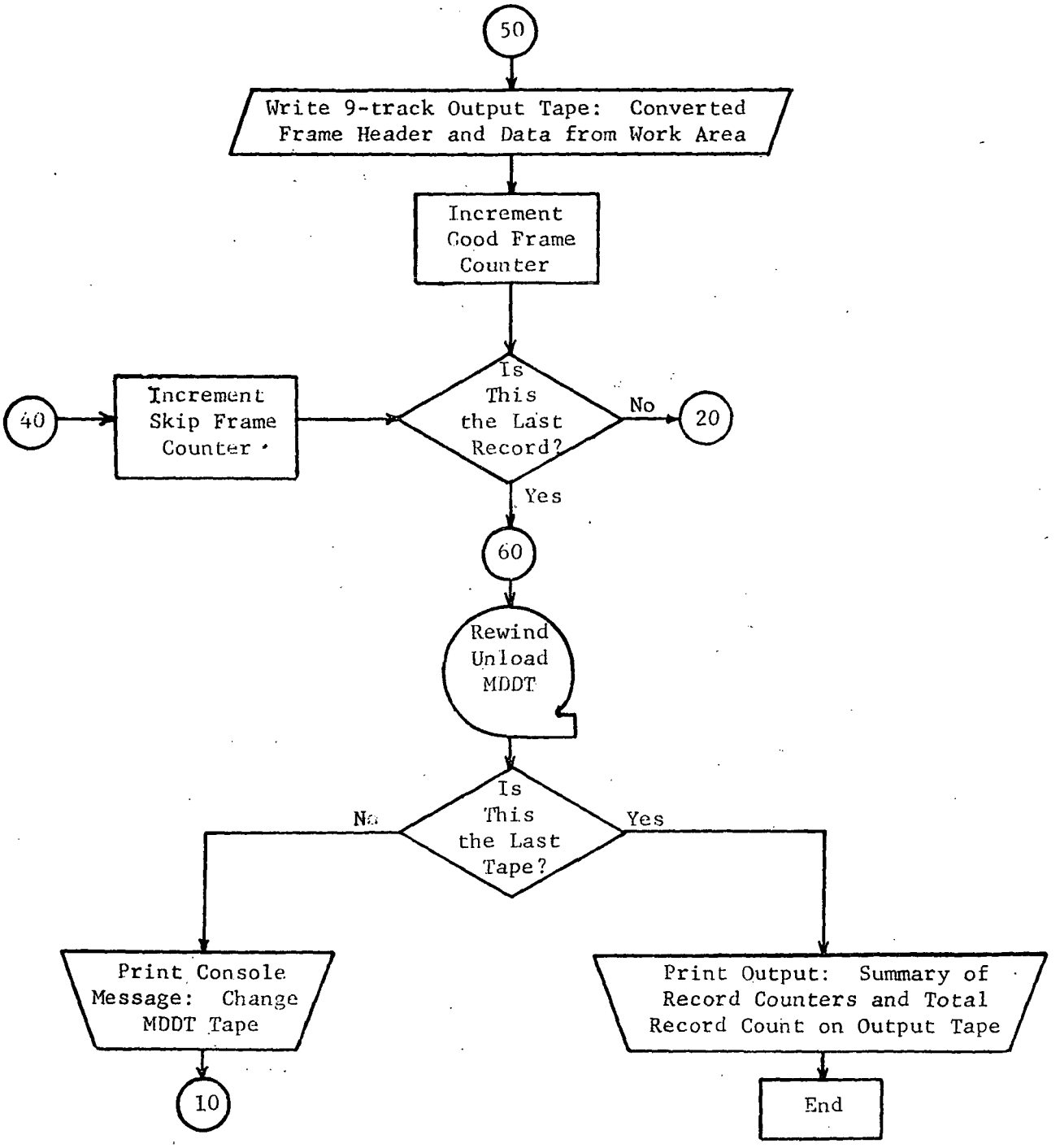

Fig. 3-1. (CONTINUED)

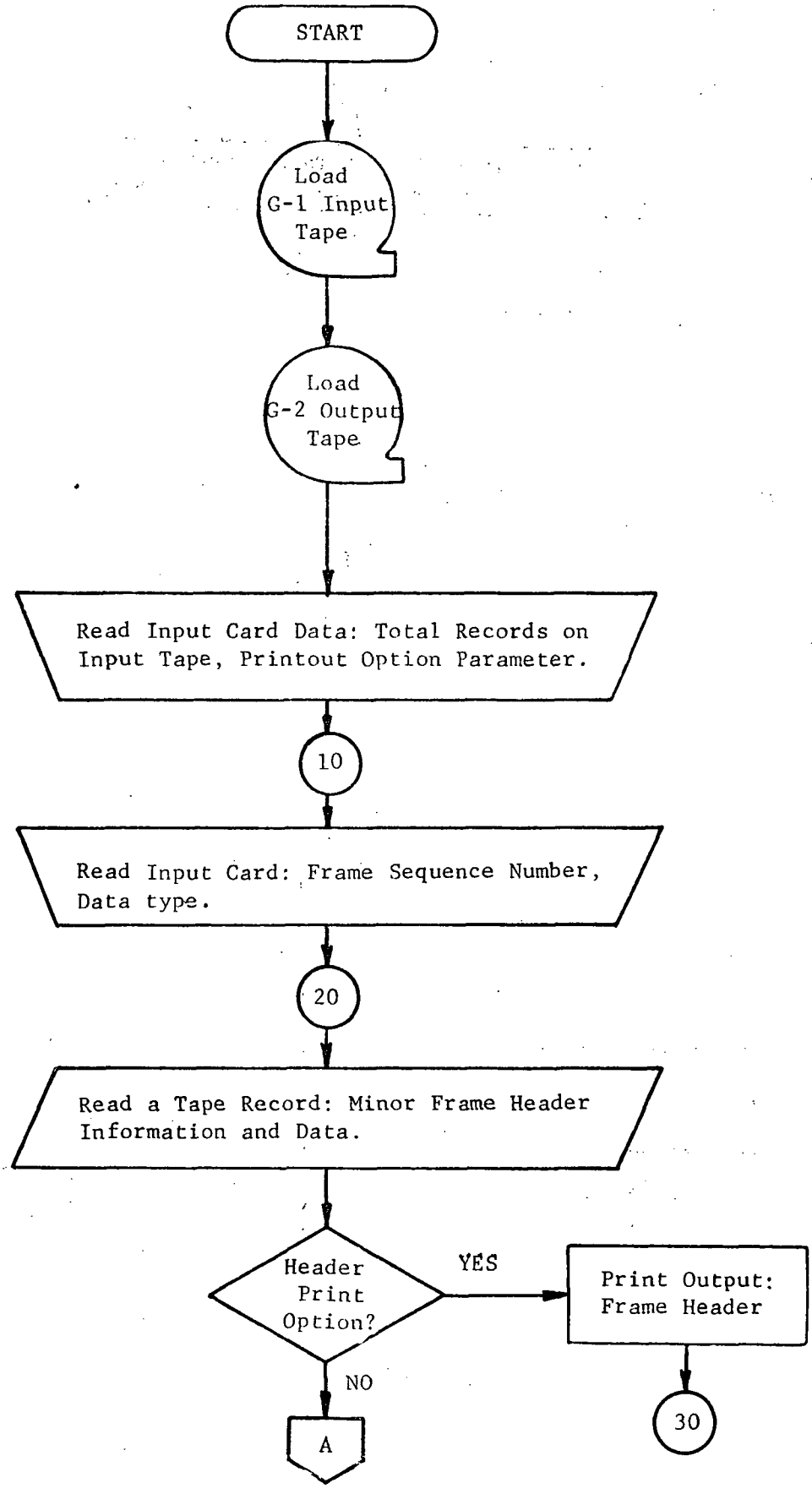

Fig. 3-2. SCHEMATIC FLOW OF RRA-119 TAPE TRANSLATION PROGRAM WHICH SELECTED GOOD QUALITY DATA FROM THE RMS MDDT, TRANSLATED THE DATA INTO SINGLE WORD OUTPUT FORMAT, AND WROTE THE RESULTS IN A NINE-TRACK FORMAT ON TAPE G-1.

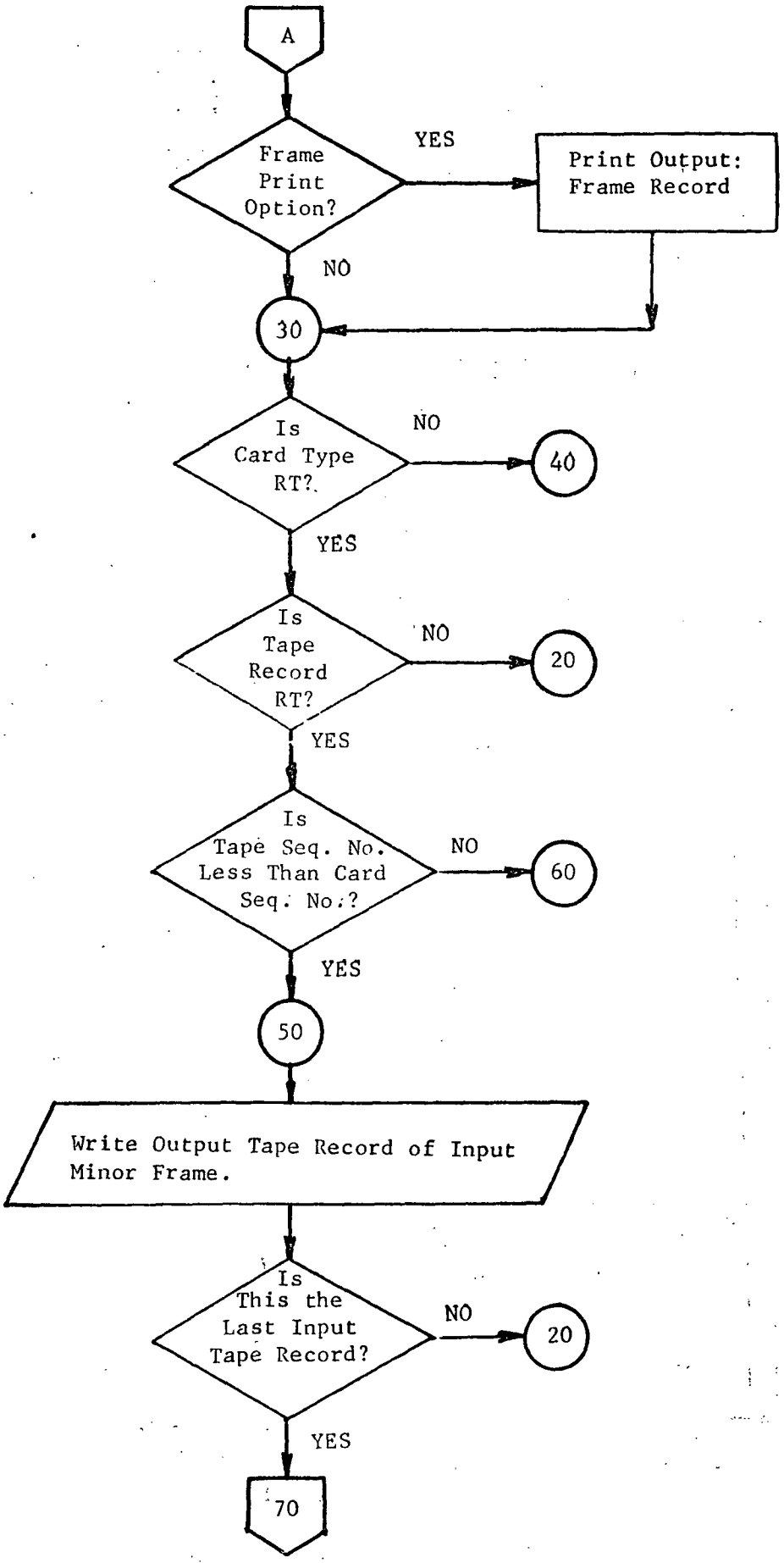

Fig. 3-2. (CONTINUED)

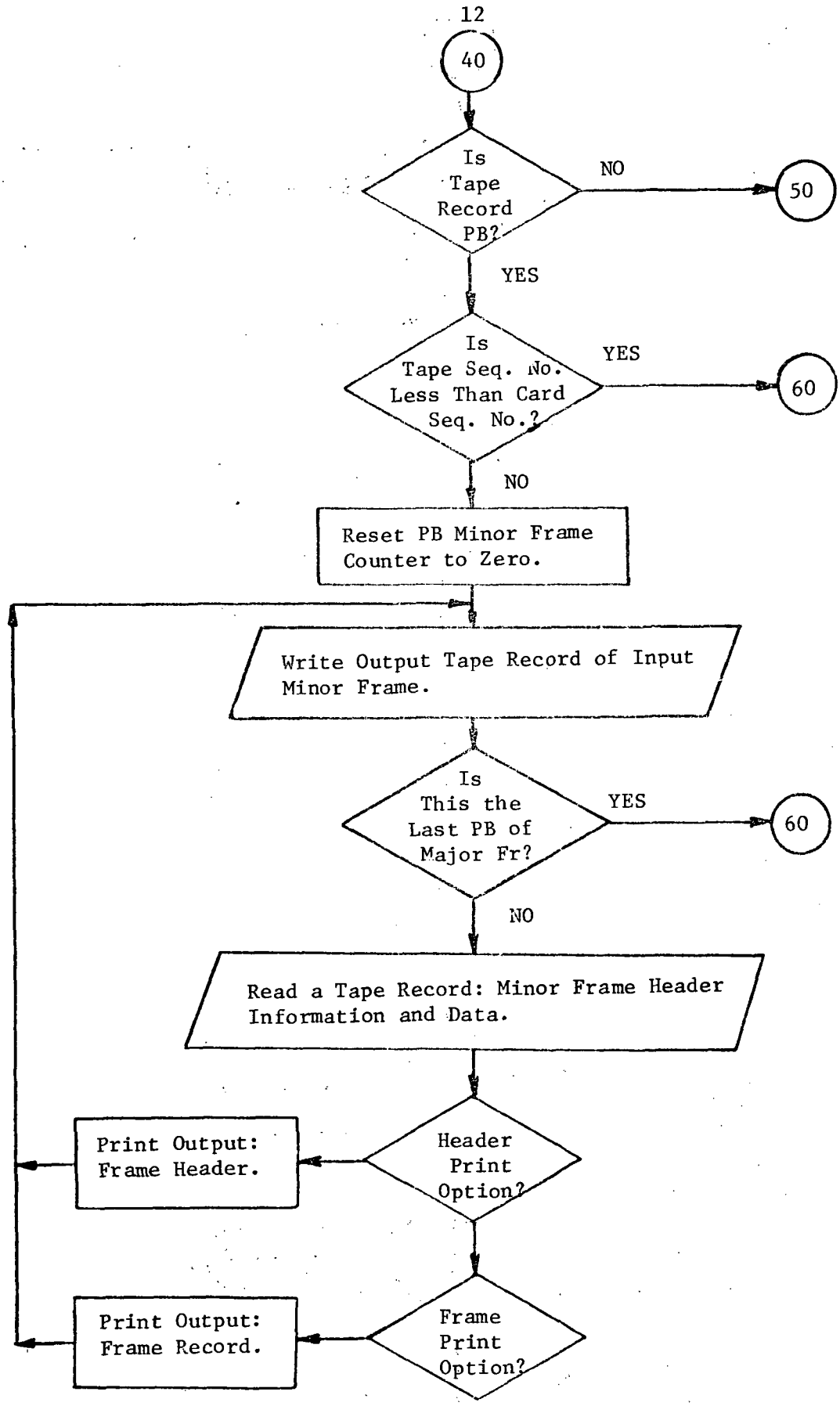

Fig. 3-2. (CONTINUED)

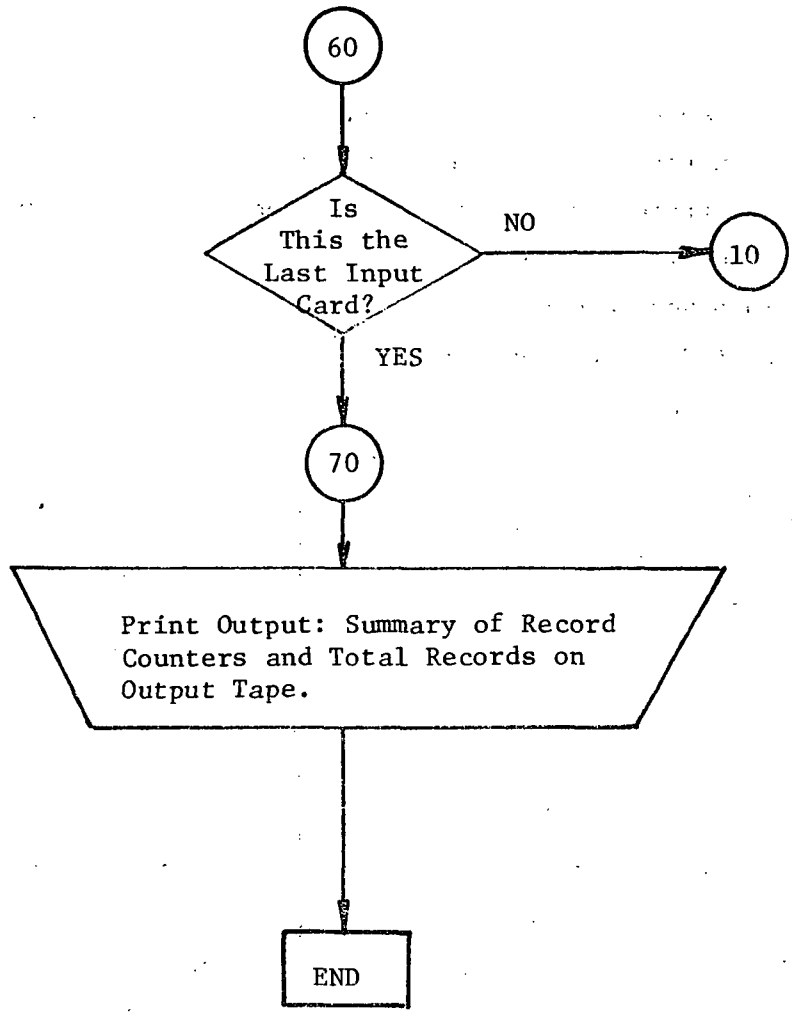

Fig. 3-2. (CONTINUED)

transmission time in the data frame. In addition, the raw data collection for the MDDT tapes included numerous runs of bad quality data. These bad frames occurred at the beginning of each data transmission from the satellite before lock on the signal had been established at the station. In other cases, the data from a given station-pass was accidentally repeated two or more times on the MDDT.

The most time-consuming of the problems encountered in this program was associated with the correlation of the spacecraft clock with the GMT. The correlations made by Goddard Space Flight Center were in error in nearly all cases. There were three major sources of error found:

(a) correlation with time of transmission from the receiving station to GSFC instead of time of transmission to station from satellite;

(b) locking of minute and .1 second integers in GMT clock;

(c) miscorrelation of time with data frames (probably occurring in digital transmission from station to GSFC.)

Many attempts to remove the systematic errors by the computer proved unsuccessful and in order to obtain correlation it was found necessary to use the time when the command was sent to the satellite from the station which were obtained from the pass summaries. This data was entered into the computer on cards and the final correlation to the exact frame was made by the computer by adding the time per frame times the frame number to the command time, plus 4.75 seconds which is the delay from the time the command button was pressed by the station operator until the satellite began transmitting the zeroth frame.

To apply the corrections and demonstrate the accuracy of the final correlations, a least-square-fit was made of the command time GMTs to the spacecraft clock. The resulting curve is given in Fig. 3-3. This curve shows that the spacecraft clock oscillator was running at one average rate during the first part of the satellite's lifetime and a slower rate during the latter part. Change in rate correlates with the change in the satellite's motion from a spin to an end-over-end tumble. At this time, the average temperature of the satellite control unit decreased, since

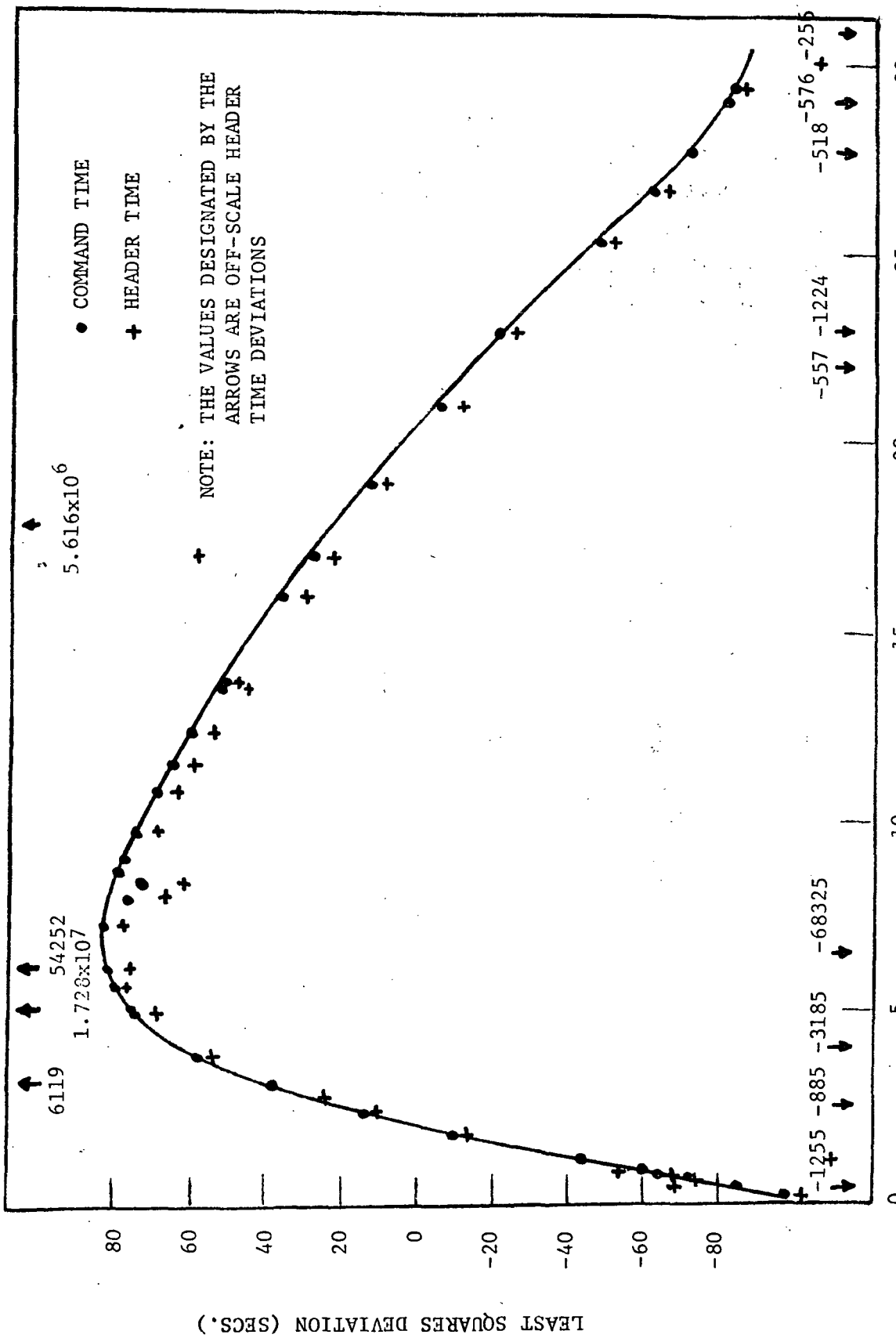

Fig. 3-3. DEVIATION OF COMMAND CORRELATED GMT FROM LEAST SQUARES CURVE FIT OF COMMAND GMT VERSUS SPACECRAFT CLOCK

that unit was facing away from the sun. The correlation of the GMTs obtained from the command times is seen to follow the curve with only slight deviations. In contrast, the GSFC-provided GMTs, shown as "+" on the curve, are seen to scatter wildly. The numbers with the arrows indicate the large deviation in some times. The systematically low values of most of the points result from the shifting of data frames with respect to the time.

After the analysis, it is believed that the resulting error in time, within a one sigma limit, is of the order of ± 3 seconds, which corresponds to a position uncertainty of approximately 15 nautical miles. This is well within the accuracy required for the correlation of the data to the B and L coordinates. Because of these errors, considerable time was required in reviewing the printouts of the headers from the MDDT files and comparing them with the station-pass summaries. This review did, however, make it possible to establish a complete history of the RMS mission.

3.2 Ephemeris Tape Translation

The RMS ephemeris tape which was supplied by Goddard Space Flight Center was in the ORB-3A format. The information contained on the tapes included the spacecraft's position in two coordinate systems as a function of GMT and other data such as the time of terminator crossing. The most important information on the tapes, relative to this program, was the position in the B and L geomagnetic coordinate system. This information was given as a function of GMT at one minute intervals during the RMS mission lifetime.

The data was first translated from the seven-track to nine-track tapes which were compatible with the IBM 360 computer series. A program was then written (shown schematically in Figure 3-4) which extracted the B and L values from the tape and produced a tape in which the data could be merged with the RMS data using the FORTRAN computer language.

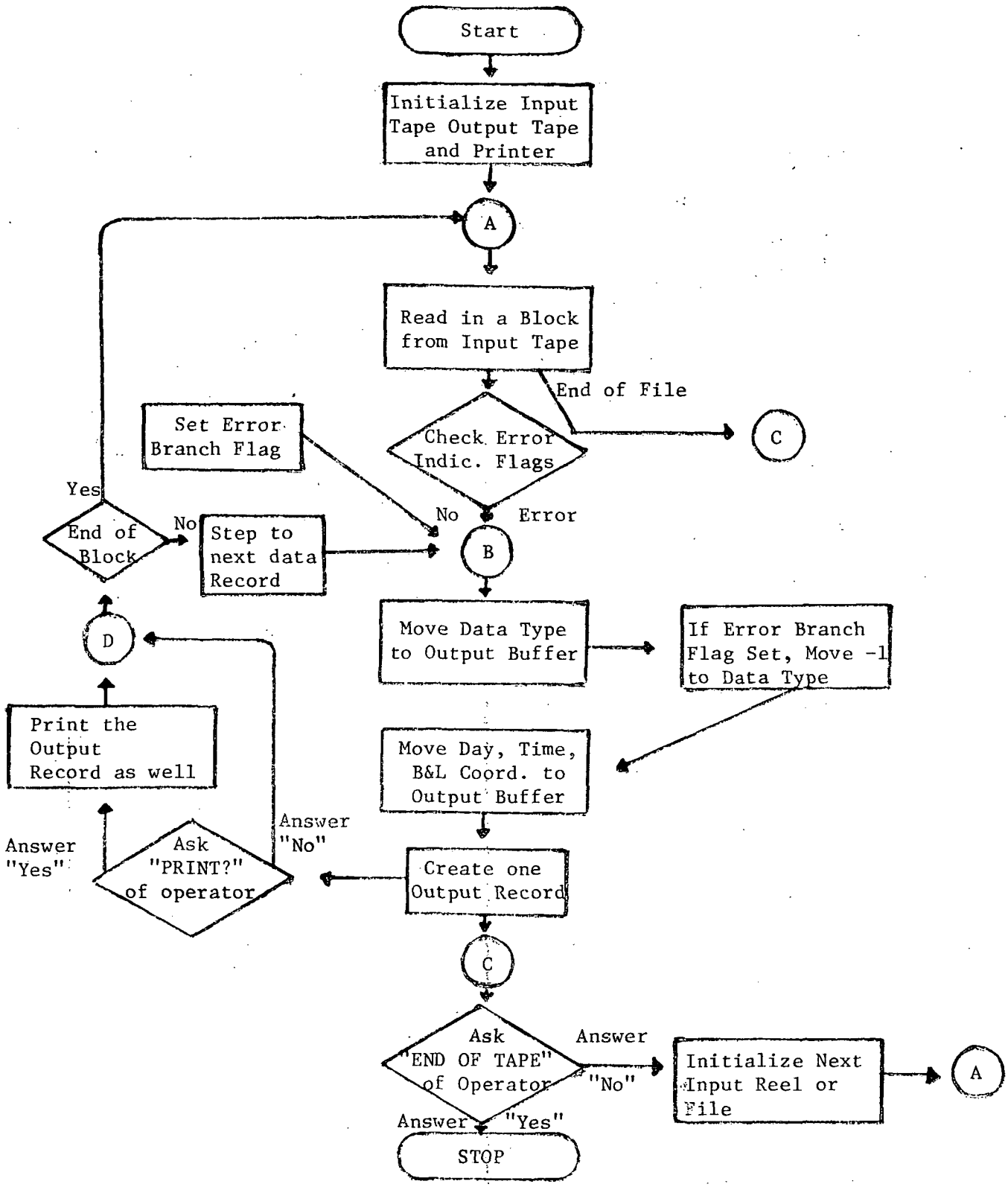

Fig. 3-4. Schematic Flow Chart of Program to Extract B and L Coordinates from the Ephemeris Tape

IV. ANALYSIS OF RADIATION DATA

4.1 Introduction

The radiation experiment aboard RMS consisted of three basic systems:

(a) a proton-electron spectrometer,

(b) a pulse-height spectrum-to-dose conversion system, and

(c) a triad of standard Manned Spacecraft Center ionization chambers.

The primary objective of this experiment was to demonstrate the feasibility and accuracy of the spectrum-to-dose conversion concept (as discussed in Ref. 4) and instrumentation in a real-time mode and in the actual space radiation environment. This objective was met in general, as discussed in Ref. 1; however, in the fullest sense, valuable data was lost due to instrument malfunctions which prevented a detailed analysis of the accuracy of the system for both electrons and protons. The loss of this data in no way reflects on the pulse-height spectrum-to-dose conversion system on board the satellite, since this system did actually convert to dose, in real-time, the information it received from the spectrometer.

The secondary objective of the radiation experiment was to provide data to develop dose and spectral maps in the South Atlantic magnetic anomaly.

In line with the original objectives of the radiation experiment the current data analysis program consisted of two basic tasks:

(a) the evaluation of the success of the RMS mission in light of the OFO/RMS separation problems at insertion into orbit and

(b) the computation of electron and proton doses and the preparation of orbital and spectral dose maps.

4.2 Mission Anomalies

Before any of the radiation data obtained by the satellite could

be accepted as being accurate, it was necessary to review the overall mission in light of the launch anomaly and the instrument malfunctions. Cross comparisons of the information from the various instruments and comparisons of these data to the models of the radiation bells have led to confidence in the spectral and dose maps presented in paragraph 4.3.

4.2.1 Launch Separation Anomaly

From data obtained from the OFO beacon signal modulations it was determined that the spin rates of the vehicle were not as predicted for the launch sequence. Also,the OFO accelerometers indicated a rather large impact at the time of separation. The detailed sequence of events as well as could be established, is discussed in Refs. 1 and 5. In brief the Scout fourth-stage sequence timer apparently ran at twice its normal speed. Because of the timing error it is believed that the two satellites impacted at separation and in some way damaged the radiation experiment. Preflight tests indicated that the instruments were working properly just prior to launch; however, the first orbital data contained dose readings from the spectrometer which were higher than those obtained by the ionization chambers. These and other data anomalies are discussed in the following paragraphs.

4.2.2 Data Anomalies

To accomplish the objectives of the radiation experiment, onboard comparisons between the doses measured by the NASA ionization chambers and those computed from the spectrometer measurements were to be made in real time, the supposition being that if the readings from both instruments matched, then one could have confidence in the pulse-height spectrum to-dose-conversion system,which potentially has a far wider range of applications than the ionization chamber system.

Unfortunately a malfunction occured in the spectrometer which first became apparent when the proton doses from the spectrum-to-dose conversion system were found to be much higher than those measured by

the ionization chambers. The comparisons were available immediately after a data dump from the GSFC "quick look" printouts.

4.2.2.1 Spectrometer Anomalies

In an attempt to understand the problem, spectra were taken with each of these spectrometer heads independently and it was found that head 2 recorded no proton spectra, indicating that the signal from the main detector stack was not reaching the total energy summing amplifier. The spectra obtained from heads 1 and 3 were found to be distorted, having an excess of counts at high energies. To allow early comparisons to the Vette models two runs were made by Mr. Tim White at NASA/MSC in which spectra were obtained from the models for two actual RMS orbits. The Vette spectra for both electrons and protons were computed with the GSFC updated RMS orbital locations. Latitude, longitude, and height above the surface of the earth were supplied to MSC at one-minute intervals covering the data collection time of the radiation experiment for that particular orbit. The results of a comparison for orbit 52 for spectrometer head 1 are shown in Figs. 4-1 and 4-2. The electron spectra match quite nicely, which gives a high degree of confidence in the spectrometer. The overall view of the comparisons of the proton spectra is not as good. This is partly due to the fact that the Vette spectrum is composed of three separate models: the AP1, between 30 and 50 MeV; AP6, below 30 MeV; and AP7, above 50 MeV. The discontinuities of the composite spectrum at the boundary of each model make comparisons difficult. It is obvious, however, that the RMS data is too high above 50 MeV. The spectra obtained with spectrometer head 3 (Figs. 4-3 and 4-4) show the same basic characteristics as those of head 1. A closer examination of the head 3 spectra revealed additional differences between the data and the Vette model. There was an excess in high energy electron counts and in the high energy portion of the Proton I proton spectrum (that part below 42 MeV). When data were available from the B and L maps of the radiation belts these spectral distortions were even more obvious.

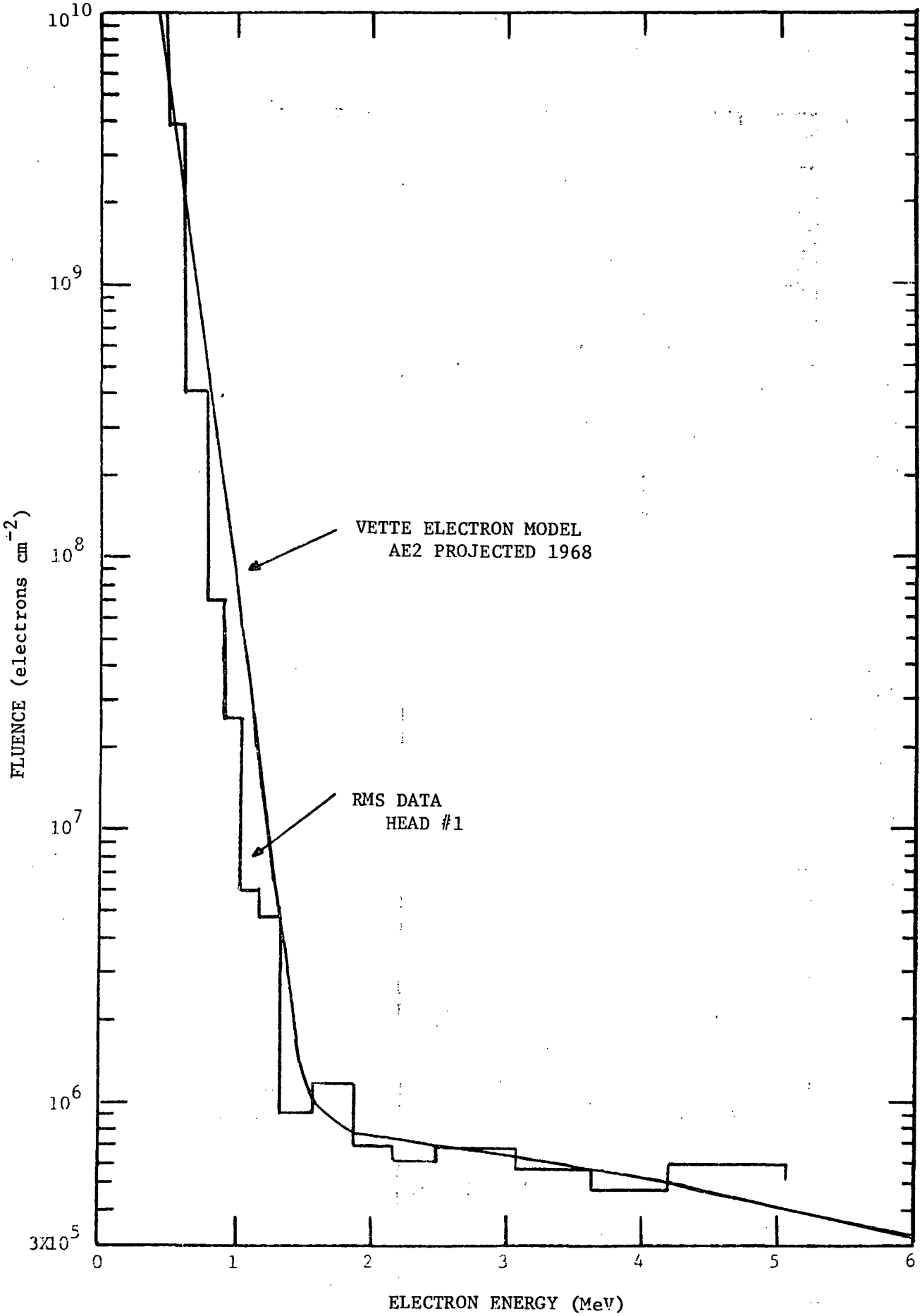

Fig. 4-1. Electron Spectra Integrated over RMS Orbit 52

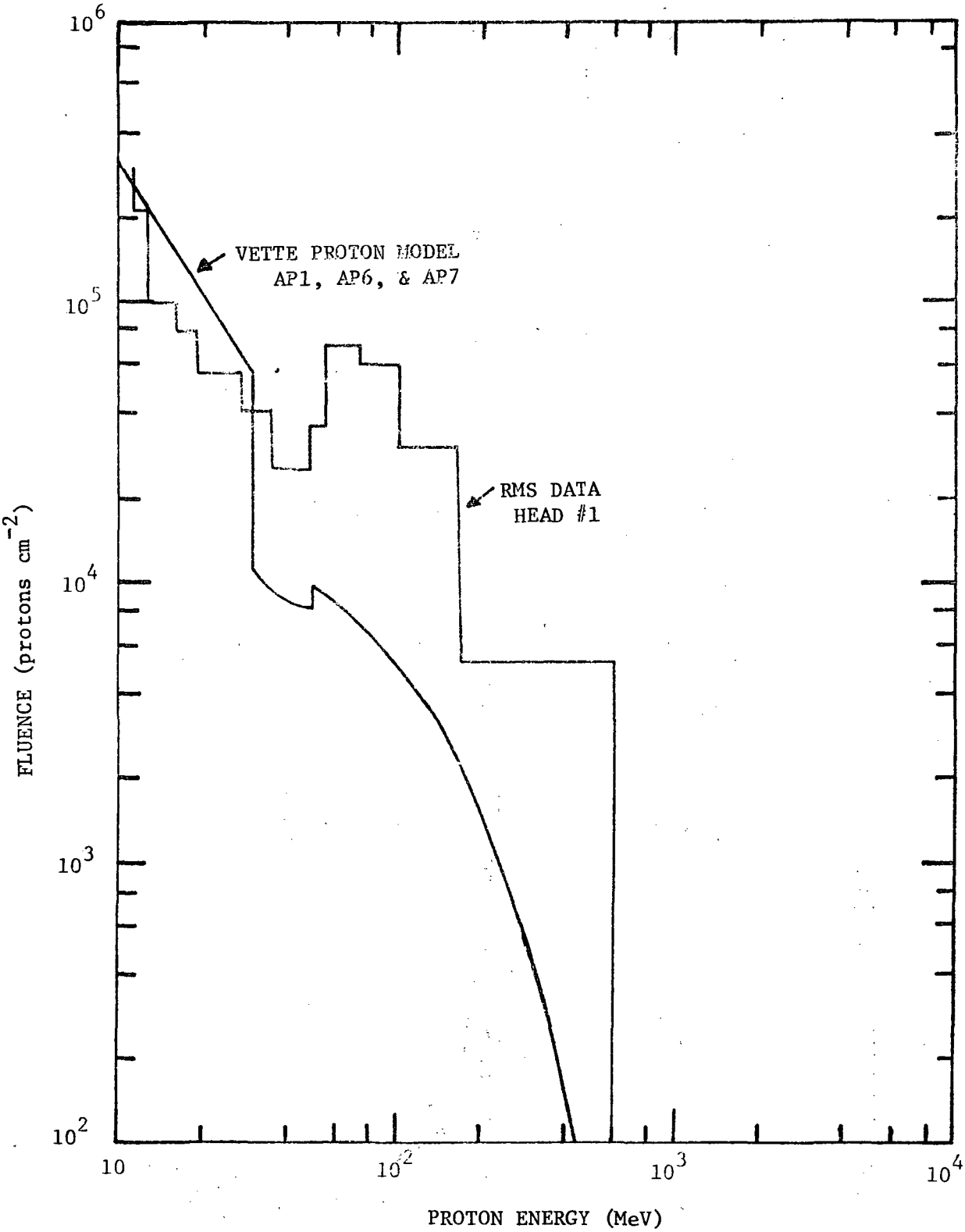

Fig. 4-2. Proton Spectra Integrated over RMS Orbit 52

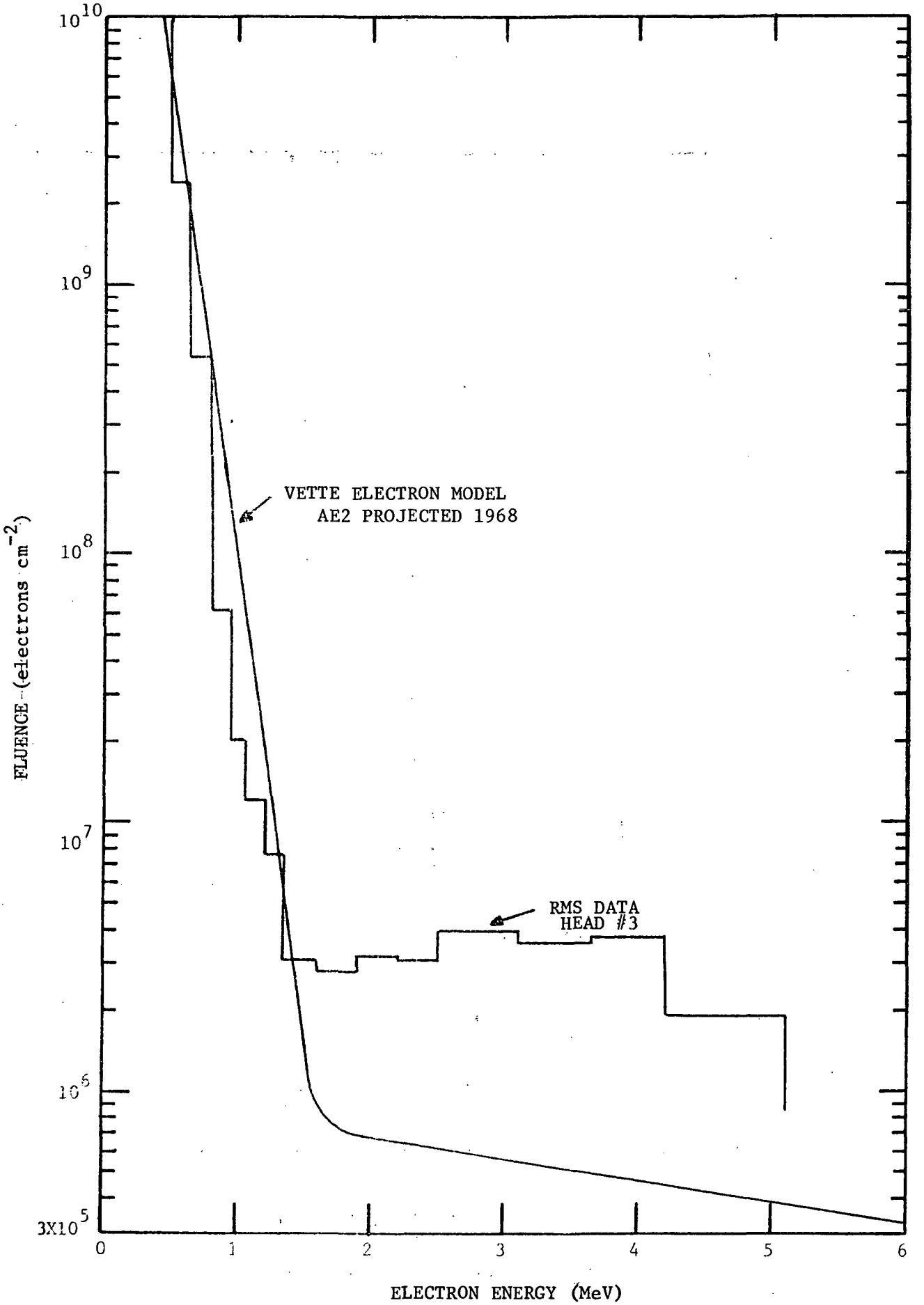

Fig. 4-3. Electron Spectra Integrated over RMS Orbit 67

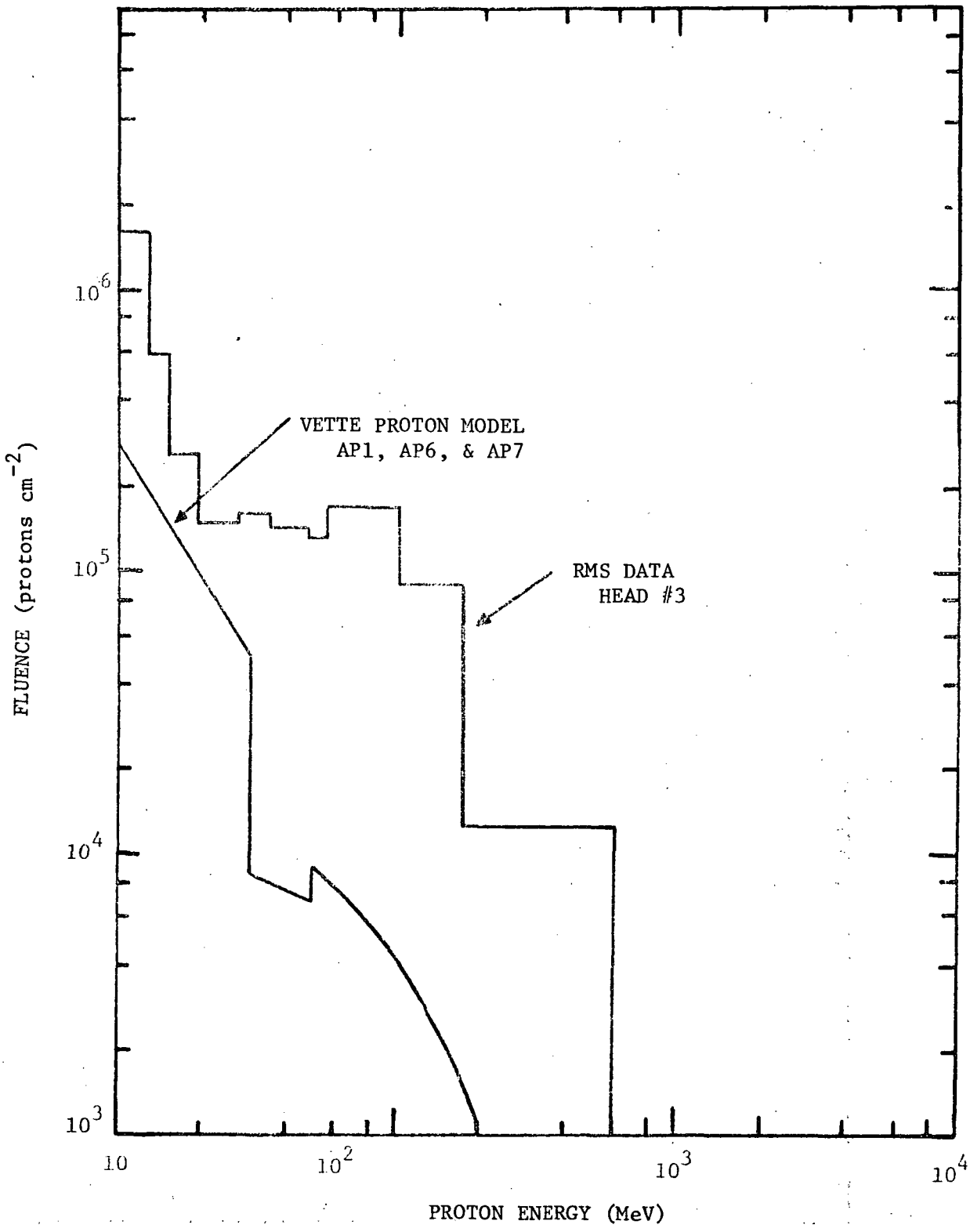

Fig. 4-4. Proton Spectra Integrated over RMS Orbit 67

Examples of the data for heads 1 and 3 at the same B and L locations are given in Figures 4-5 and 4-6 for electrons and 4-7 and 4-8 for protons. In the last four figures the data are compared to the Vette models and normalized over the region of the RMS data. These curves show conclusively the more subtle distortions in the electron and low energy proton spectra (Proton I) of head 3.

An explanation of the malfunctions can be most easily understood by referring to the drawing of the spectrometer telescope in Fig. 4-9 and the calibration curves in Fig. 4-10, both of which were taken from Ref. 1. The problem of excessive counts in the Proton II portion of the spectra, which is common to both head 1 and head 3 is believed to be due to an instrument grounding problem. The most plausible explanation for the excessive counting is that the instrument was sensitive to particles which penetrated the walls of the telescope and lost energy in both the total energy stack and the back penetration detector. It appears that the level detector circuit from the penetration detector activated the coincidence circuit between the first two detectors and produced a false logic signal which deposited the count in the Proton II channels. Such malfunctions had been observed in the laboratory when grounding leads were disconnected.

The more subtle spectral distortions in head 3 are believed result from protons which penetrated the walls of the telescope and deposited energy in both the second detector of the telescope and the stack but not the back detector. The signal resulting from the stack apparently activated the detector 1 and 2 coincidence circuit and caused the accumulation of false counts.

Attempts were made to model the failures and restore the data, however, the uncertainties involved in the penetrations of the particles through the telescope walls and satellite structure increased the errors in the spectra to an unacceptable level, rendering them useless. The work did show, however, that the number of particles, which would be expected to penetrate the walls, was in the order of the spectral distortions observed.

FIG. 4-5. RMS ELECTRON SPECTRA

FIG. 4-6. RMS ELECTRON SPECTRA

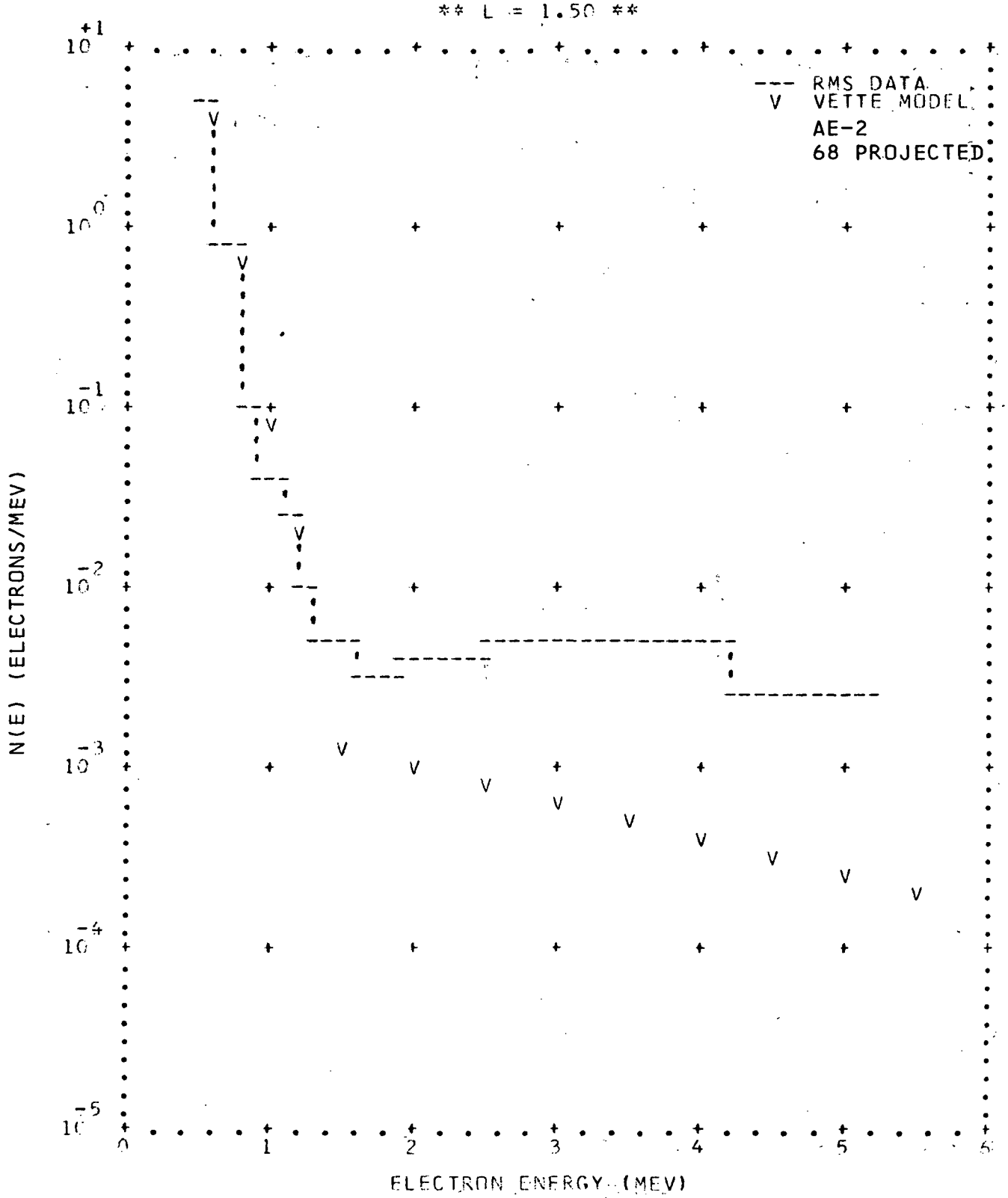

FIG. 4-7. RMS PROTON SPECTRA
(HEAD 1 ENABLED)
** L = 1.40 **
** B = .220 **

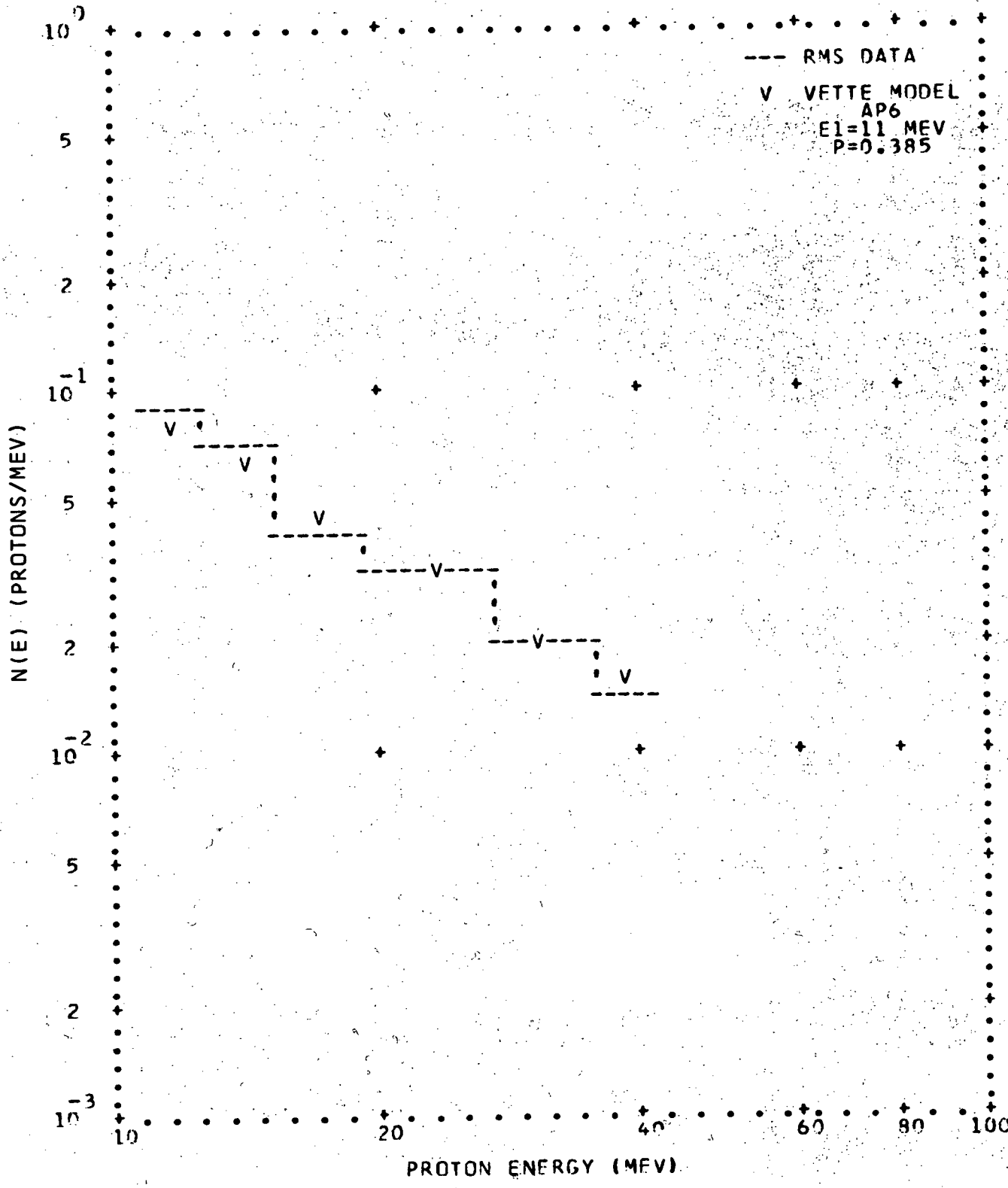

FIG. 4-8. RMS PROTON SPECTRA

(HEAD 3 ENABLED)

** L = 1.40 **

** B = .220 **

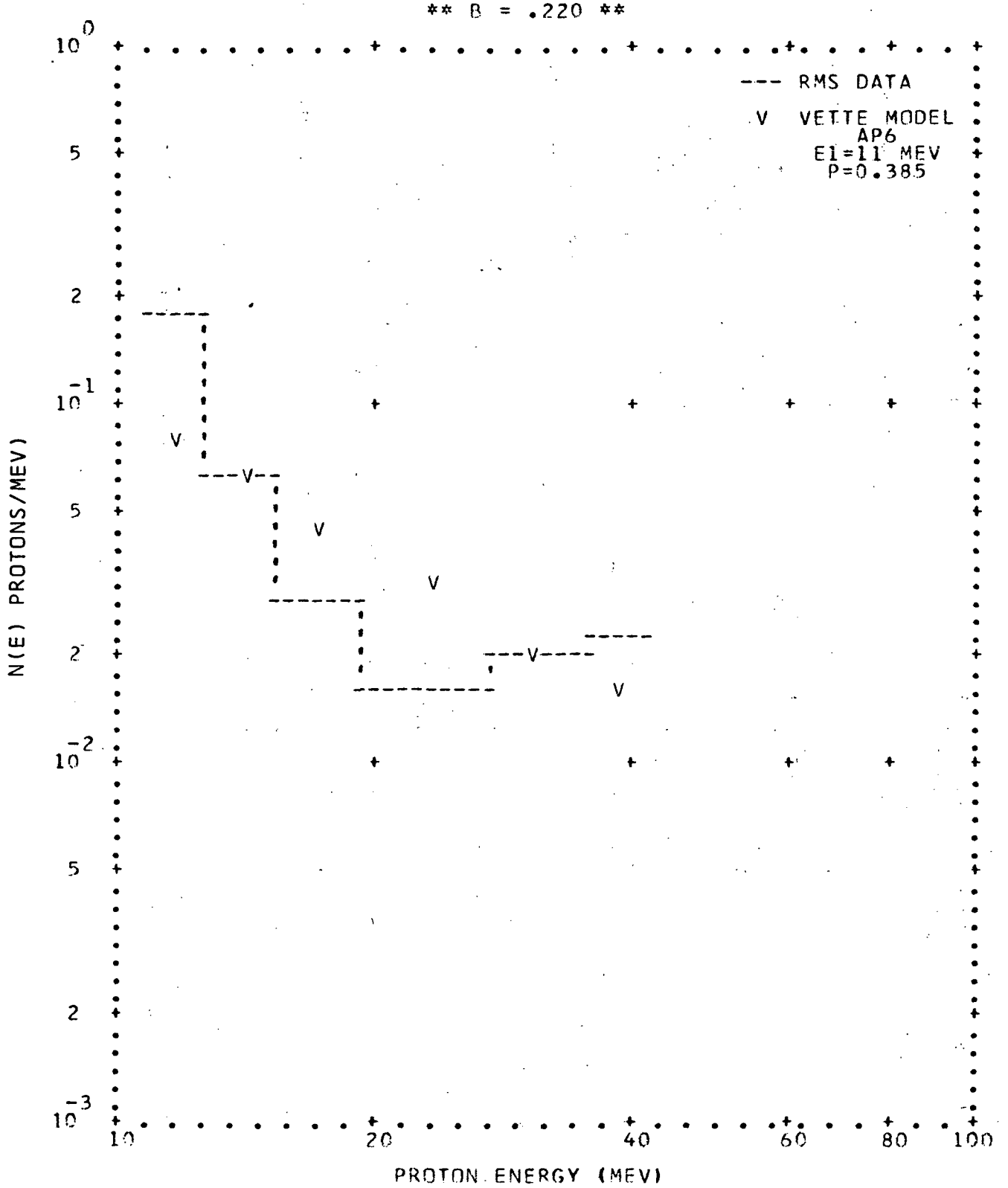

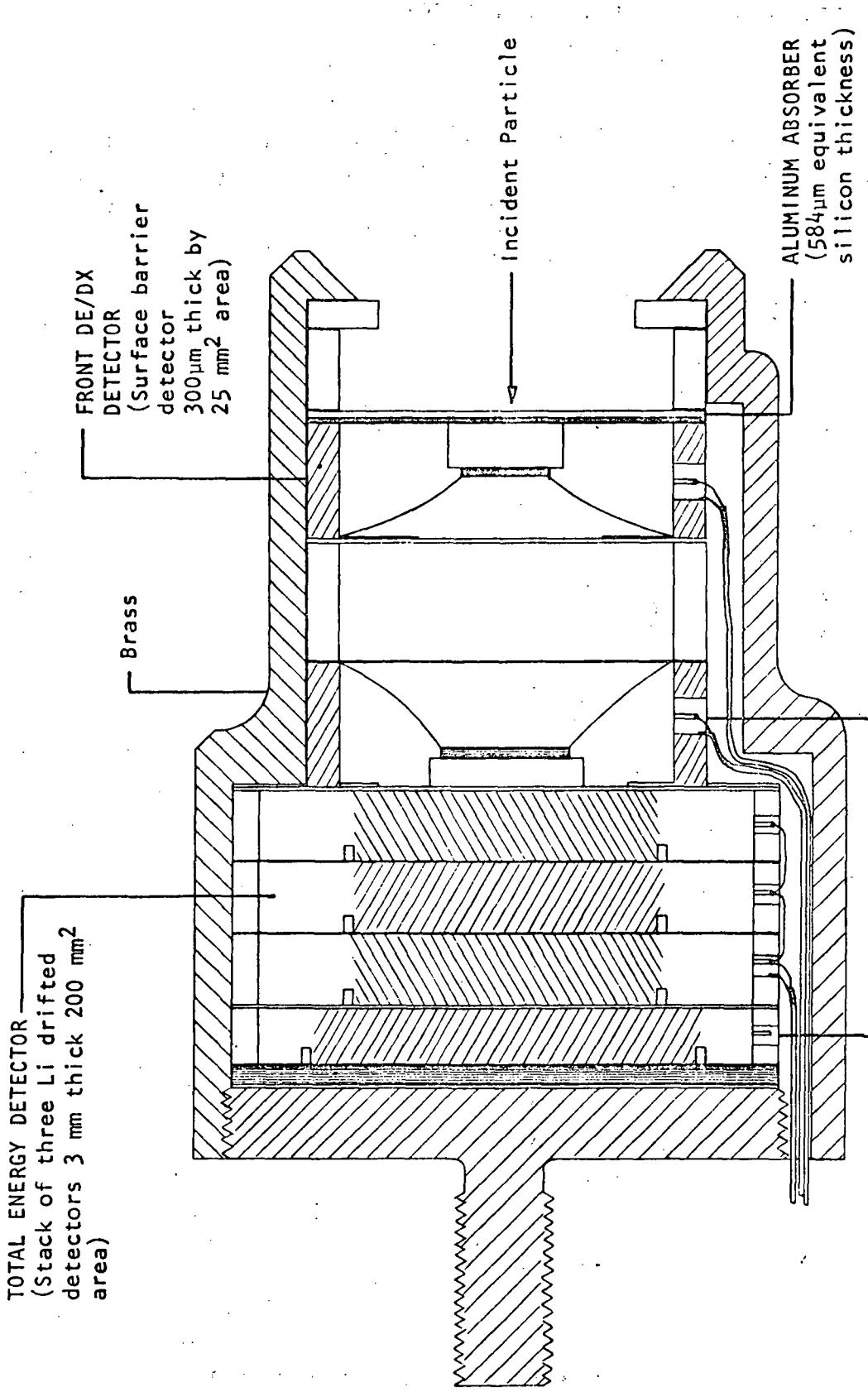

FIGURE 4-9. SPECTROMETER TELESCOPE

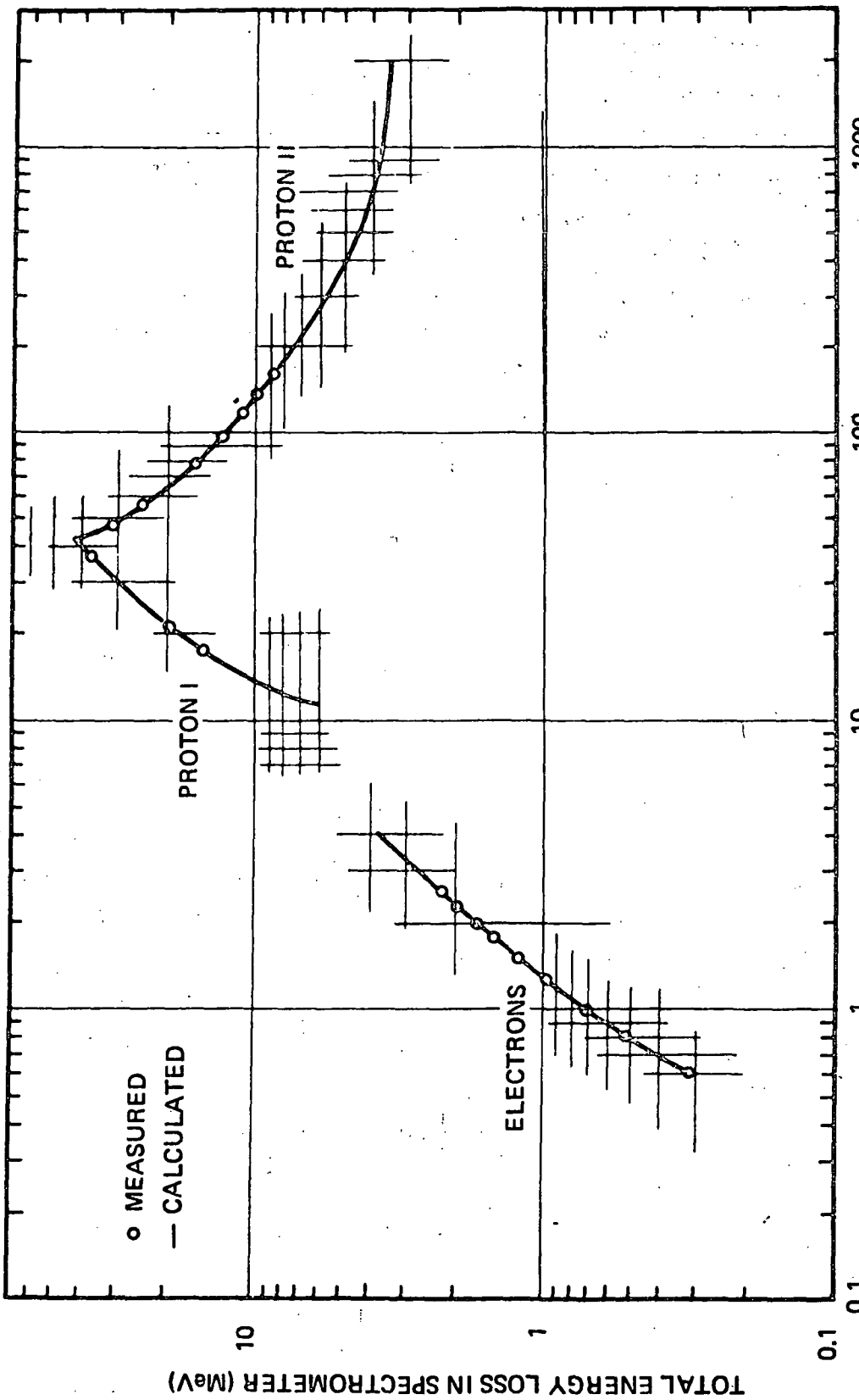

FIGURE 4-10 ELECTRON-PROTON SPECTROMETER CALIBRATION CURVES

4.2.2.2 Ionization Chamber Anomalies

It was thought until the last phases of this program that the ionization chamber readings were reliable. It was not until the correlations were made in the B and L coordinate system that it was possible to make accurate comparisons between the dose readings and those doses computed from the Vette models with the ionization chamber response functions. To make these comparisons the overlap integrals of the response functions (Figs. 4-11 through 4-14) and the Vette distributions were computed. These are presented in Table 4-1 with the average of the RMS ionization chamber readings for the corresponding grid locations. The values for the thin and thick shields are not unreasonably divergent. In general the computed doses are of the order of 80% higher than the measured values. The situation for the unshielded chamber is quite different. The calculations are from 5 to 10 times higher than the readings. This prompted a careful examination of the ionization chamber calibration and final checkout data of the satellite.

The gamma-ray calibrations were studied and it was found that the latest available data taken during the final acceptance test (Ref. 6) of the satellite was consistent with the original calibrations of dose rate as a function of voltage output (Ref. 1). This indicated that over this period the three chambers gave reliable readings.

The only explanation is that the sensitivity of the bare chamber changed during or after launch. Several attempts were made to determine the nature of the change and, thus, obtain a new calibration relative to the other chambers. This was unsuccessful, since the ratio of the readings to the computations was neither constant with reading nor with spectrum shape. This implied that the sensitivity change occurred in the nonlinear portion of the logarithmic amplifiers.

Further investigations did show that the ratio of the readings of the unshielded chamber to those of the shielded chambers did remain constant at the same B and L locations for different orbits, indicating

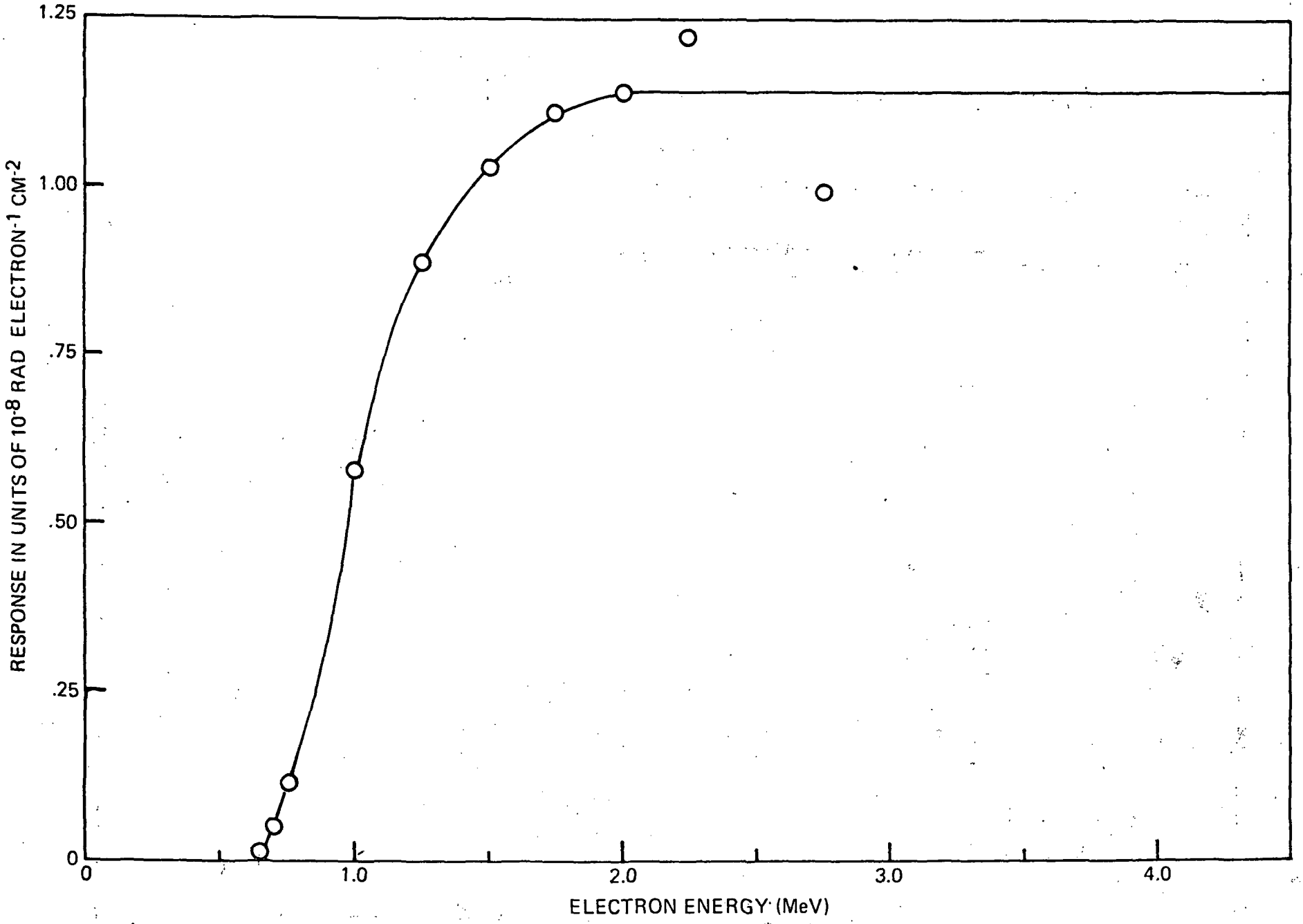

FIGURE 4-11. RESPONSE OF THE UNSHIELDED IONIZATION CHAMBER TO OMNIDIRECTION ELECTRONS

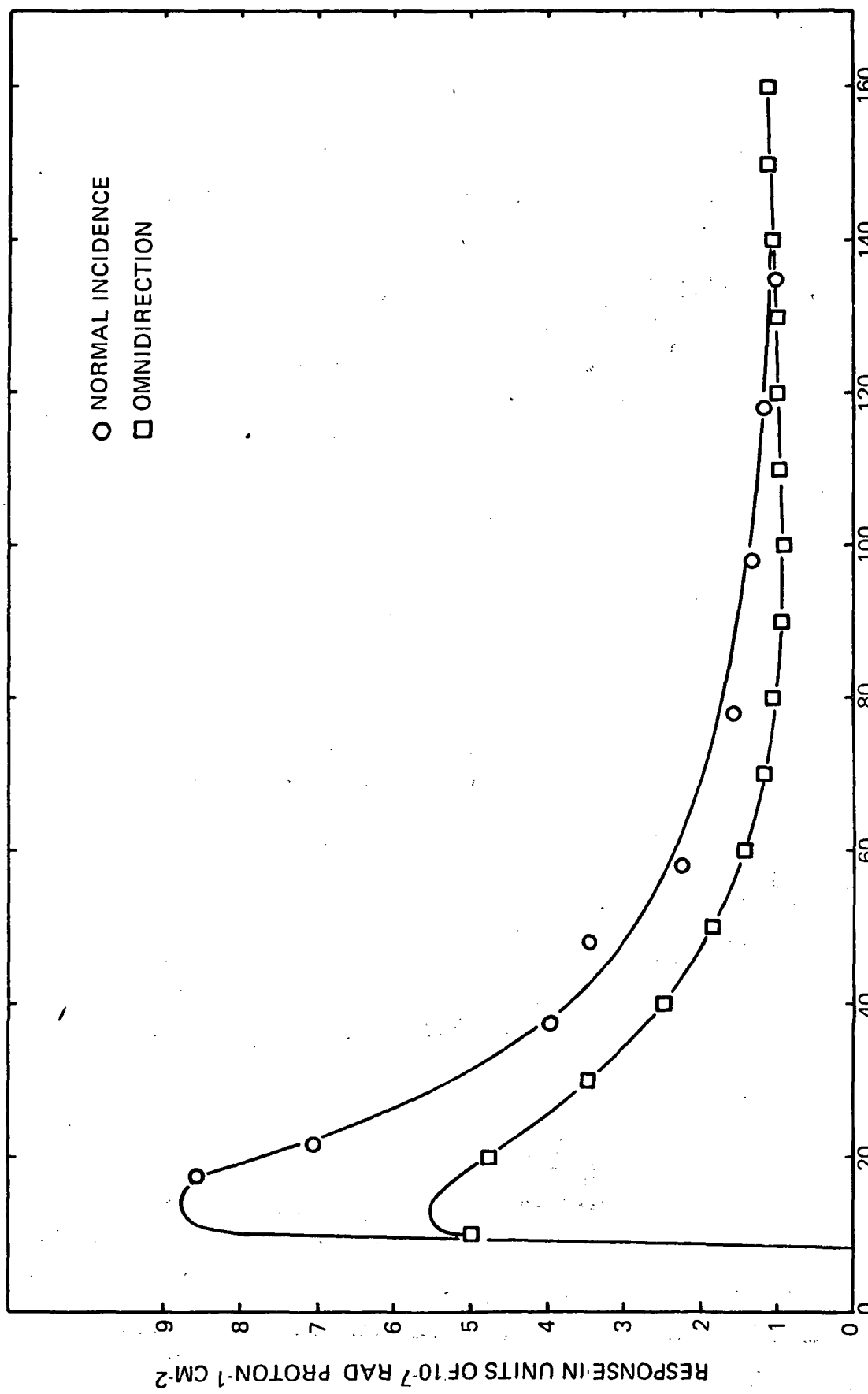

FIGURE 4-12. RESPONSE OF UNSHIELDED IONIZATION CHAMBER TO PROTONS AT NORMAL INCIDENCE AND OMNIDIRECTION

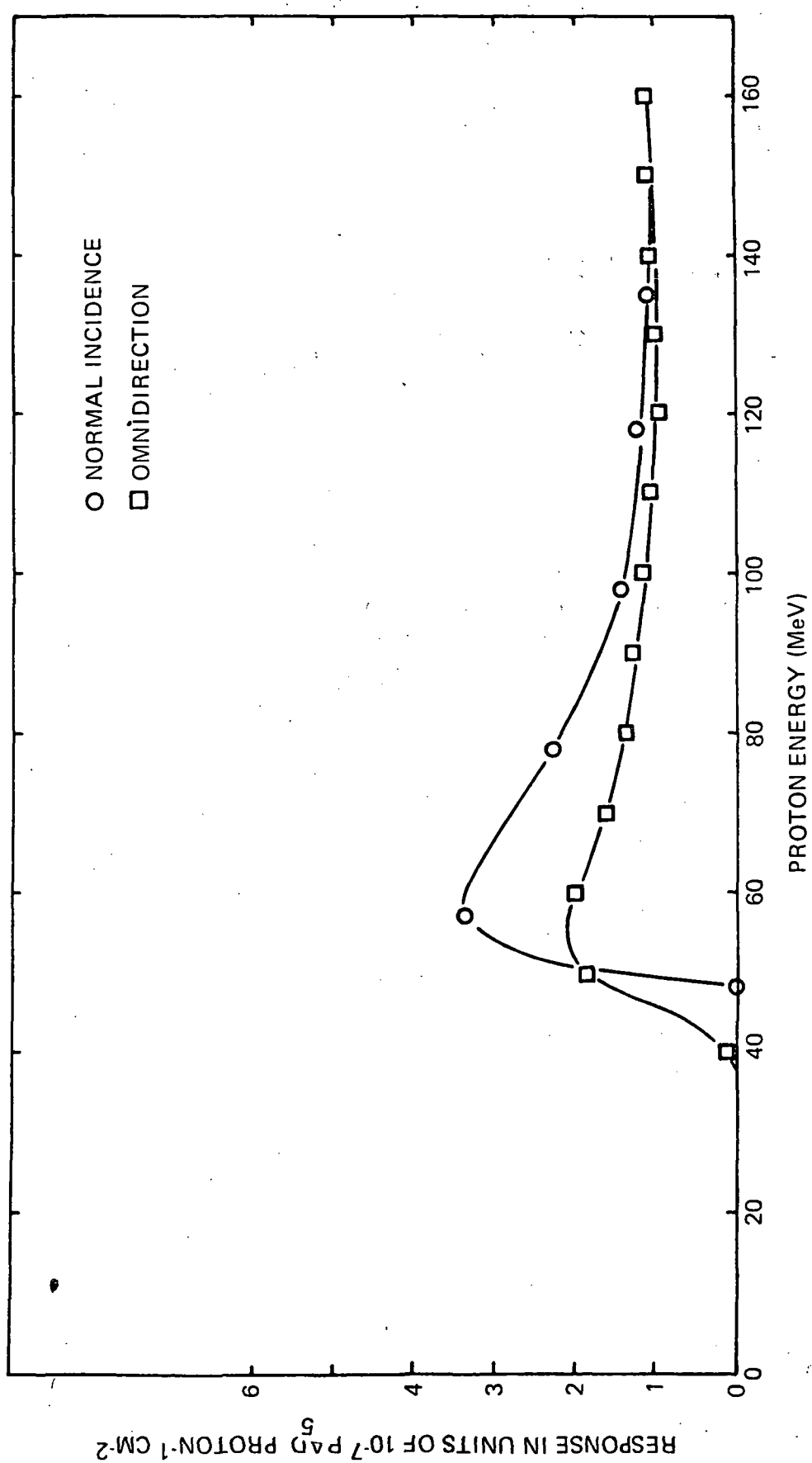

FIGURE 4-13. RESPONSE OF THIN-SHIELDED IONIZATION CHAMBER TO PROTONS AT NORMAL INCIDENCE AND OMNIDIRECTION

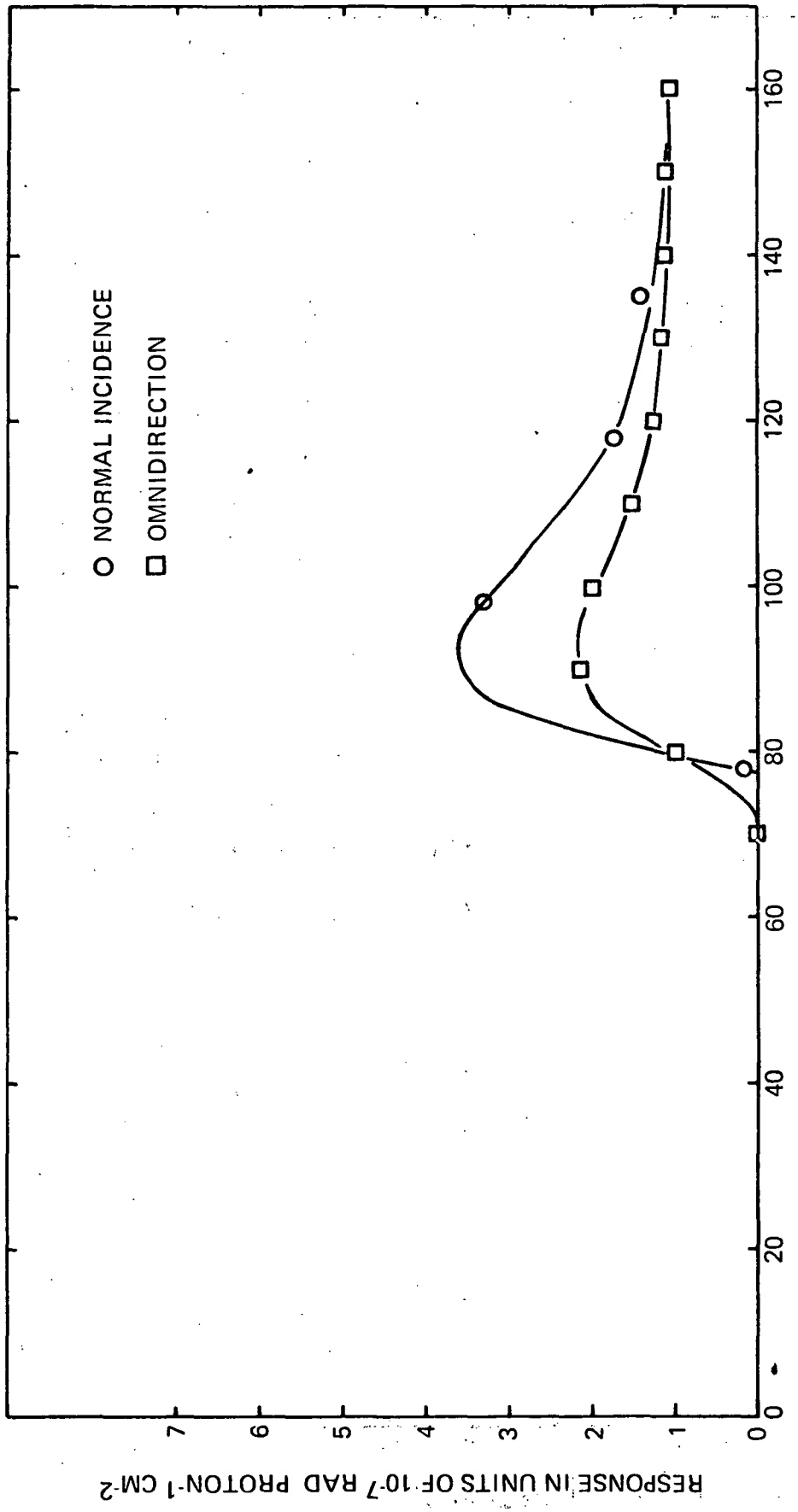

FIGURE 4-14. RESPONSE OF THICK SHIELDED IONIZATION CHAMBER TO PROTONS AT NORMAL INCIDENCE AND OMNIDIRECTION

TABLE 4-1.
COMPARISONS OF RMS IONIZATION CHAMBER DOSE READINGS TO THOSE COMPUTED FROM VETTE MODELS USING IONIZATION CHAMBER RESPONSE FUNCTIONS

** L = 1.20 **

B (GAUSS)	DATA TYPE	DOSE (RAD/HR) NO SHIELD	THIN SHIELD	THICK SHIELD
0.196	ELECTRON	3.702E-01		
	PROTON	1.813E 00	4.311E-01	3.349E-01
	TOTAL	2.183E 00	4.311E-01	3.349E-01
	RMS DATA	3.025E-01	3.070E-01	2.154E-01
0.198	ELECTRON	2.741E-01		
	PROTON	1.477E 00	3.687E-01	2.843E-01
	TOTAL	1.751E 00	3.687E-01	2.843E-01
	RMS DATA	3.740E-01	3.276E-01	2.510E-01
0.200	ELECTRON	2.048E-01		
	PROTON	1.182E 00	3.172E-01	2.443E-01
	TOTAL	1.387E 00	3.172E-01	2.443E-01
	RMS DATA	2.562E-01	2.135E-01	1.654E-01
0.202	ELECTRON	1.465E-01		
	PROTON	9.284E-01	2.667E-01	2.010E-01
	TOTAL	1.075E 00	2.667E-01	2.010E-01
	RMS DATA	1.877E-01	1.568E-01	1.194E-01
0.204	ELECTRON	1.040E-01		
	PROTON	7.154E-01	2.178E-01	1.604E-01
	TOTAL	8.194E-01	2.178E-01	1.604E-01
	RMS DATA	1.393E-01	1.283E-01	9.226E-02
0.206	ELECTRON	7.247E-02		
	PROTON	5.339E-01	1.743E-01	1.235E-01
	TOTAL	6.064E-01	1.743E-01	1.235E-01
	RMS DATA	1.089E-01	9.863E-02	6.380E-02
0.208	ELECTRON	4.963E-02		
	PROTON	3.808E-01	1.206E-01	7.952E-02
	TOTAL	4.304E-01	1.206E-01	7.952E-02
	RMS DATA	7.648E-02	7.668E-02	4.757E-02
0.210	ELECTRON	3.387E-02		
	PROTON	2.730E-01	9.306E-02	5.692E-02
	TOTAL	3.069E-01	9.306E-02	5.692E-02
	RMS DATA	4.305E-02	4.543E-02	3.165E-02
0.212	ELECTRON	2.300E-02		
	PROTON	1.827E-01	6.267E-02	3.283E-02
	TOTAL	2.057E-01	6.267E-02	3.283E-02
	RMS DATA	< .01	2.822E-02	< .01
0.214	ELECTRON	1.544E-02		
	PROTON	1.196E-01	3.776E-02	1.699E-02
	TOTAL	1.350E-01	3.776E-02	1.699E-02
	RMS DATA	< .01	2.241E-02	< .01
0.216	ELECTRON	1.016E-02		
	PROTON	7.622E-02	2.579E-02	1.067E-02
	TOTAL	8.638E-02	2.579E-02	1.067E-02
	RMS DATA	< .01	1.459E-02	< .01

TABLE 4-1 (CONT.)
COMPARISONS OF RMS IONIZATION CHAMBER DOSE READINGS TO THOSE COMPUTED FROM VETTE MODELS USING IONIZATION CHAMBER RESPONSE FUNCTIONS

** L = 1.30 **

B (GAUSS)	DATA TYPE	DOSE (RAD/HR) NO SHIELD	THIN SHIELD	THICK SHIELD
0.200	ELECTRON	1.558E 00		
	PROTON	3.527E 00	8.699E-01	6.849E-01
	TOTAL	5.085E 00	8.699E-01	6.849E-01
	RMS DATA	6.233E-01	4.747E-01	3.830E-01
0.205	ELECTRON	9.157E-01		
	PROTON	2.356E 00	6.215E-01	4.878E-01
	TOTAL	3.272E 00	6.215E-01	4.878E-01
	RMS DATA	4.967E-01	3.977E-01	3.032E-01
0.210	ELECTRON	5.068E-01		
	PROTON	1.374E 00	4.115E-01	3.178E-01
	TOTAL	1.881E 00	4.115E-01	3.178E-01
	RMS DATA	3.184E-01	2.593E-01	1.882E-01
0.212	ELECTRON	3.916E-01		
	PROTON	1.100E 00	3.405E-01	2.603E-01
	TOTAL	1.492E 00	3.405E-01	2.603E-01
	RMS DATA	2.477E-01	1.867E-01	1.381E-01
0.214	ELECTRON	2.966E-01		
	PROTON	8.432E-01	2.862E-01	2.136E-01
	TOTAL	1.140E 00	2.862E-01	2.136E-01
	RMS DATA	1.901E-01	1.472E-01	1.034E-01
0.216	ELECTRON	2.246E-01		
	PROTON	6.510E-01	2.179E-01	1.585E-01
	TOTAL	8.756E-01	2.179E-01	1.585E-01
	RMS DATA	1.097E-01	9.110E-02	6.228E-02
0.218	ELECTRON	1.670E-01		
	PROTON	5.102E-01	1.819E-01	1.238E-01
	TOTAL	6.773E-01	1.819E-01	1.238E-01
	RMS DATA	7.710E-02	6.623E-02	4.312E-02
0.220	ELECTRON	1.264E-01		
	PROTON	3.914E-01	1.447E-01	8.915E-02
	TOTAL	5.178E-01	1.447E-01	8.915E-02
	RMS DATA	< .01	4.649E-02	< .01
0.222	ELECTRON	9.042E-02		
	PROTON	2.869E-01	9.941E-02	5.374E-02
	TOTAL	3.773E-01	9.941E-02	5.374E-02
	RMS DATA	< .01	2.850E-02	< .01

TABLE 4-1. (CONT.)
COMPARISONS OF RMS IONIZATION CHAMBER DOSE READINGS TO THOSE COMPUTED FROM VETTE MODELS USING IONIZATION CHAMBER RESPONSE FUNCTIONS

** L = 1.40 **

B (GAUSS)	DATA TYPE	DOSE (RAD/HR) NO SHIELD	THIN SHIELD	THICK SHIELD
0.210	ELECTRON	2.600E 00		
	PROTON	2.879E 00	7.310E-01	5.616E-01
	TOTAL	5.479E 00	7.310E-01	5.616E-01
	RMS DATA	6.843E-01	4.438E-01	3.337E-01
0.215	ELECTRON	1.731E 00		
	PROTON	1.908E 00	5.363E-01	4.017E-01
	TOTAL	3.639E 00	5.363E-01	4.017E-01
	RMS DATA	4.545E-01	3.246E-01	2.244E-01
0.220	ELECTRON	1.083E 00		
	PROTON	1.209E 00	3.697E-01	2.580E-01
	TOTAL	2.293E 00	3.697E-01	2.580E-01
	RMS DATA	2.220E-01	1.570E-01	9.898E-02
0.225	ELECTRON	6.234E-01		
	PROTON	6.657E-01	2.299E-01	1.465E-01
	TOTAL	1.289E 00	2.299E-01	1.465E-01
	RMS DATA	1.426E-01	9.926E-02	5.695E-02
0.230	ELECTRON	3.274E-01		
	PROTON	3.307E-01	8.911E-02	5.131E-02
	TOTAL	6.580E-01	8.911E-02	5.131E-02
	RMS DATA	3.779E-02	3.762E-02	1.726E-02
0.232	ELECTRON	2.624E-01		
	PROTON	2.462E-01	6.361E-02	3.612E-02
	TOTAL	5.086E-01	6.361E-02	3.612E-02
	RMS DATA	< .01	1.478E-02	< .01

TABLE 4-1. (CONT.)
COMPARISONS OF RMS IONIZATION CHAMBER DOSE READINGS TO THOSE COMPUTED FROM VETTE MODELS USING IONIZATION CHAMBER RESPONSE FUNCTIONS

** L = 1.50 **

B (GAUSS)	DATA TYPE	DOSE (RAD/HR) NO SHIELD	THIN SHIELD	THICK SHIELD
0.210	ELECTRON	3.487E 00		
	PROTON	4.554E 00	7.002E-01	5.186E-01
	TOTAL	8.041E 00	7.002E-01	5.186E-01
	RMS DATA	6.180E-01	3.586E-01	2.519E-01
0.220	ELECTRON	1.847E 00		
	PROTON	2.364E 00	4.020E-01	2.748E-01
	TOTAL	4.211E 00	4.020E-01	2.748E-01
	RMS DATA	4.057E-01	2.590E-01	1.632E-01
0.225	ELECTRON	1.244E 00		
	PROTON	1.555E 00	3.021E-01	1.908E-01
	TOTAL	2.799E 00	3.021E-01	1.908E-01
	RMS DATA	2.558E-01	1.505E-01	8.730E-02
0.230	ELECTRON	7.841E-01		
	PROTON	9.582E-01	2.020E-01	1.182E-01
	TOTAL	1.742E 00	2.020E-01	1.182E-01
	RMS DATA	1.393E-01	8.892E-02	4.595E-02
0.235	ELECTRON	4.712E-01		
	PROTON	5.508E-01	1.213E-01	6.884E-02
	TOTAL	1.022E 00	1.213E-01	6.884E-02
	RMS DATA	< .01	5.116E-02	< .01

** L = 1.60 **

B (GAUSS)	DATA TYPE	DOSE (RAD/HR) NO SHIELD	THIN SHIELD	THICK SHIELD
0.220	ELECTRON	4.026E-01		
	PROTON	3.354E 00	3.101E-01	1.908E-01
	TOTAL	3.757E 00	3.101E-01	1.908E-01
	RMS DATA	3.410E-01	1.876E-01	1.090E-01
0.230	ELECTRON	2.193E-01		
	PROTON	1.737E 00	1.782E-01	9.998E-02
	TOTAL	1.957E 00	1.782E-01	9.998E-02
	RMS DATA	2.320E-01	1.255E-01	6.276E-02
0.240	ELECTRON	1.104E-01		
	PROTON	7.267E-01	8.503E-02	4.742E-02
	TOTAL	8.371E-01	8.503E-02	4.742E-02
	RMS DATA	9.766E-02	5.895E-02	< .01

TABLE 4-1. (CONT.)
COMPARISONS OF RMS IONIZATION CHAMBER DOSE READINGS TO THOSE COMPUTED FROM VETTE MODELS USING IONIZATION CHAMBER RESPONSE FUNCTIONS

** L = 1.70 **

B (GAUSS)	DATA TYPE	DOSE (RAD/HR) NO SHIELD	THIN SHIELD	THICK SHIELD
0.240	ELECTRON	3.130E-02		
	PROTON	1.279E 00	7.571E-02	3.968E-02
	TOTAL	1.310E 00	7.571E-02	3.968E-02
	RMS DATA	9.757E-02	5.211E-02	< .01

** L = 1.80 **

B (GAUSS)	DATA TYPE	DOSE (RAD/HR) NO SHIELD	THIN SHIELD	THICK SHIELD
0.240	ELECTRON	1.436E-02		
	PROTON	1.664E 00	5.044E-02	2.323E-02
	TOTAL	1.679E 00	5.044E-02	2.323E-02
	RMS DATA	1.043E-01	4.629E-02	< .01
0.250	ELECTRON	1.037E-02		
	PROTON	8.781E-01	3.025E-02	1.415E-02
	TOTAL	8.885E-01	3.025E-02	1.415E-02
	RMS DATA	7.984E-02	3.797E-02	< .01

** L = 1.90 **

B (GAUSS)	DATA TYPE	DOSE (RAD/HR) NO SHIELD	THIN SHIELD	THICK SHIELD
0.250	ELECTRON	8.051E-03		
	PROTON	1.134E 00	2.123E-02	7.883E-03
	TOTAL	1.142E 00	2.123E-02	7.883E-03
	RMS DATA	5.974E-02	2.425E-02	< .01

** L = 2.00 **

B (GAUSS)	DATA TYPE	DOSE (RAD/HR) NO SHIELD	THIN SHIELD	THICK SHIELD
0.250	ELECTRON	6.371E-03		
	PROTON	1.321E 00	1.619E-02	3.933E-03
	TOTAL	1.328E 00	1.619E-02	3.933E-03
	RMS DATA	4.754E-02	1.674E-02	< .01

that the change in sensitivity did remain constant for the life of the experiment. A detailed examination of the NASA/MSC data logs, if these are still available, should provide the necessary information to salvage the data; however, at this point the readings of the bare chamber must be considered to be in error. This in no way reflects on the validity of the data from the shielded chambers. The ratio in the readings of these chambers to the computations is simply the adjustment required in the flux values of the Vette models if the spectra are assumed to be even reasonably accurate.

4.2.3 Spectrometer Efficiency and Satellite Dynamics

A brief analysis was made to determine the effect of the "pancake" trajectories of particles incident on the spectrometer telescope. Since the radiations encountered by the satellite were very low in the radiation trapping zone, the particles were very near their mirror points and the pitch angles of the particles (both electrons and protons) were nearly 90° with respect to the magnetic field lines. Because of the small acceptance angle of the telescope, the number of particles counted could be from zero to several times that obtained in an omnidirectional flux, depending on the orientation of the telescope with respect to the field line. This was further complicated by the complex motion of the satellite which consisted of a spin with precession in the most general case. Using the measured angular response functions of the satellite which are given in Fig. 4-15, computations of the effective efficiency of the spectrometer were made for various precession angles as a function of the orientation of the total angular momentum vector of the satellite with respect to the magnetic field. These curves are presented in Fig. 4-16. The calculations were made for both head 1 at 35° with respect to the spin axis of the satellite and head 3 at 66°. These curves have several interesting features. The efficiency for either head is seen to vary greatly, especially at low precession angles. However, in most cases for precession angles 30° or greater, the average of the outputs from the two heads is very

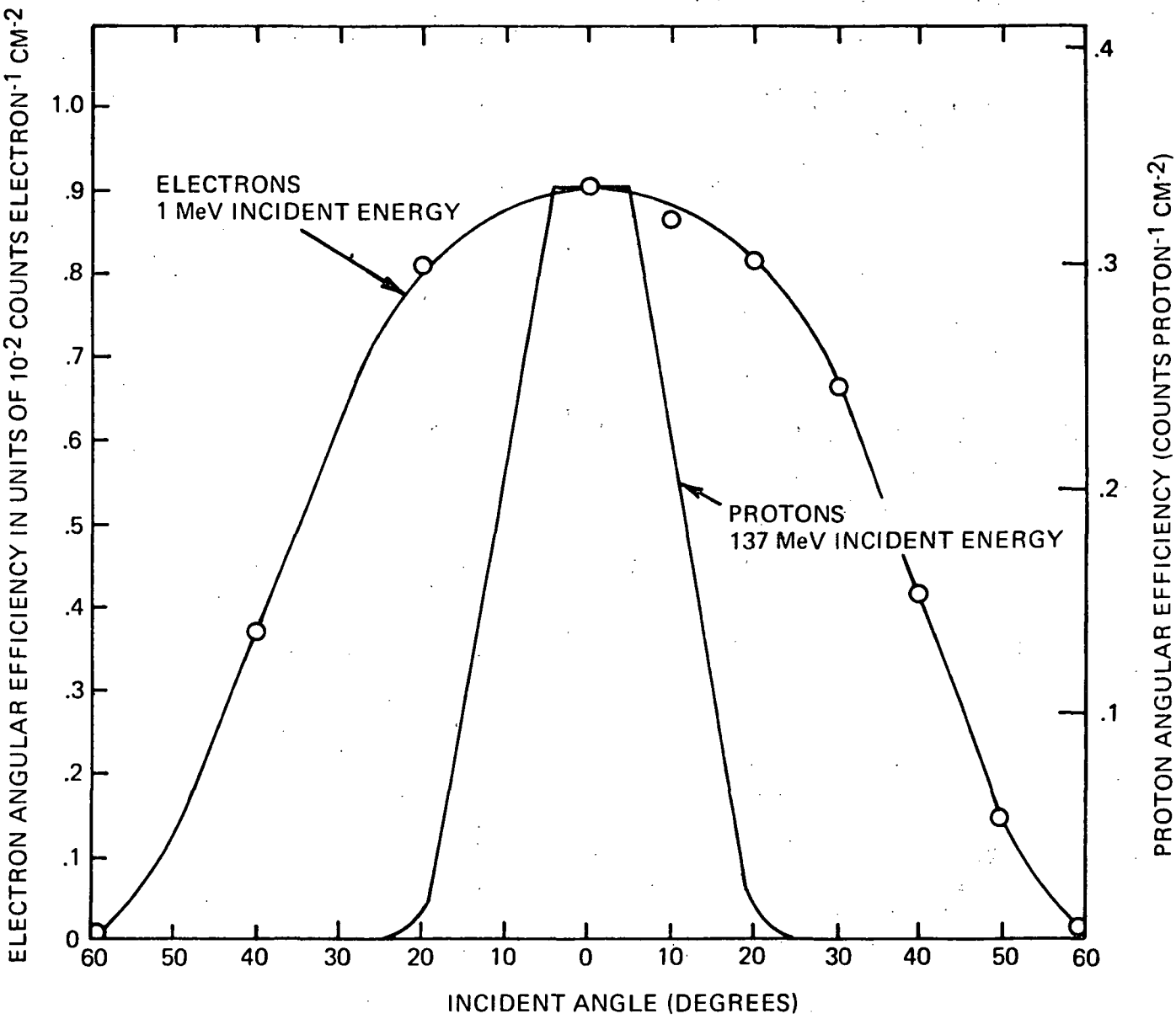

FIGURE 4-15. TYPICAL ANGULAR EFFICIENCIES OF THE ELECTRON-PROTON SPECTROMETER

FIGURE 4-16. COMPARISON OF EFFICIENCIES OF ELECTRON-PROTON TELESCOPE FOR OMNIDIRECTIONAL AND PANCAKE FLUXES AS A FUNCTION OF SATELLITE ORIENTATION WITH RESPECT TO MAGNETIC FIELD LINES AT VARIOUS SATELLITE PRECESSION ANGLES

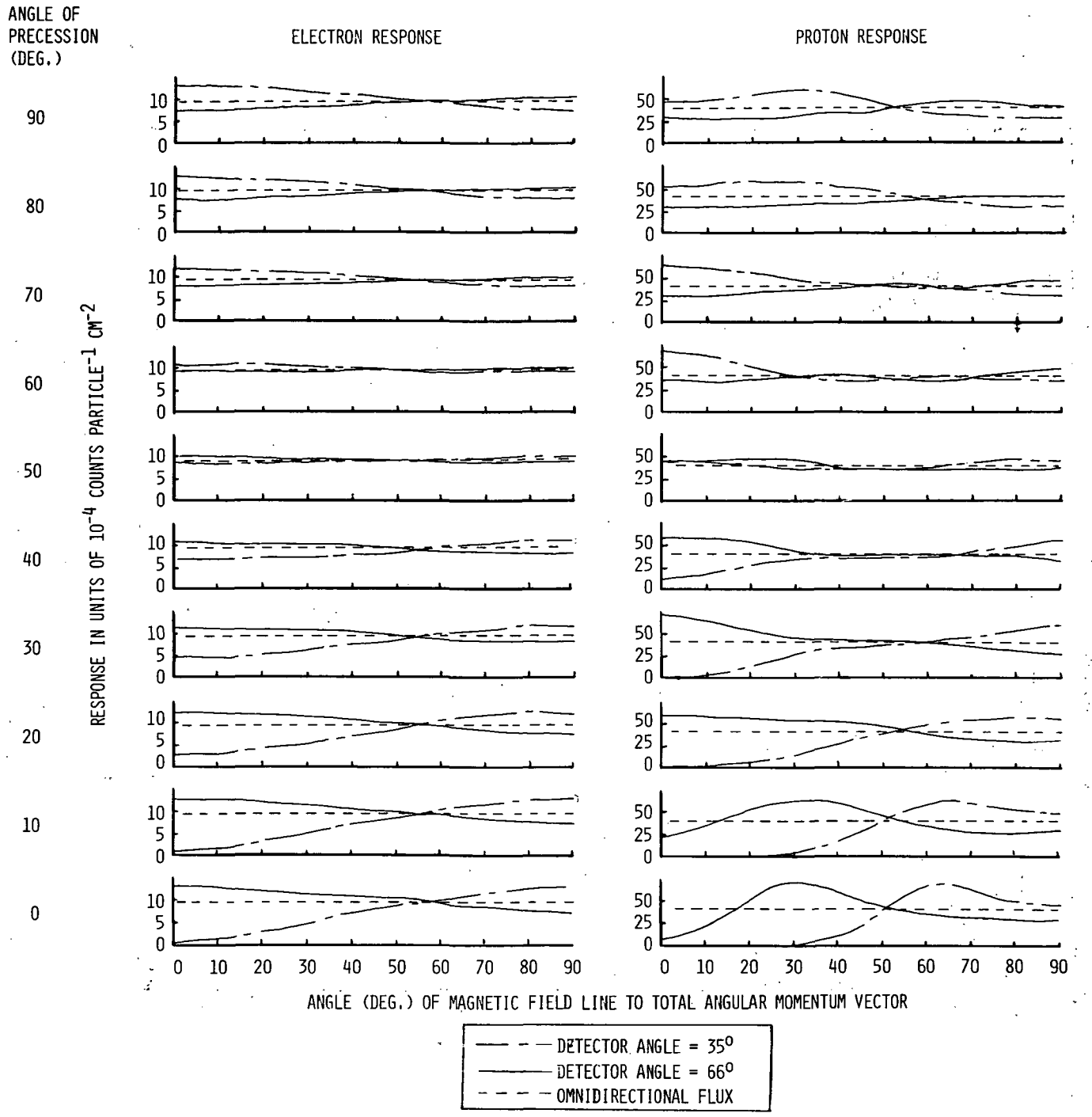

nearly equal to the omnidirectional efficiency. The implication is that if the two heads had functioned properly, the error in the absolute value of the flux measurements would have been increased only slightly.

Considerable time was spent in an attempt to determine the dynamics of the satellite in order to assign an accurate efficiency to the spectral measurements. Automatic gain control (AGC) recordings from the station receivers were made of the RMS beacon and telemetering transmitters. In addition plots of the satellite solar panel current were made as a function of time and rather unsuccessful attempts were made to correlate these data. The solar panel data indicated the changing angle of the cylindrical solar panel array with respect to the sun. Thus, it was possible to measure the precession period and the period of tumble after spin stopped. (These periods should be constant and equal, theoretically). Such measurements made throughout the lifetime of the satellite showed this to be essentially true. Precession periods of the order of 36 seconds were observed. This was not corroborated by the AGC data, however. The relatively simple pattern which was received after spin stopped indicated a tumble period of 6.7 seconds. The complex patterns before spin stopped could not be reliably correlated at all. Since spin stopped relatively fast (about orbit 169), the evidence strongly suggests that the precession angle was large, certainly greater than 30°, during the time the radiation data were taken. Thus, an uncertainty can be placed on the data from an examination of Fig. 4-16. An error of the order of ± 20% for one standard deviation appears reasonable. This dictates the highest precision which could be obtained in making spectrum-to-dose comparisons. Such comparisons are made and discussed in Section 4.3.3.

4.3 Presentation of Data

As described in the preceding paragraphs, two forms of useful data were obtained by the RMS radiation experiment:

(a) Spectral maps obtained by the spectrometer telescope and

(b) Dose maps obtained by the NASA ionization chambers.

Both of these types of data were obtained in the South Atlantic magnetic anomaly and are presented in the B and L coordinate system.

4.3.1 Spectral Maps

The spectral maps were obtained from the G-II tape on which had been written the correlated B and L coordinates. The coordinates were taken as the point at the center of the 8 second data period. The resulting tabulations and plots were taken from the entire RMS mission for spectrometer head 1. The B and L grid used is identical to that used in the Vette model. Data were placed in a particular grid location according to the simple criteria of one half the distance between B or L values. The resulting data for electrons and protons are presented in tabular form in Tables 4-2 and 4-3 respectively. Plots are presented in Figs. 4-17 and 4-18. The channel boundaries of the spectrometer and mean efficiences over the boundaries are taken from Ref. (1) and presented in Table 4-4. The regions of poor statistics are indicated in both the tables and the figures. The data are normalized as indicated in the table and figure captions. This is the form for presentation of the data which is most useful, since it offers the best comparison to the Vette models.

4.3.2 Dose Maps

The dose maps were obtained from the outputs of the three NASA ionization chambers. The chambers are described in detail in Ref. (1) and are shielded in a manner to provide proton thresholds of approximately 11 MeV for the chamber with no shield, 40 MeV for the thin shield and 80 MeV for the thick shield. As discussed in Section 4.2.2.2, Ionization Chamber Anomalies, the data from the unshielded ionization chamber did not agree with the computations from the spectrometer data or the Vette models. The no shield data is included here only for reference. The calibration curves for the chambers were presented earlier in Fig. 4-11 through 4-14.

TABLE 4-2. TABULATION OF RMS ELECTRON SPECTRA.

(HEAD 1 ENABLED)

ENERGY GROUP (MEV)	L = 1.10 *	L = 1.20 *	L = 1.30 *	L = 1.40	L = 1.50	L = 1.70 *	L = 2.00 *	L = 2.50 *
0.50-0.65	9.440E-01	5.596E 00	5.699E 00	6.119E 00	6.084E 00	5.944E 00	5.986E 00	6.243E 00
0.65-0.79	1.604E-02	4.068E-01	1.762E-01	4.411E-01	4.560E-01	5.294E-01	4.714E-01	2.090E-01
0.79-0.93	3.947E-03	7.614E-02	9.093E-02	8.896E-02	1.082E-01	1.481E-01	1.328E-01	1.167E-01
0.93-1.06	1.342E-02	5.184E-01	3.901E-02	2.982E-02	3.902E-02	7.161E-02	7.101E-02	0.0
1.06-1.20	5.519E-04	5.217E-03	1.794E-03	6.399E-03	1.006E-02	2.018E-02	1.880E-02	0.0
1.20-1.35	3.038E 00	1.786E-02	2.264E-01	4.014E-03	3.073E-03	2.454E-03	7.048E-03	0.0
1.35-1.62	5.434E-05	1.644E-03	1.332E-01	1.078E-03	1.108E-03	1.208E-03	1.388E-03	0.0
1.62-1.91	0.0	7.750E-04	4.691E-04	1.152E-03	4.669E-04	5.316E-04	0.0	0.0
1.91-2.20	1.259E 00	5.812E-04	3.776E-04	7.725E-04	3.557E-04	6.076E-04	1.309E-03	6.210E-02
2.20-2.53	0.0	6.527E-04	2.413E-04	5.598E-04	3.321E-04	0.0	0.0	0.0
2.53-3.10	5.342E-02	1.594E-03	2.833E-04	7.102E-04	2.941E-04	2.318E-04	3.995E-03	0.0
3.10-3.65	4.377E-03	4.938E-04	2.715E-04	5.145E-04	3.634E-04	2.403E-04	0.0	0.0
3.65-4.20	2.702E-05	3.548E-02	2.976E-04	4.359E-04	3.400E-04	2.002E-04	2.070E-03	0.0
4.20-5.20	0.0	4.495E-04	3.178E-02	5.777E-04	2.708E-04	4.405E-05	3.795E-04	0.0

*INDICATES POOR STATISTICS

TABLE 4-3. TABULATION OF RMS PROTON SPECTRA.

(HEAD 1 ENABLED)

** L = 1.10 **

B (GAUSS)	ENERGY GROUP (MEV) 11.0-12.7	12.7-15.5	15.5-19.0	19.0-27.0	27.0-35.0	35.0-42.0
*0.200	0.0	0.0	0.0	0.0	0.0	0.0
*0.205	0.0	0.0	0.0	4.167E-02	8.333E-02	0.0
*0.210	1.681E-01	5.102E-02	5.102E-02	2.232E-02	1.339E-02	1.531E-02
*0.215	5.602E-02	1.701E-02	2.177E-01	5.952E-03	5.952E-03	0.0

** L = 1.20 **

B (GAUSS)	ENERGY GROUP (MEV) 11.0-12.7	12.7-15.5	15.5-19.0	19.0-27.0	27.0-35.0	35.0-42.0
*0.196	0.0	0.0	0.0	0.0	0.0	0.0
*0.198	1.665E-01	9.466E-02	2.926E-02	2.259E-02	1.506E-02	6.885E-03
*0.200	1.631E-01	8.604E-02	3.714E-02	1.906E-02	1.408E-02	1.238E-02
0.202	1.350E-01	6.238E-02	4.207E-02	2.654E-02	1.841E-02	1.272E-02
0.204	1.420E-01	6.158E-02	4.269E-02	2.874E-02	1.580E-02	1.149E-02
*0.206	1.681E-01	8.291E-02	5.102E-03	2.455E-02	2.902E-02	5.102E-03
*0.208	1.563E-01	4.464E-02	3.571E-02	2.148E-02	1.953E-02	2.232E-02
*0.210	1.858E-01	7.519E-02	3.008E-02	2.303E-02	1.316E-02	1.128E-02
*0.212	3.885E-02	3.032E-02	8.086E-03	1.415E-02	1.061E-02	8.895E-02
*0.214	1.420E-01	8.621E-02	2.956E-02	2.155E-02	1.724E-02	1.478E-02

** L = 1.30 **

B (GAUSS)	ENERGY GROUP (MEV) 11.0-12.7	12.7-15.5	15.5-19.0	19.0-27.0	27.0-35.0	35.0-42.0
0.200	1.288E-01	7.071E-02	3.932E-02	2.778E-02	1.915E-02	9.994E-03
0.205	1.396E-01	6.498E-02	3.899E-02	2.790E-02	1.724E-02	1.188E-02
0.210	1.292E-01	7.114E-02	4.405E-02	2.643E-02	1.671E-02	1.169E-02
0.212	1.388E-01	7.424E-02	3.531E-02	2.142E-02	1.791E-02	1.685E-02
0.214	1.353E-01	7.857E-02	3.000E-02	2.500E-02	1.812E-02	1.429E-02
*0.216	1.101E-01	5.069E-02	6.083E-02	2.742E-02	1.774E-02	1.382E-02
*0.218	1.894E-01	4.843E-02	2.663E-02	2.860E-02	1.801E-02	1.090E-02
*0.220	1.264E-01	6.008E-02	4.005E-02	2.687E-02	2.220E-02	1.202E-02
*0.222	2.124E-01	2.976E-02	3.968E-02	1.736E-02	2.083E-02	1.587E-02
*0.224	1.307E-01	5.952E-02	6.349E-02	2.778E-02	1.389E-02	7.937E-03

* INDICATES POOR STATISTICS

TABLE 4-3. RMS PROTON SPECTRA TABULATIONS (CONT.)

(HEAD 1 ENABLED)

** L = 1.40 **

B (GAUSS)	ENERGY GROUP (MEV) 11.0-12.7	12.7-15.5	15.5-19.0	19.0-27.0	27.0-35.0	35.0-42.0
*0.200	0.0	0.0	0.0	0.0	0.0	0.0
*0.205	0.0	0.0	0.0	0.0	0.0	0.0
0.210	1.124E-01	6.508E-02	4.042E-02	3.167E-02	1.954E-02	1.079E-02
0.215	1.159E-01	6.253E-02	3.944E-02	2.904E-02	2.210E-02	1.154E-02
0.220	8.489E-02	6.787E-02	4.210E-02	3.163E-02	2.096E-02	1.394E-02
0.225	9.727E-02	5.343E-02	3.975E-02	3.248E-02	2.100E-02	1.687E-02
*0.230	1.730E-01	2.101E-02	5.042E-02	3.676E-02	1.471E-02	8.403E-03
*0.232	1.681E-01	5.102E-02	4.082E-02	1.786E-02	1.786E-02	2.041E-02

** L = 1.50 **

B (GAUSS)	ENERGY GROUP (MEV) 11.0-12.7	12.7-15.5	15.5-19.0	19.0-27.0	27.0-35.0	35.0-42.0
*0.200	0.0	0.0	0.0	0.0	0.0	0.0
*0.205	0.0	0.0	0.0	0.0	0.0	0.0
*0.210	0.0	0.0	0.0	0.0	0.0	0.0
0.215	8.218E-02	5.252E-02	4.202E-02	3.493E-02	2.022E-02	1.786E-02
0.220	8.739E-02	4.490E-02	4.082E-02	3.857E-02	2.429E-02	1.143E-02
0.225	8.403E-02	5.777E-02	3.340E-02	3.335E-02	2.627E-02	1.450E-02
0.230	7.791E-02	4.376E-02	4.447E-02	3.642E-02	2.442E-02	1.466E-02
*0.232	5.530E-02	3.663E-02	4.884E-02	3.632E-02	3.098E-02	1.343E-02
*0.234	1.094E-01	2.492E-02	4.319E-02	2.471E-02	3.488E-02	1.661E-02

** L = 1.60 **

B (GAUSS)	ENERGY GROUP (MEV) 11.0-12.7	12.7-15.5	15.5-19.0	19.0-27.0	27.0-35.0	35.0-42.0
*0.200	0.0	0.0	0.0	0.0	0.0	0.0
*0.205	0.0	0.0	0.0	0.0	0.0	0.0
*0.210	0.0	0.0	0.0	0.0	0.0	0.0
*0.215	0.0	0.0	0.0	0.0	0.0	0.0
*0.220	0.0	0.0	0.0	0.0	0.0	0.0
*0.225	0.0	0.0	0.0	0.0	0.0	0.0
*0.230	2.558E-02	6.211E-02	6.211E-02	3.804E-02	2.174E-02	1.242E-02
*0.235	6.146E-02	6.219E-02	3.269E-02	3.794E-02	2.425E-02	1.564E-02
*0.240	3.728E-02	4.779E-02	3.421E-02	3.873E-02	3.345E-02	1.509E-02
0.245	1.038E-01	6.303E-02	5.042E-02	2.941E-02	2.206E-02	8.403E-03

*INDICATES POOR STATISTICS

TABLE 4-4. Channel Energy Boundaries, Efficiences and Spectrum-to-Dose Conversion Factors for Electron-Proton Spectrometer

Channel Number	ELECTRONS Energy Band (MeV)	Efficiency (counts/electrons)	S-to-D Factors Unshielded Chamber (rad/count)
1	Not Used	-	-
2	Not Used	-	-
3	0.50 - 0.65	6.0 (-5)	0.0
4	0.65 - 0.79	4.8 (-4)	1.23 (-6)
5	0.79 - 0.93	8.6 (-4)	4.16 (-6)
6	0.93 - 1.06	9.3 (-4)	6.60 (-6)
7	1.06 - 1.20	9.0 (-4)	9.35 (-6)
8	1.20 - 1.35	8.4 (-4)	1.34 (-5)
9	1.35 - 1.62	7.9 (-4)	2.04 (-5)
10	1.62 - 1.91	7.8 (-4)	2.95 (-5)
11	1.91 - 2.20	7.8 (-4)	3.00 (-5)
12	2.20 - 2.53	7.8 (-4)	3.20 (-5)
13	2.53 - 3.10	7.8 (-4)	3.20 (-5)
14	3.10 - 3.65	7.8 (-4)	3.20 (-5)
15	3.65 - 4.20	7.8 (-4)	3.20 (-5)
16	4.20 - 5.20	7.8 (-4)	3.20 (-5)

TABLE 4-4. (Continued)

PROTONS

Channel Number	Energy Band (MeV)	Efficiency (counts/protons)	S-to-D Factors		
			No Shield (rad/count)	Thin Shield (rad/count)	Thick Shield (rad/count)
PI 1	Not Used	-	-	-	-
2	11.0-12.7	5.0(-3)	1.15(-4)	0.0	0.0
3	12.7-15.5	5.0(-3)	1.10(-4)	0.0	0.0
4	15.5-19.0	5.0(-3)	1.05(-4)	0.0	0.0
5	19.0-27.0	5.0(-3)	8.80(-5)	0.0	0.0
6	27.0-35.0	5.0(-3)	6.80(-5)	0.0	0.0
7	35.0-42.0	5.0(-3)	5.50(-5)	3.00(-6)	0.0
8	Not Used	-	-	-	-
PII 1	620-∞	1.0(-2)	1.20(-5)	1.10(-5)	1.03(-5)
2	167-620	1.0(-2)	1.20(-5)	1.10(-5)	1.03(-5)
3	100-167	5.0(-3)	2.10(-5)	2.10(-5)	2.30(-5)
4	75-100	5.0(-3)	2.00(-5)	2.80(-5)	3.00(-5)
5	54-75	5.0(-3)	2.80(-5)	3.60(-5)	5.00(-7)
6	46-54	5.0(-3)	3.80(-5)	3.20(-5)	0.0
7	42-54	5.0(-3)	4.40(-5)	1.30(-5)	0.0
8	Not Used	-	-	-	-

FIG. 4-17. RMS ELECTRON SPECTRA COMPARED TO VETTE AE2 PROJECTED 1968 SPECTRA. BOTH SPECTRA ARE NORMALIZED TO ONE ABOVE 0.5 MEV

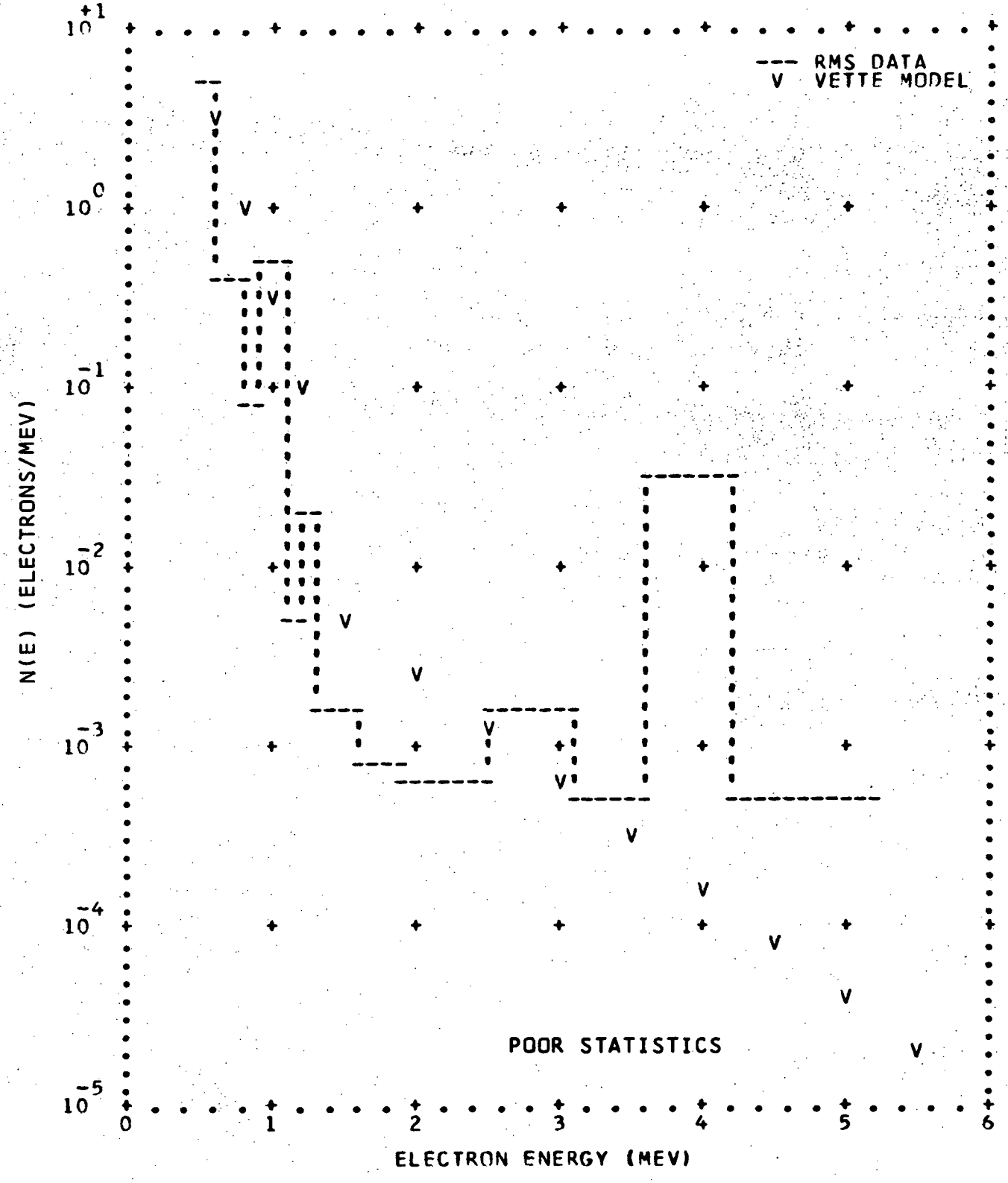

FIG. 4-17. RMS ELECTRON SPECTRA (CONT.)

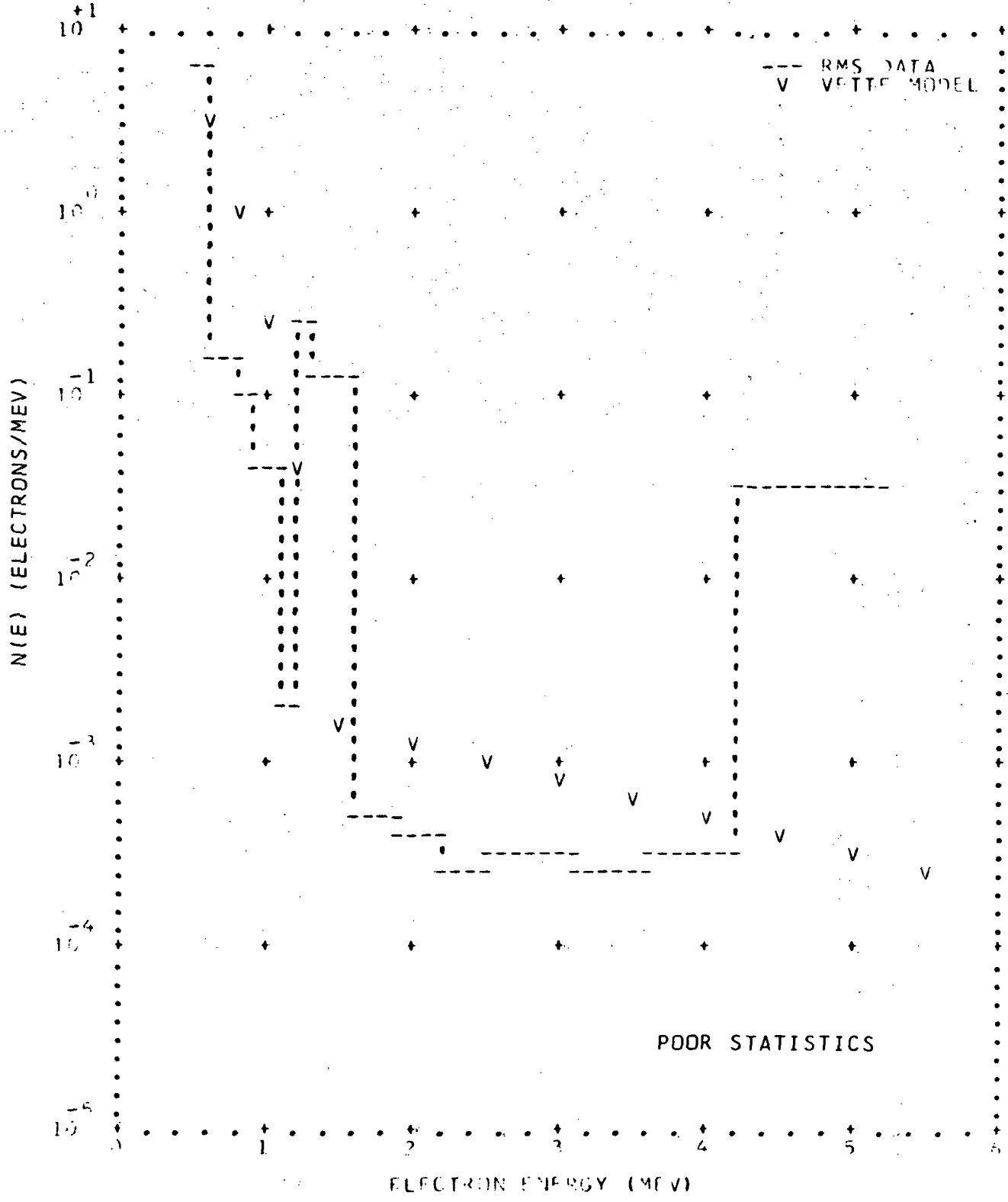

FIG. 4-17. RMS ELECTRON SPECTRA (CONT.)

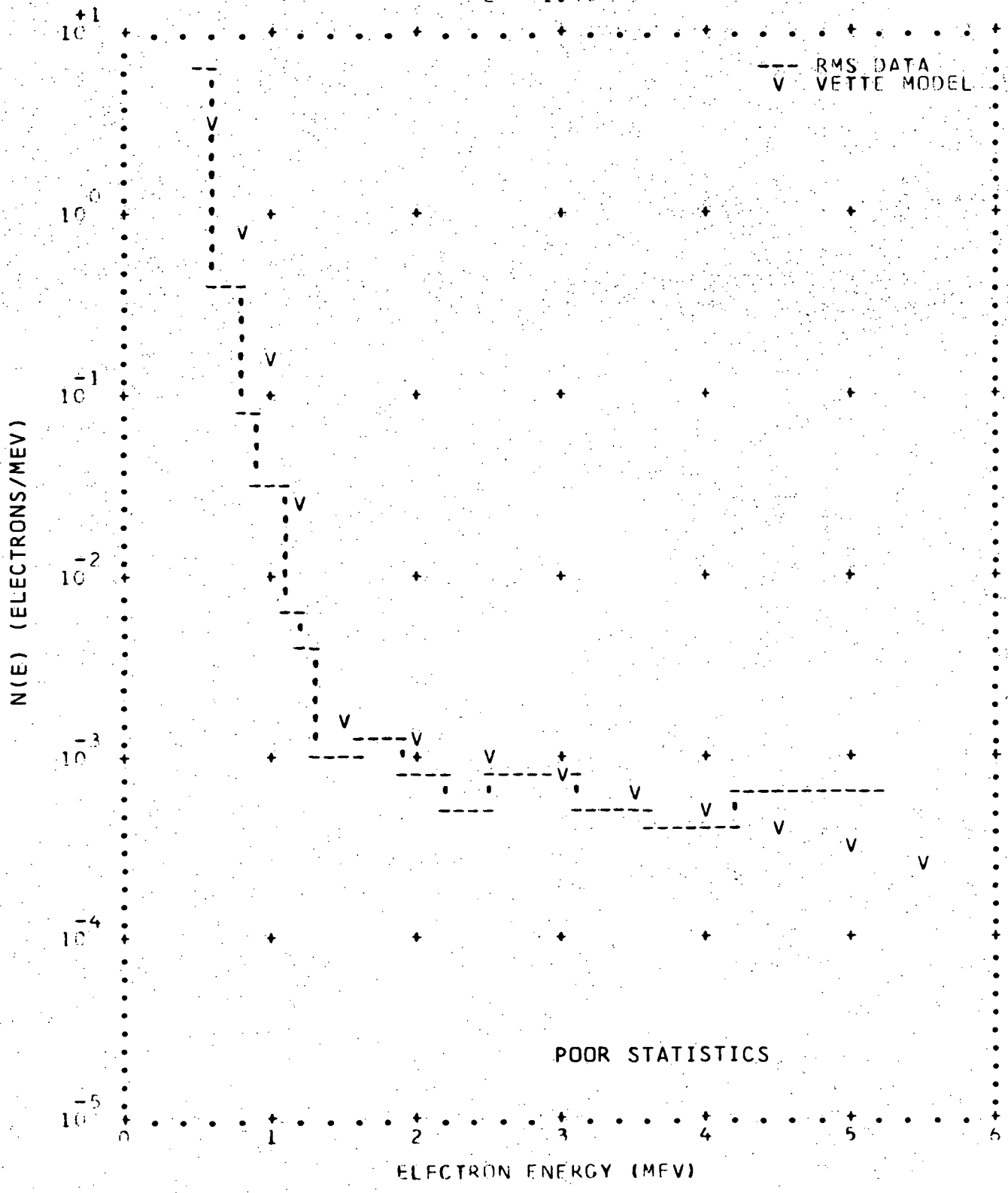

FIG. 4-17. RMS ELECTRON SPECTRA (CONT.)

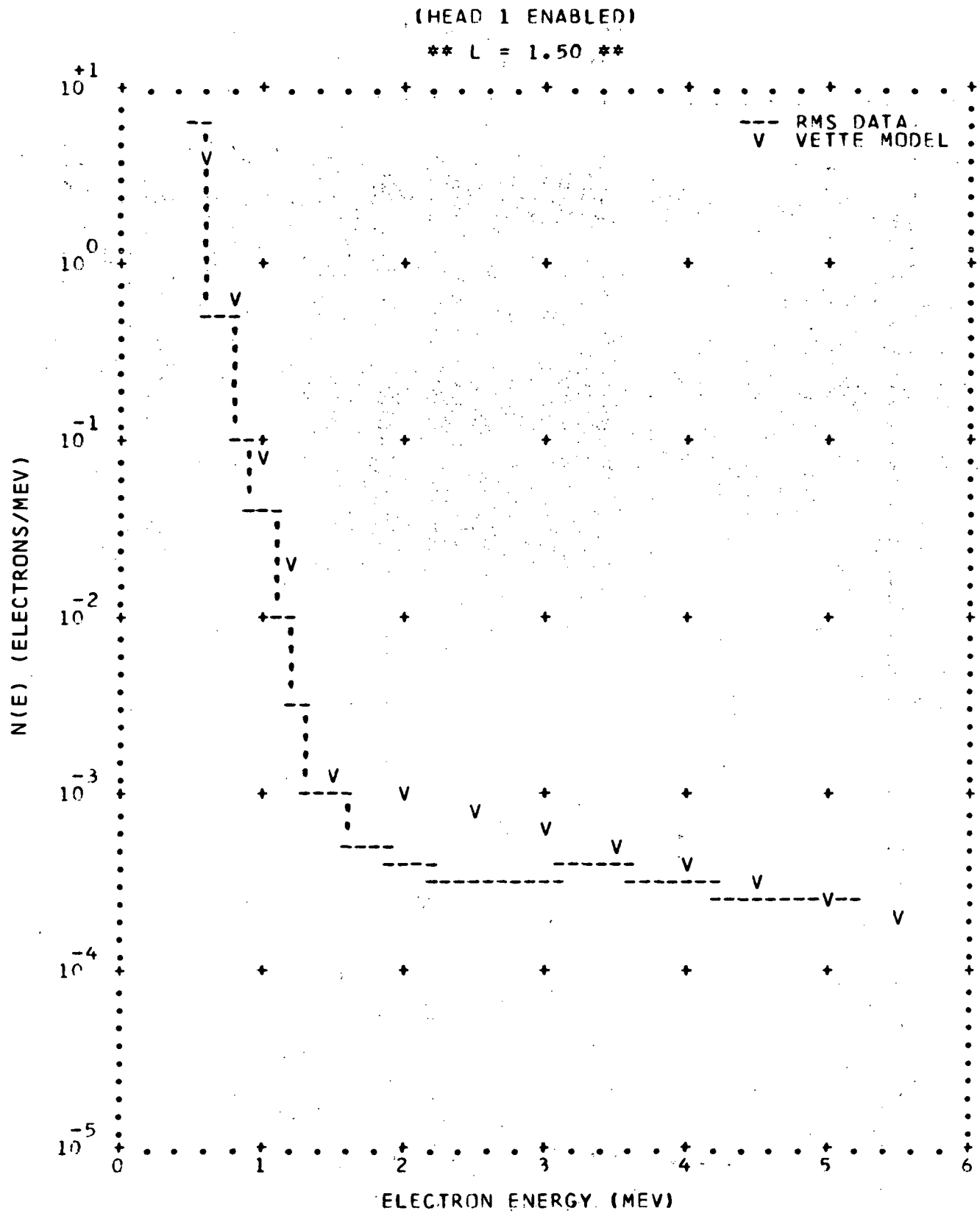

FIG. 4-17. RMS ELECTRON SPECTRA

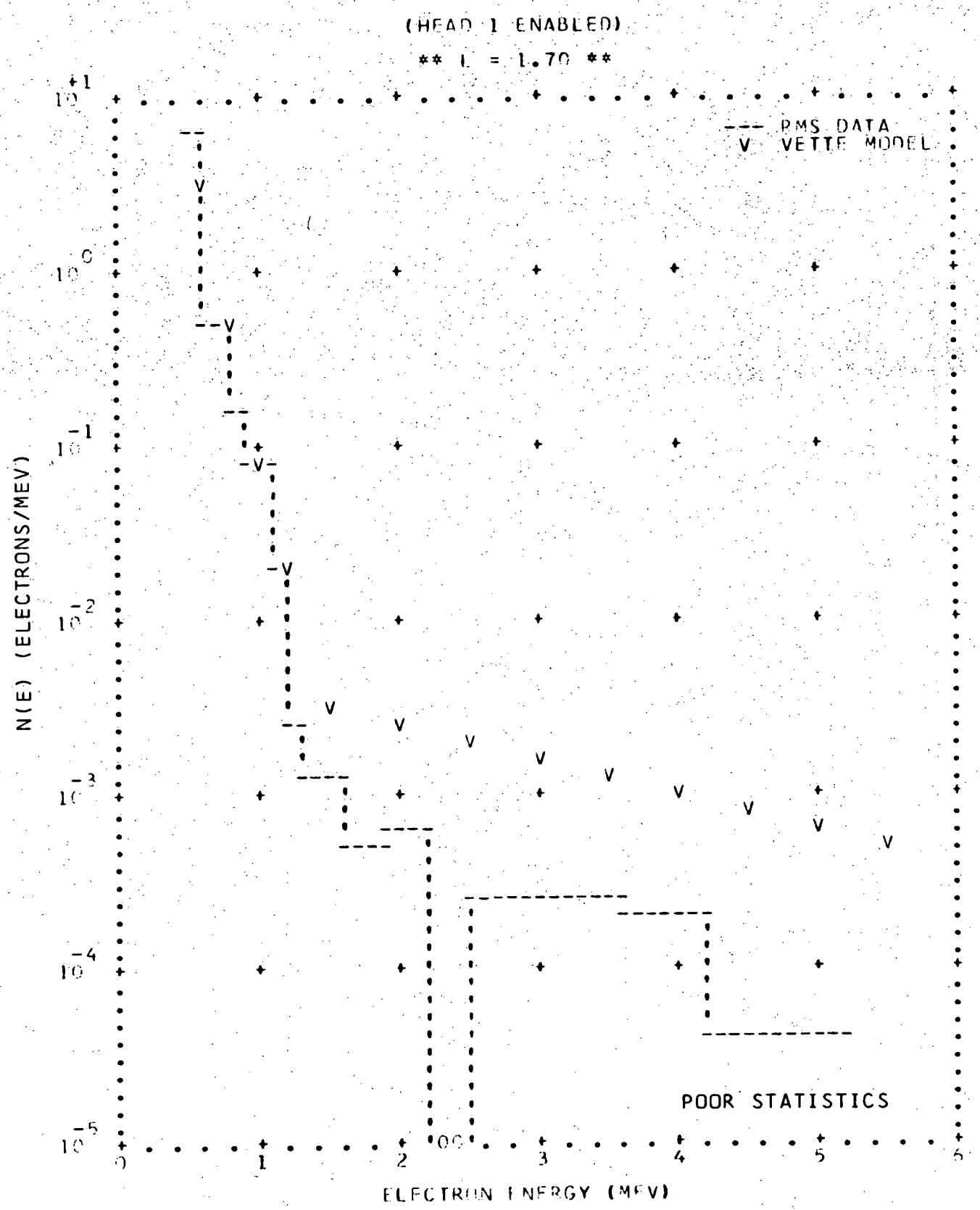

FIG. 4-18. RMS PROTON SPECTRA COMPARED TO VETTE MODEL AP6. BOTH SPECTRA ARE NORMALIZED TO ONE OVER THE REGION OF THE RMS DATA (11 TO 42 MEV)

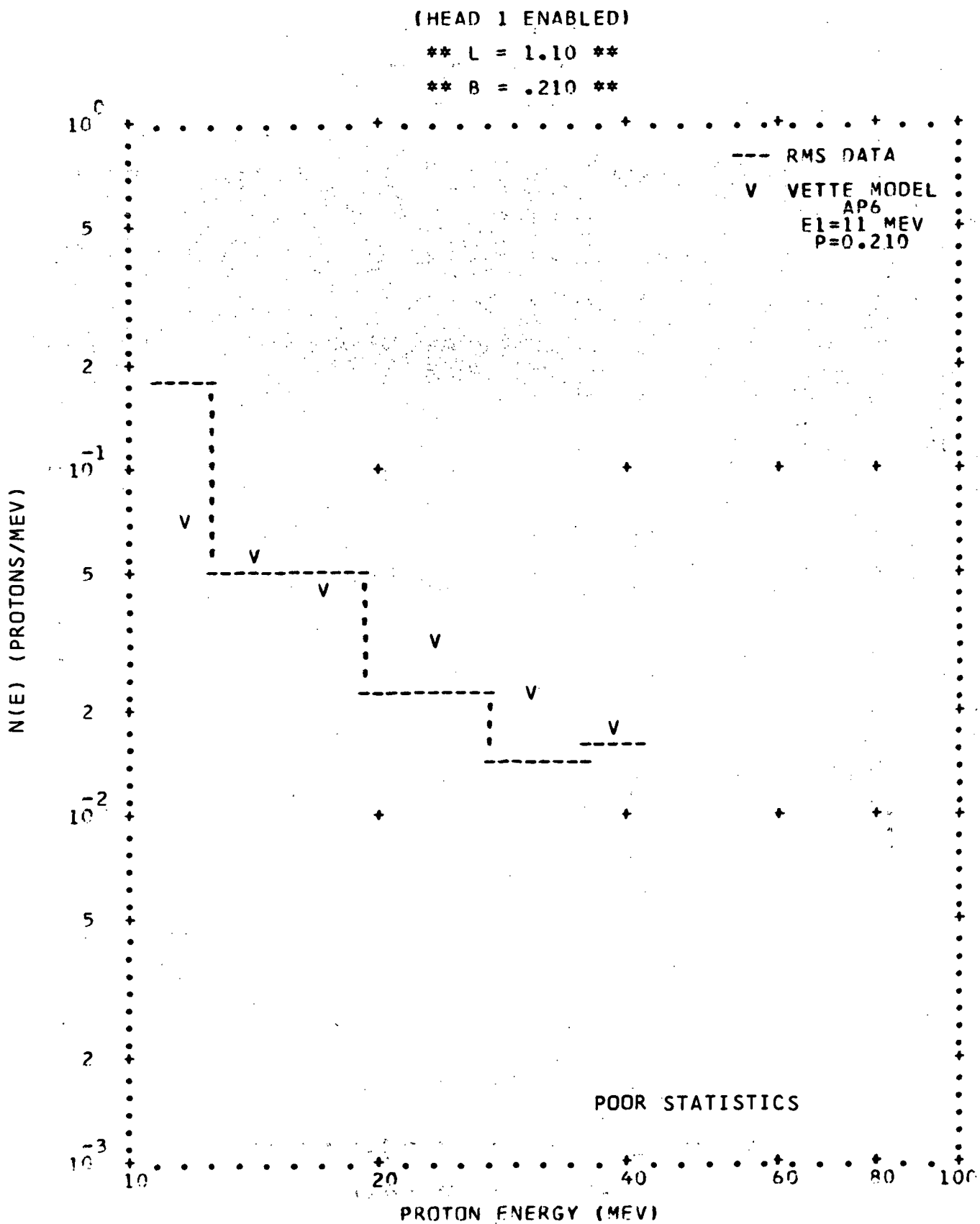

FIG. 4-18. RMS PROTON SPECTRA (CONT.)

(HEAD 1 ENABLED)

** L = 1.20 **

** B = .200 **

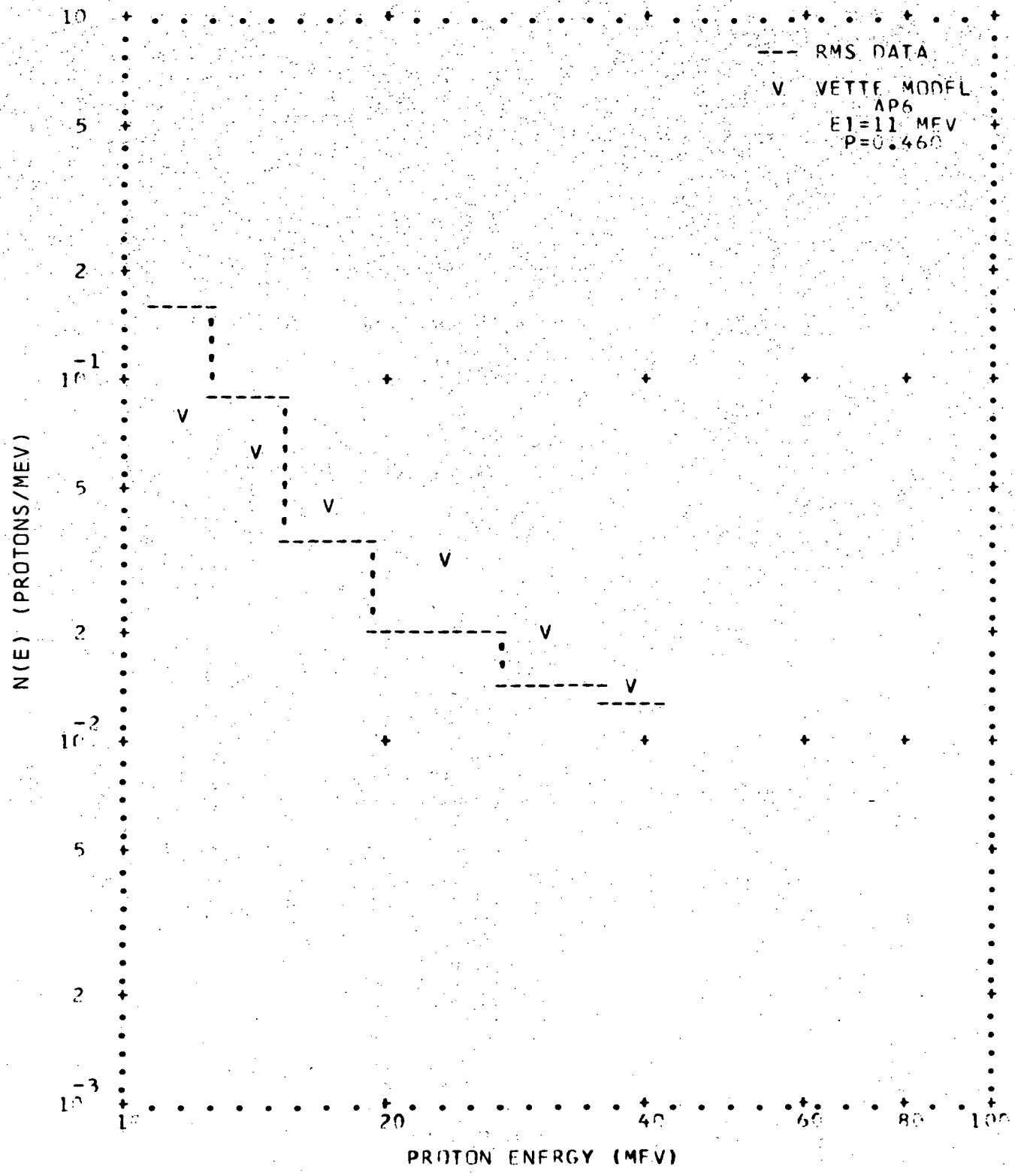

FIG. 4-18. RMS PROTON SPECTRA (CONT.)

(HEAD 1 ENABLED)

** L = 1.20 **

** B = .202 **

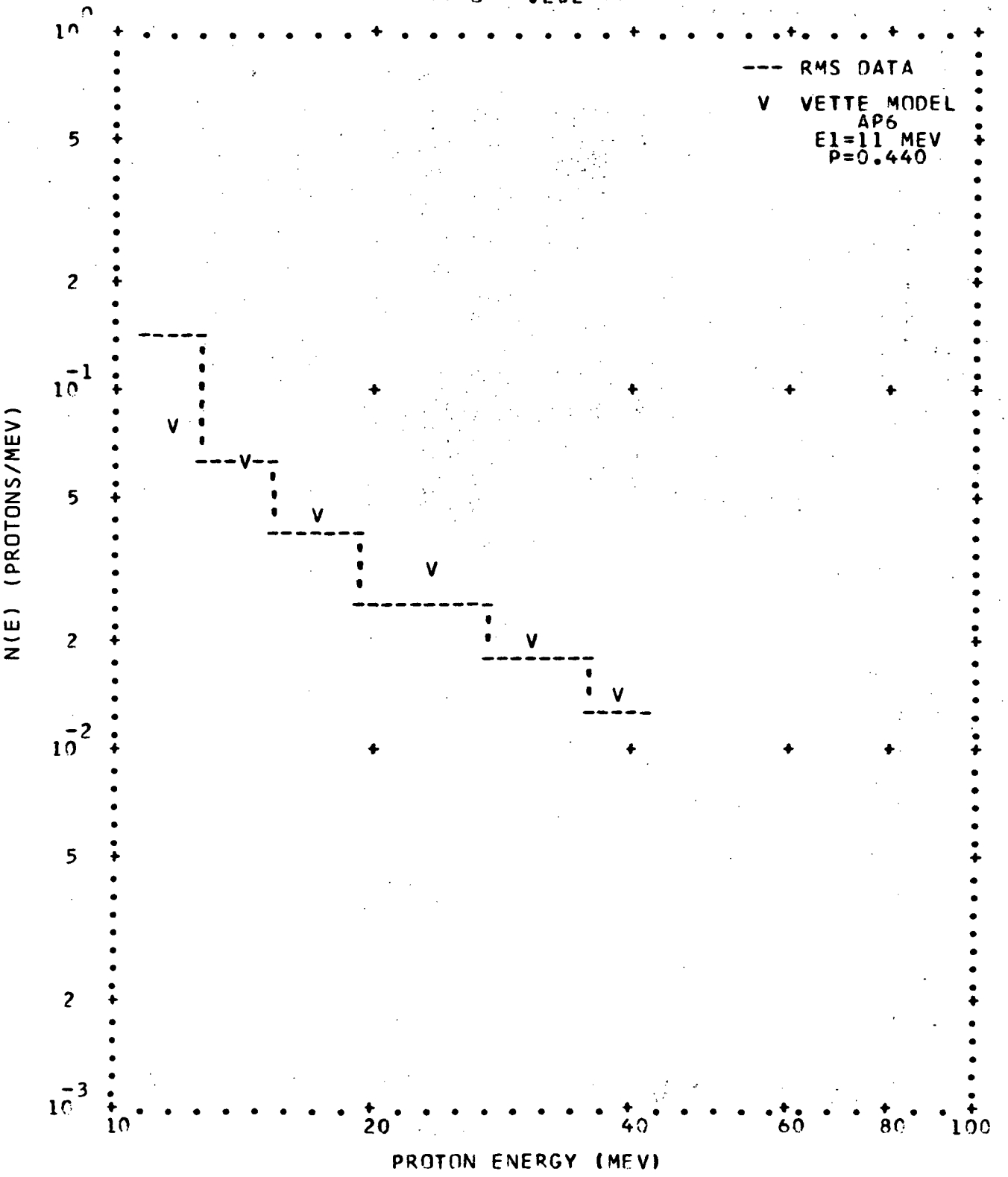

FIG. 4-18. RMS PROTON SPECTRA (CONT.)

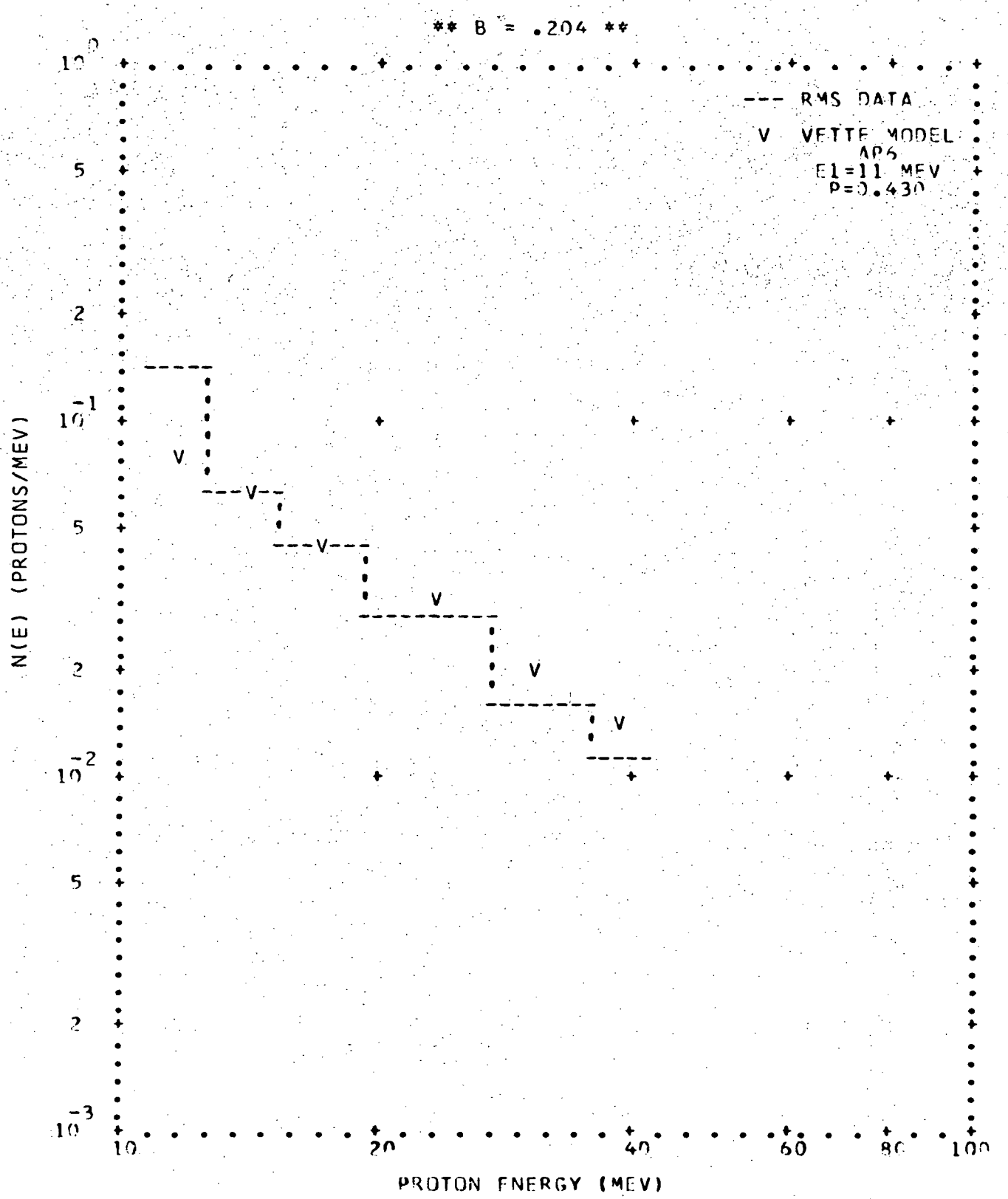

FIG. 4-18. RMS PROTON SPECTRA (CONT.)

(HEAD 1 ENABLED)

** L = 1.20 **

** B = .206 **

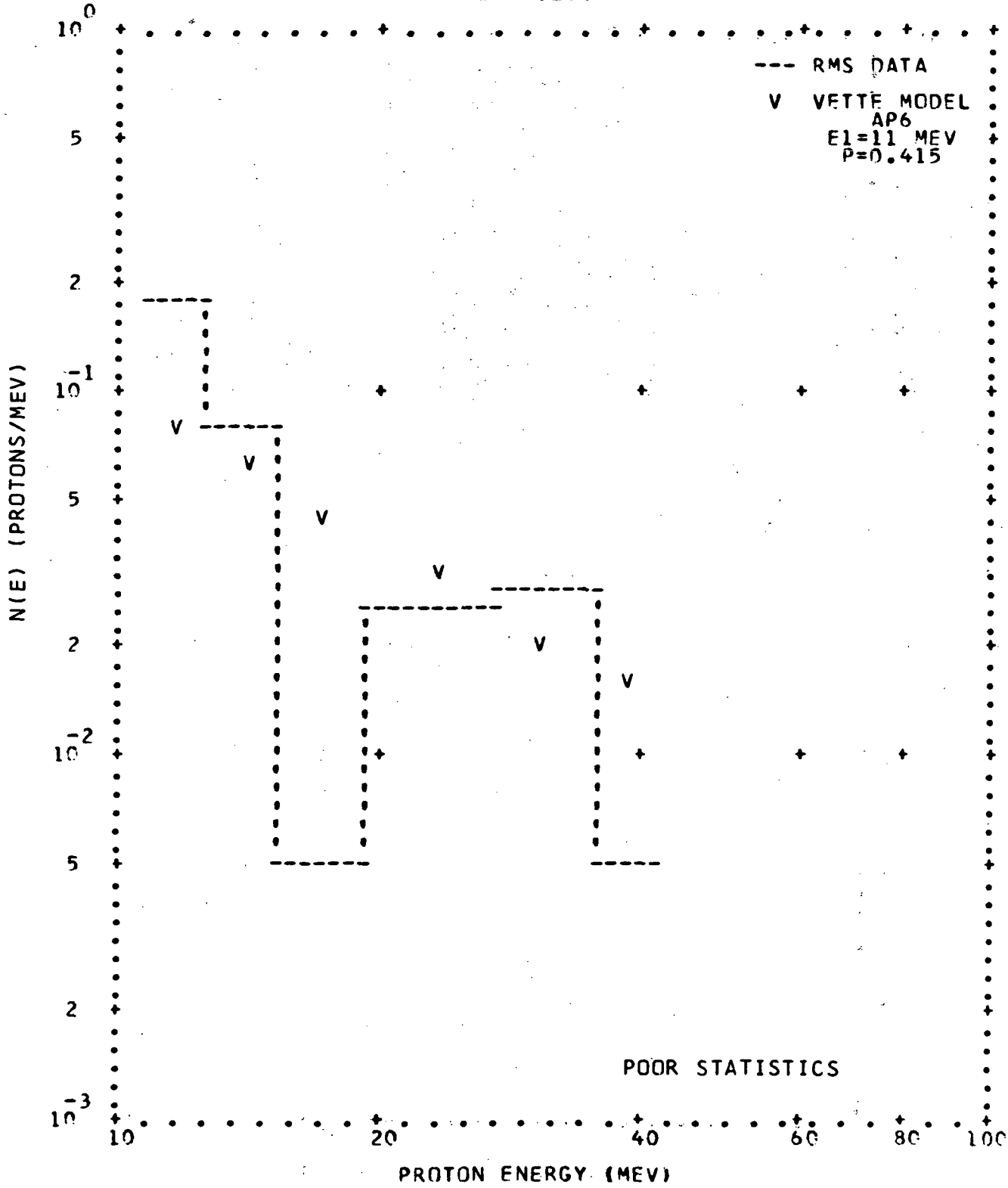

FIG. 4-18. RMS PROTON SPECTRA (CONT.)

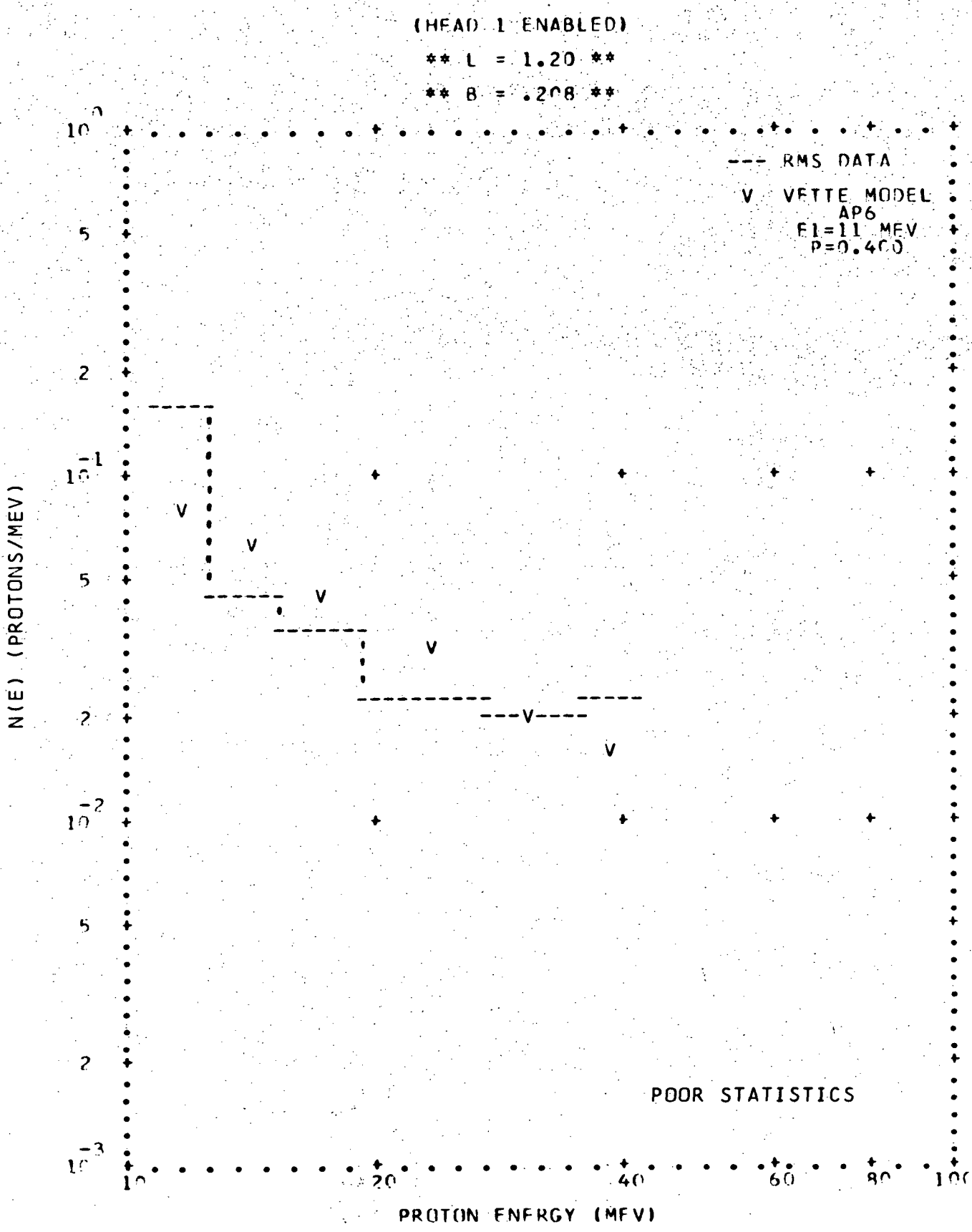

FIG. 4-18. RMS PROTON SPECTRA (CONT.)

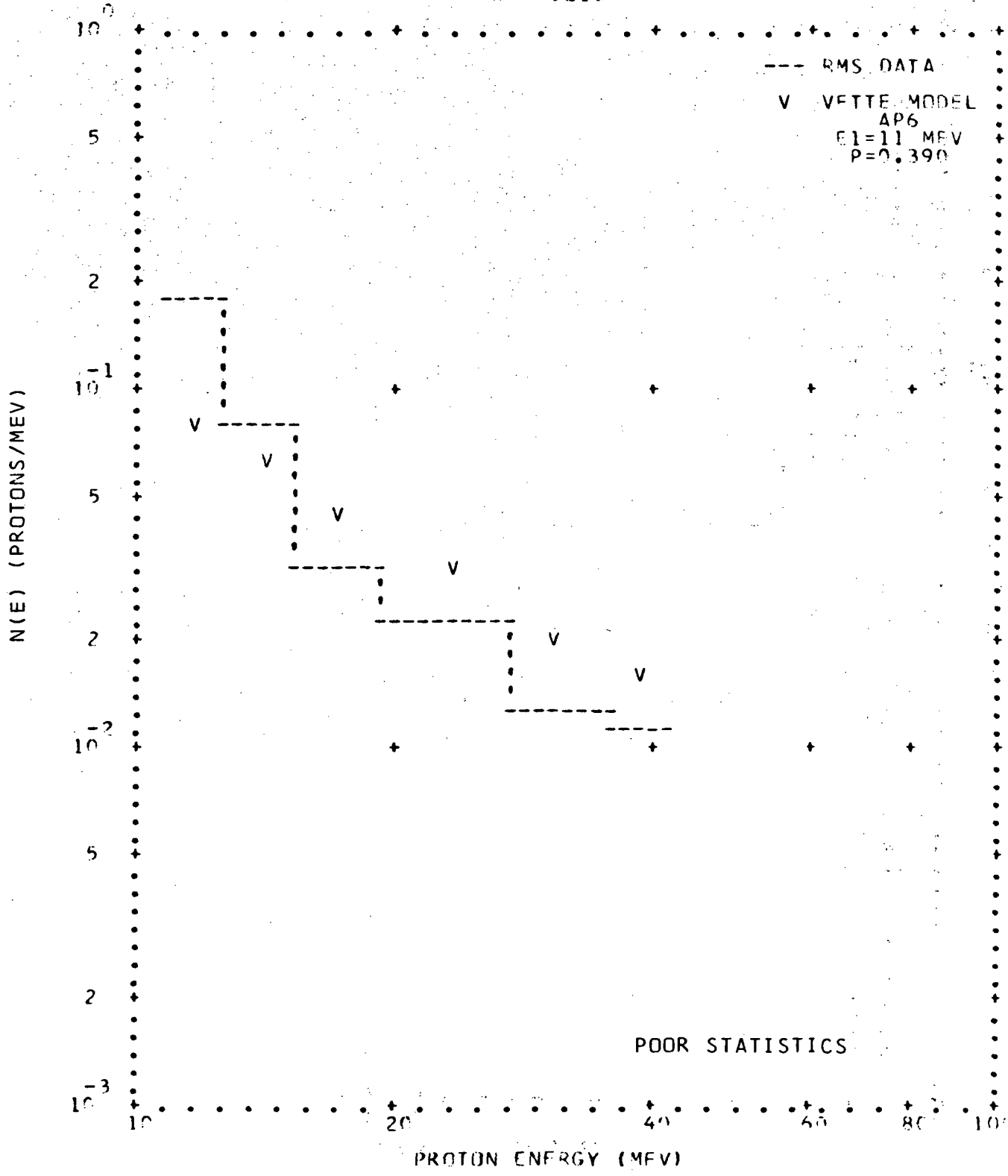

FIG. 4-18. RMS PROTON SPECTRA (CONT.)

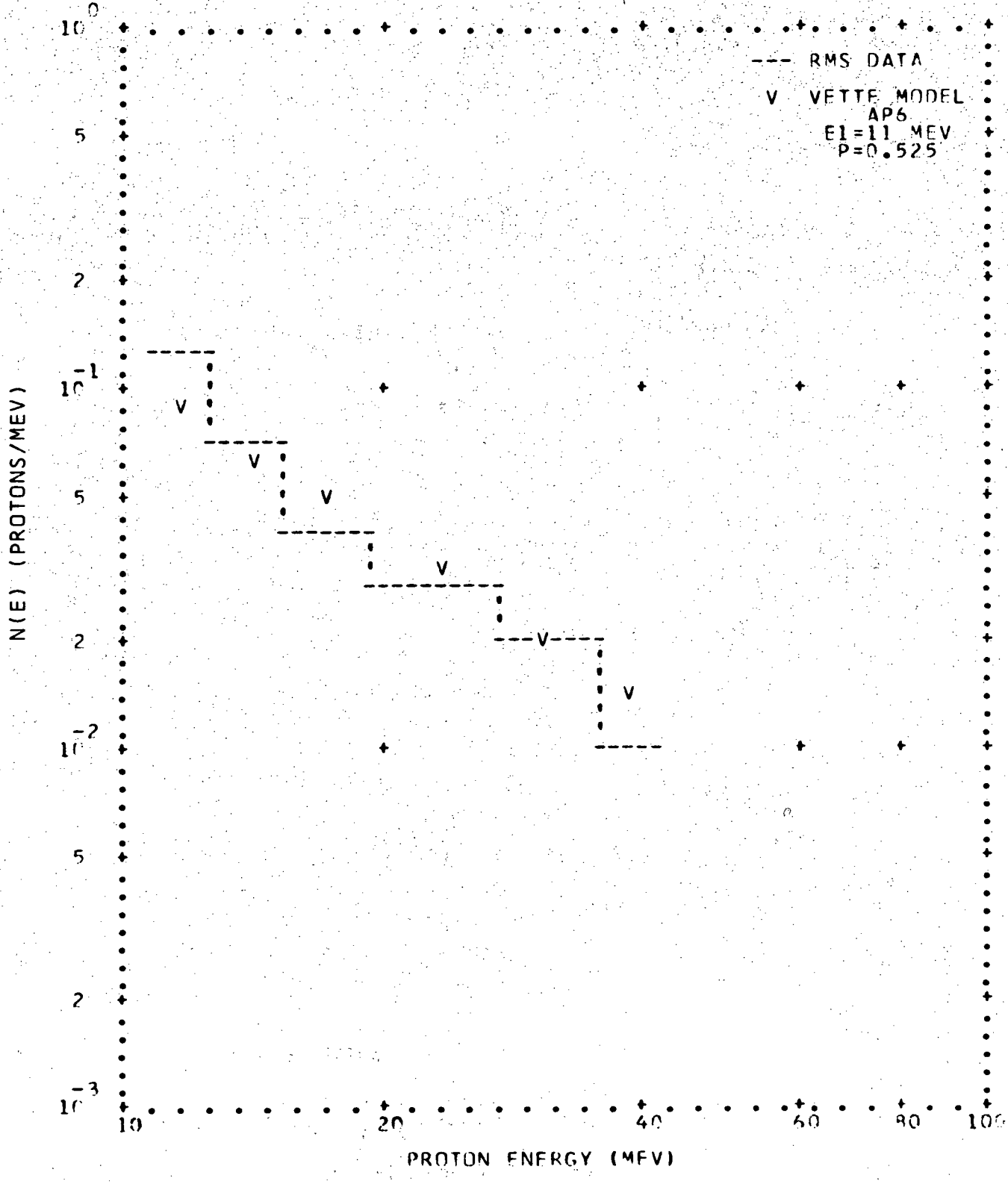

FIG. 4-18. RMS PROTON SPECTRA (CONT.)

(HEAD 1 ENABLED)

** L = 1.30 **

** B = .205 **

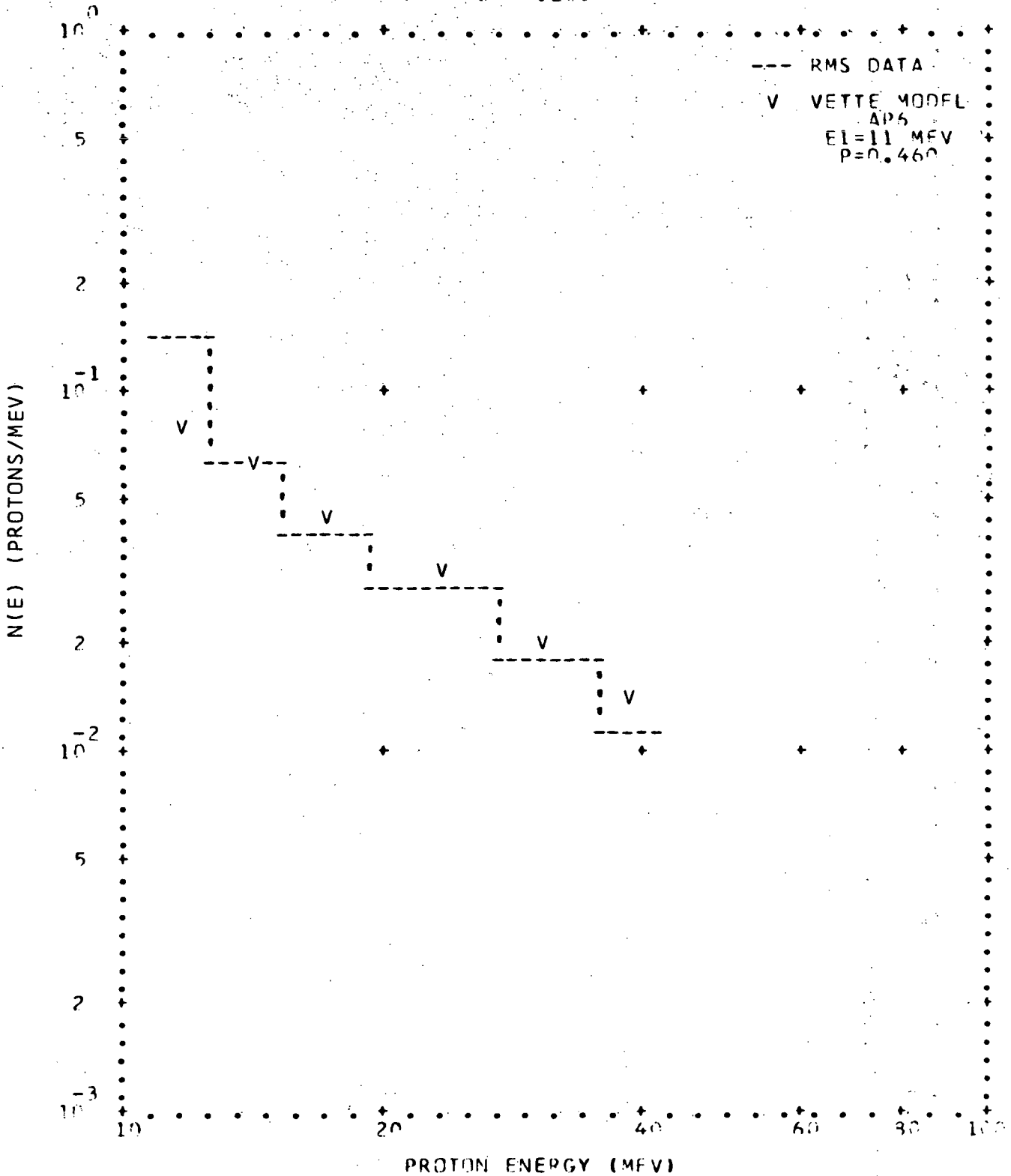

FIG. 4-18. RMS PROTON SPECTRA (CONT.)

(HEAD 1 ENABLED)

** L = 1.30 **

** B = .210 **

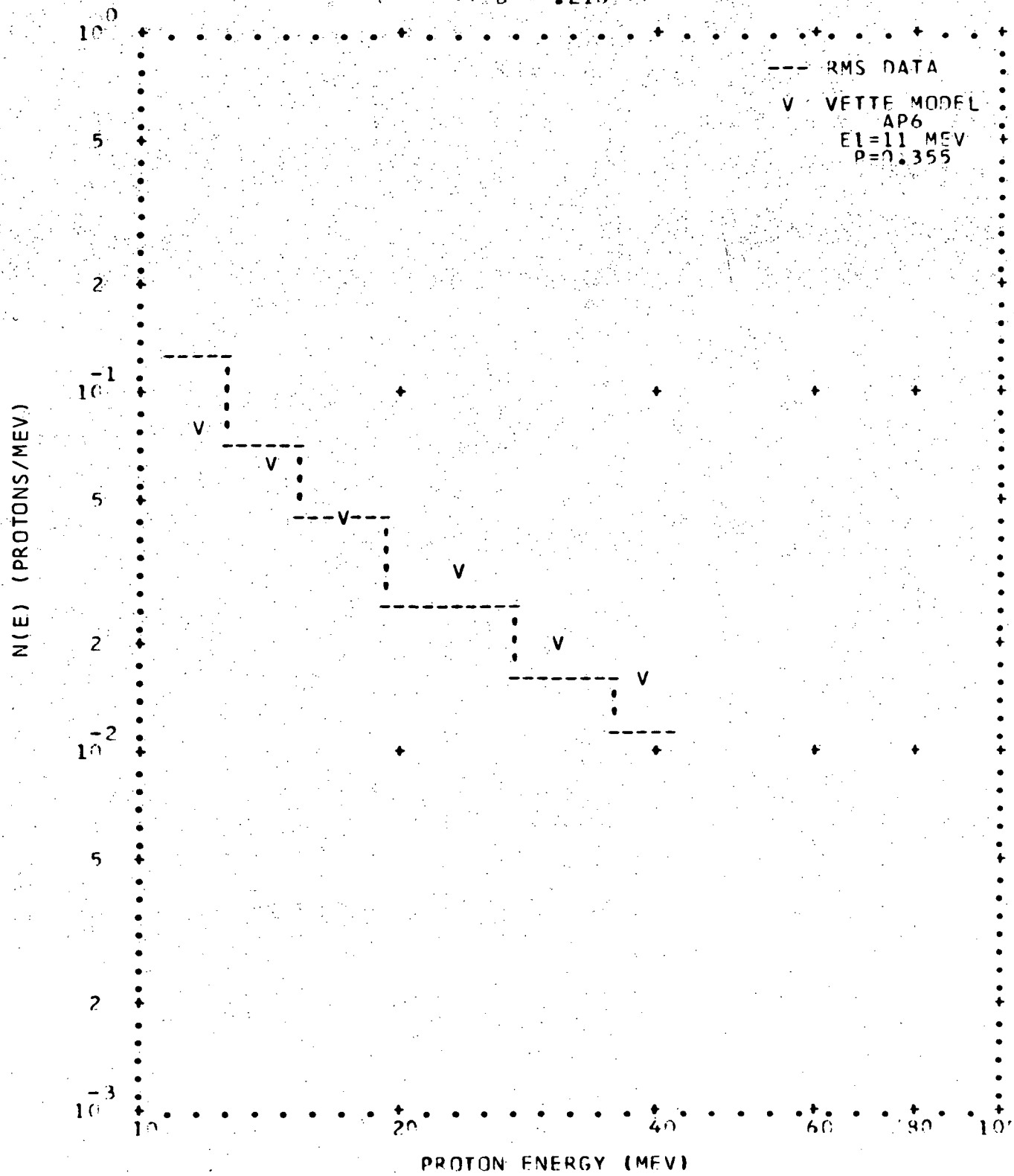

FIG. 4-18. RMS PROTON SPECTRA (CONT.)

(HEAD 1 ENABLED)

** L = 1.30 **

** B = .212 **

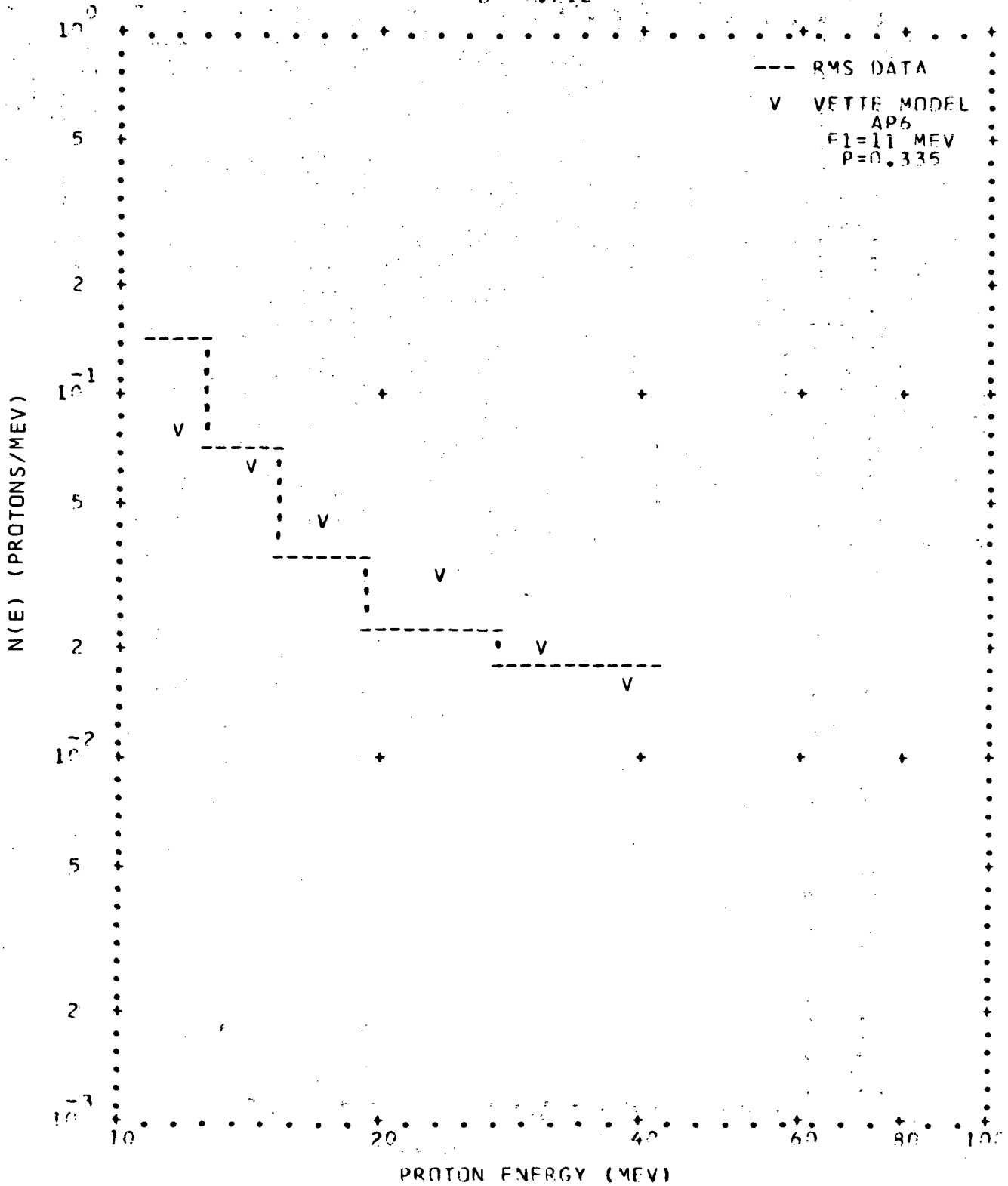

FIG. 4-18. RMS PROTON SPECTRA (CONT.)

(HEAD 1 ENABLED)

** L = 1.30 **

** B = .214 **

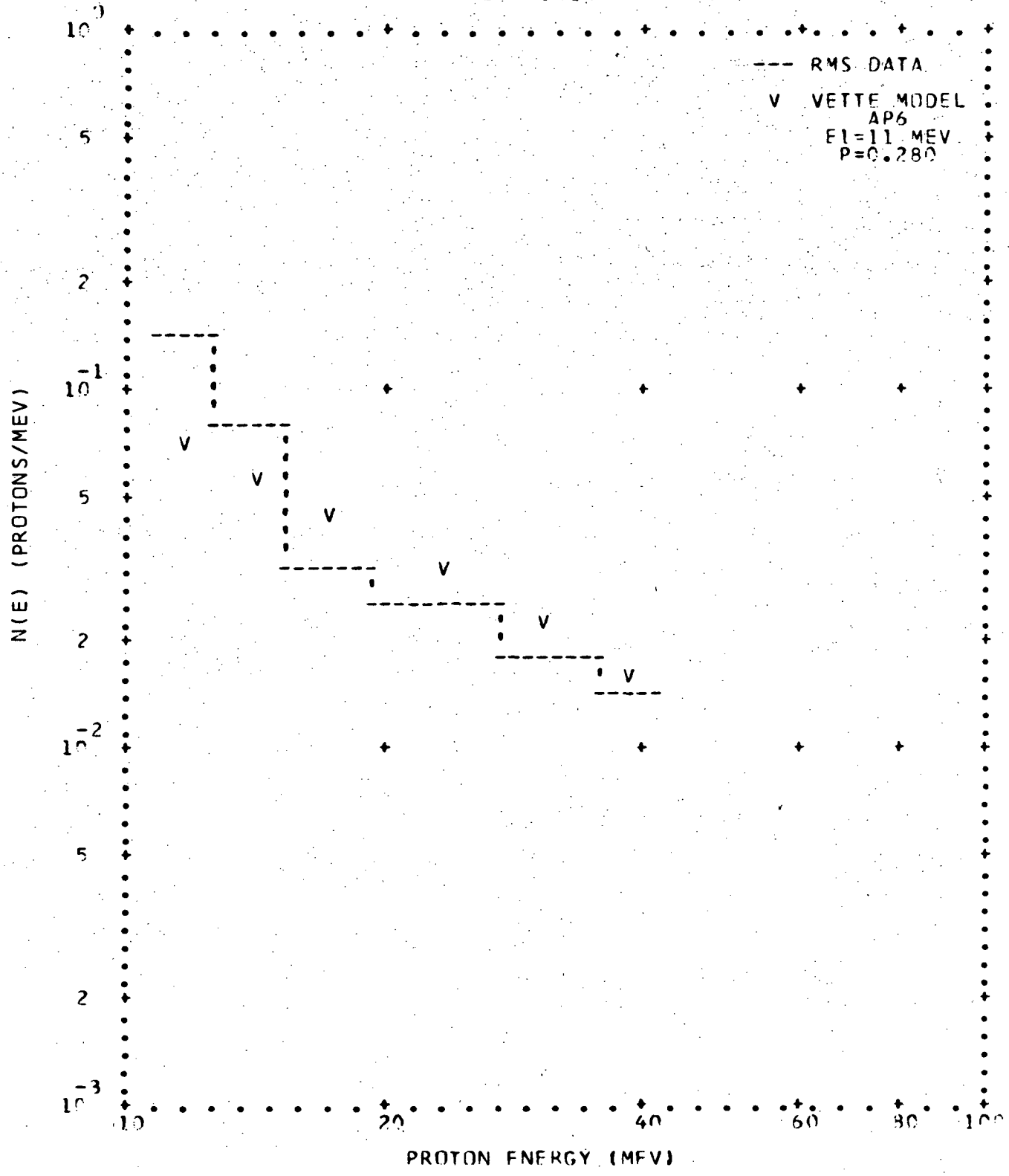

FIG. 4-18. RMS PROTON SPECTRA (CONT.)

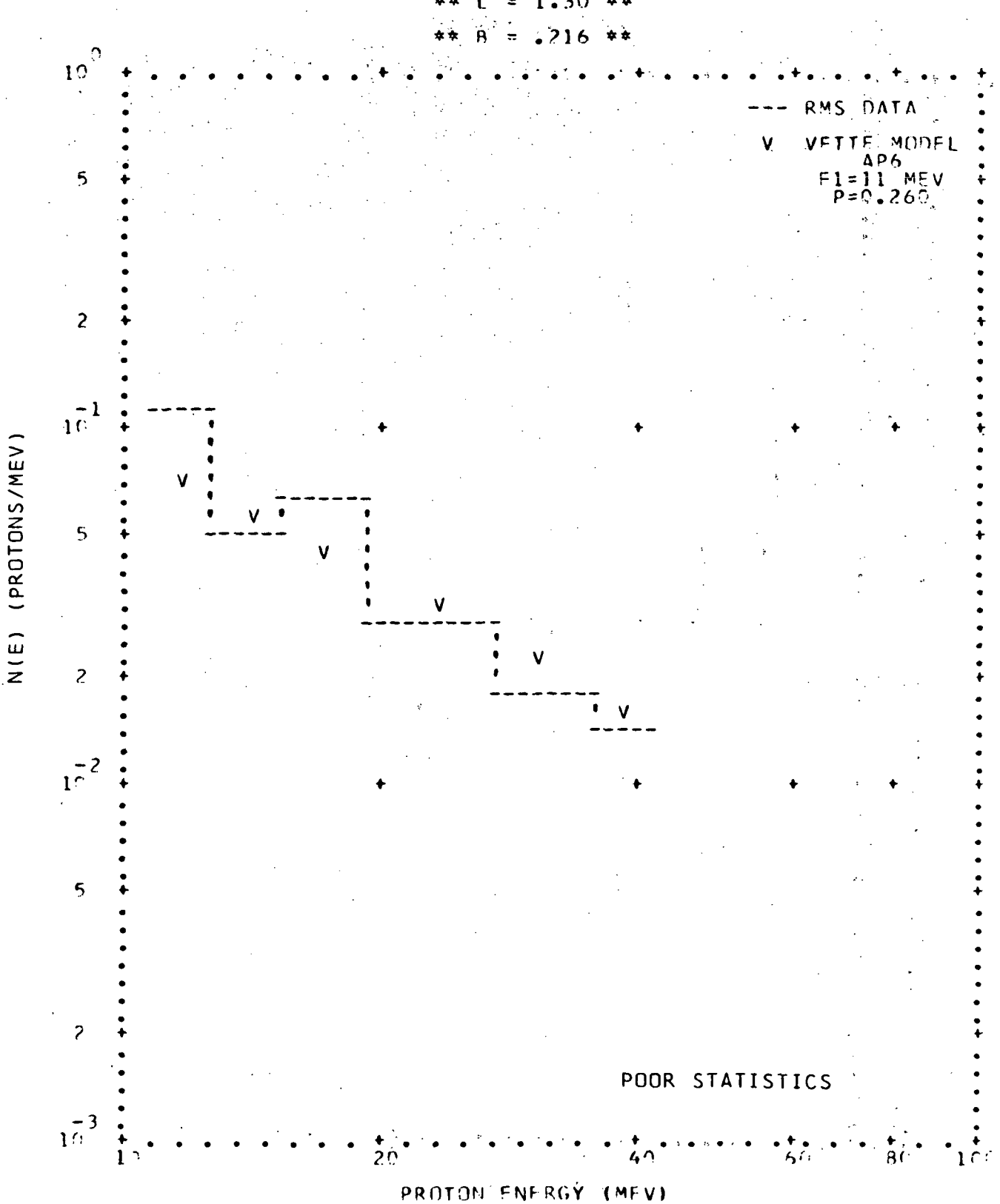

FIG. 4-18. RMS PROTON SPECTRA (CONT.)

(HEAD 1 ENABLED)

** L = 1.30 **

** B = .218 **

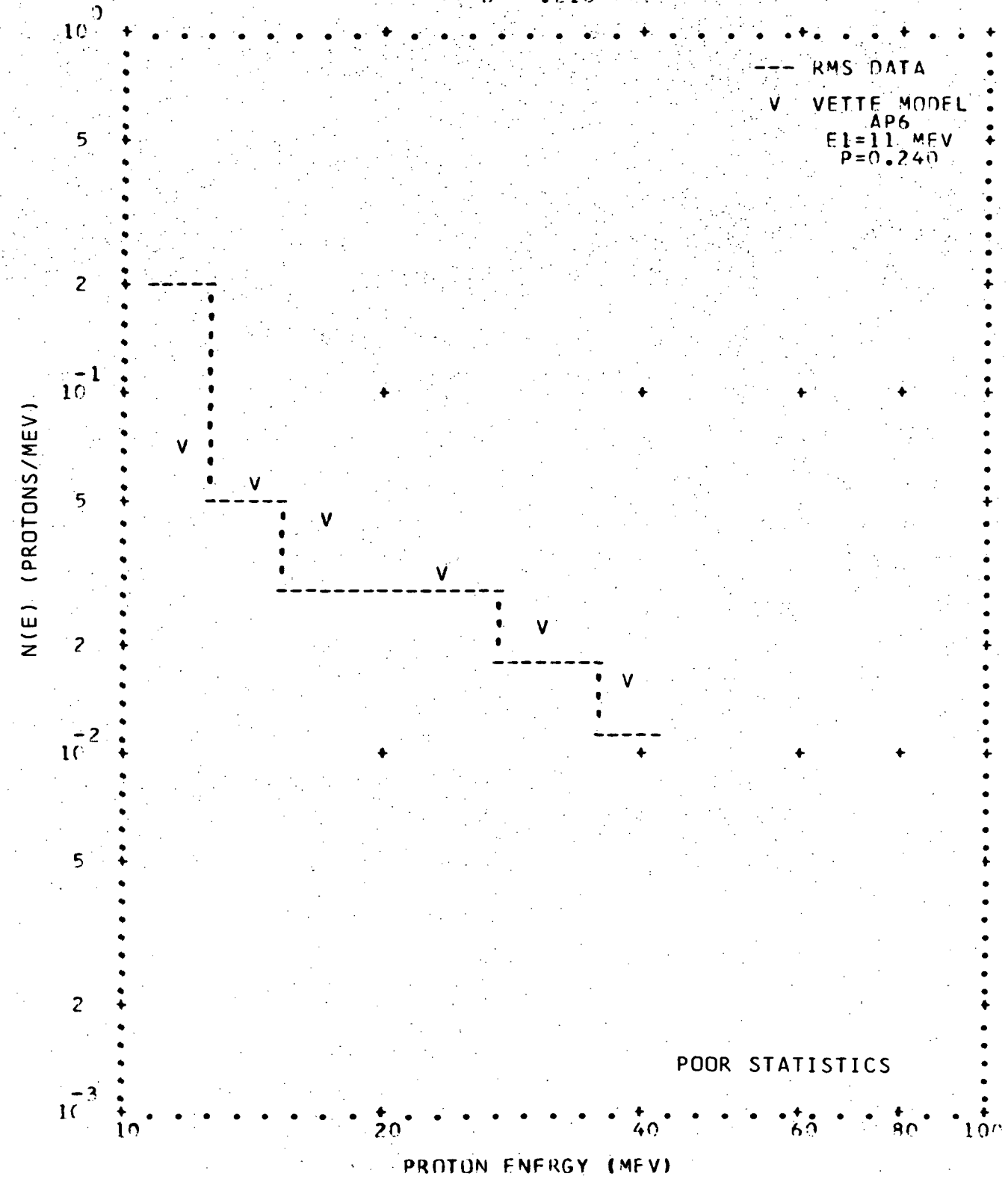

FIG. 4-18. RMS PROTON SPECTRA (CONT.)

(HEAD 1 ENABLED)

** L = 1.30 **

** B = .220 **

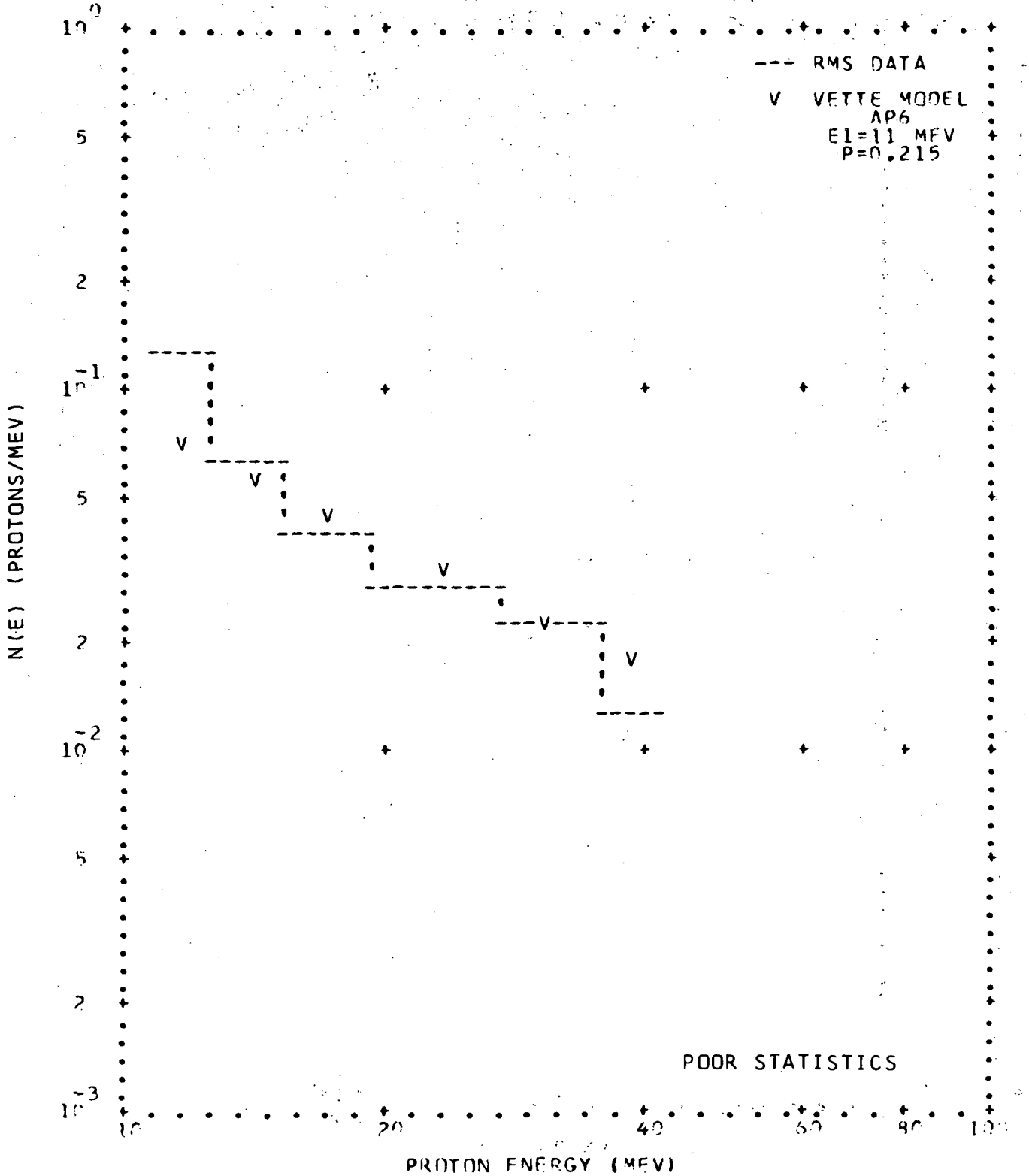

FIG. 4-18. RMS PROTON SPECTRA (CONT.)

(HEAD 1 ENABLED)

** L = 1.40 **

** B = .210 **

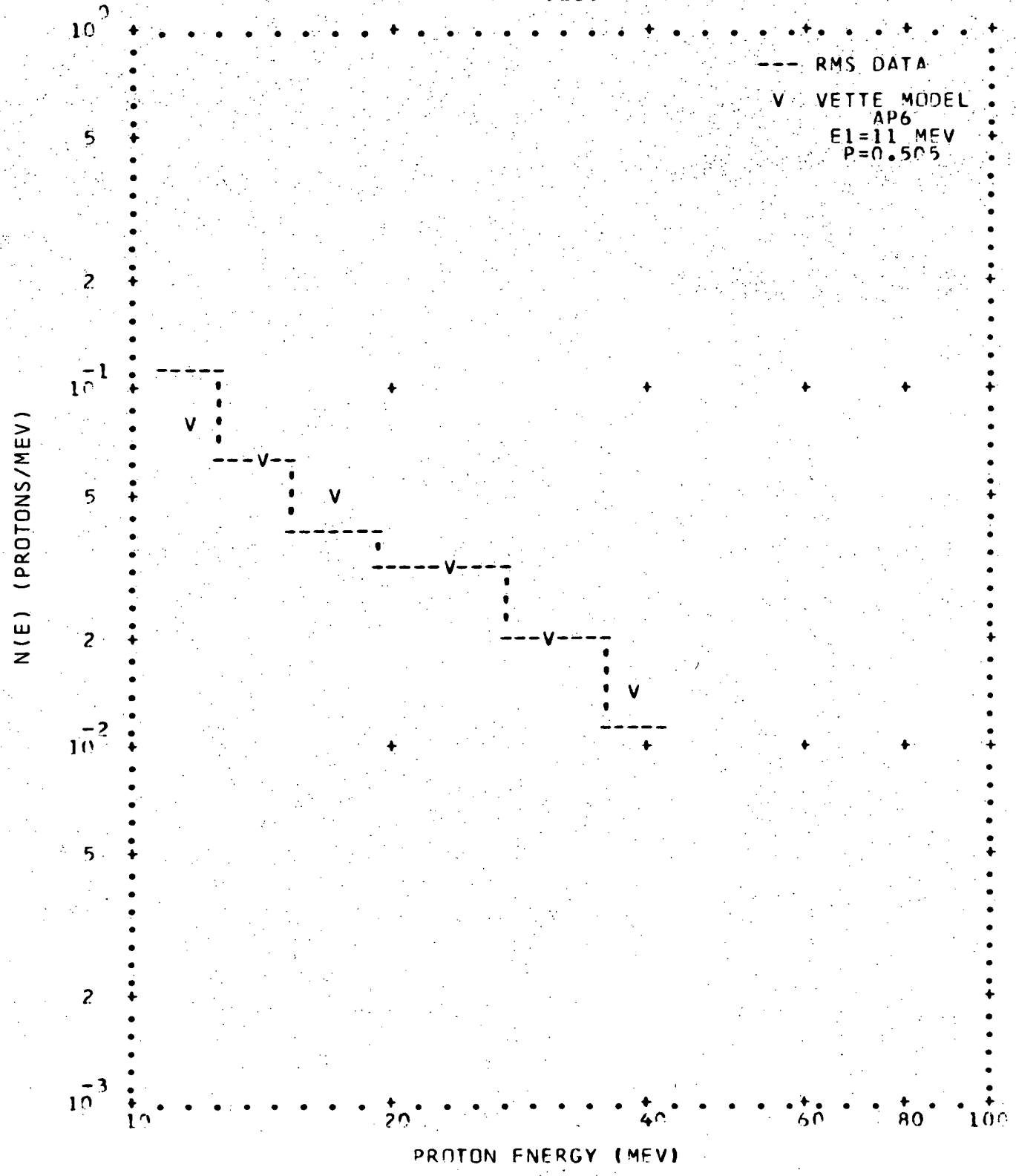

FIG. 4-18. RMS PROTON SPECTRA (CONT.)

(HEAD 1 ENABLED)

** L = 1.40 **

** B = .215 **

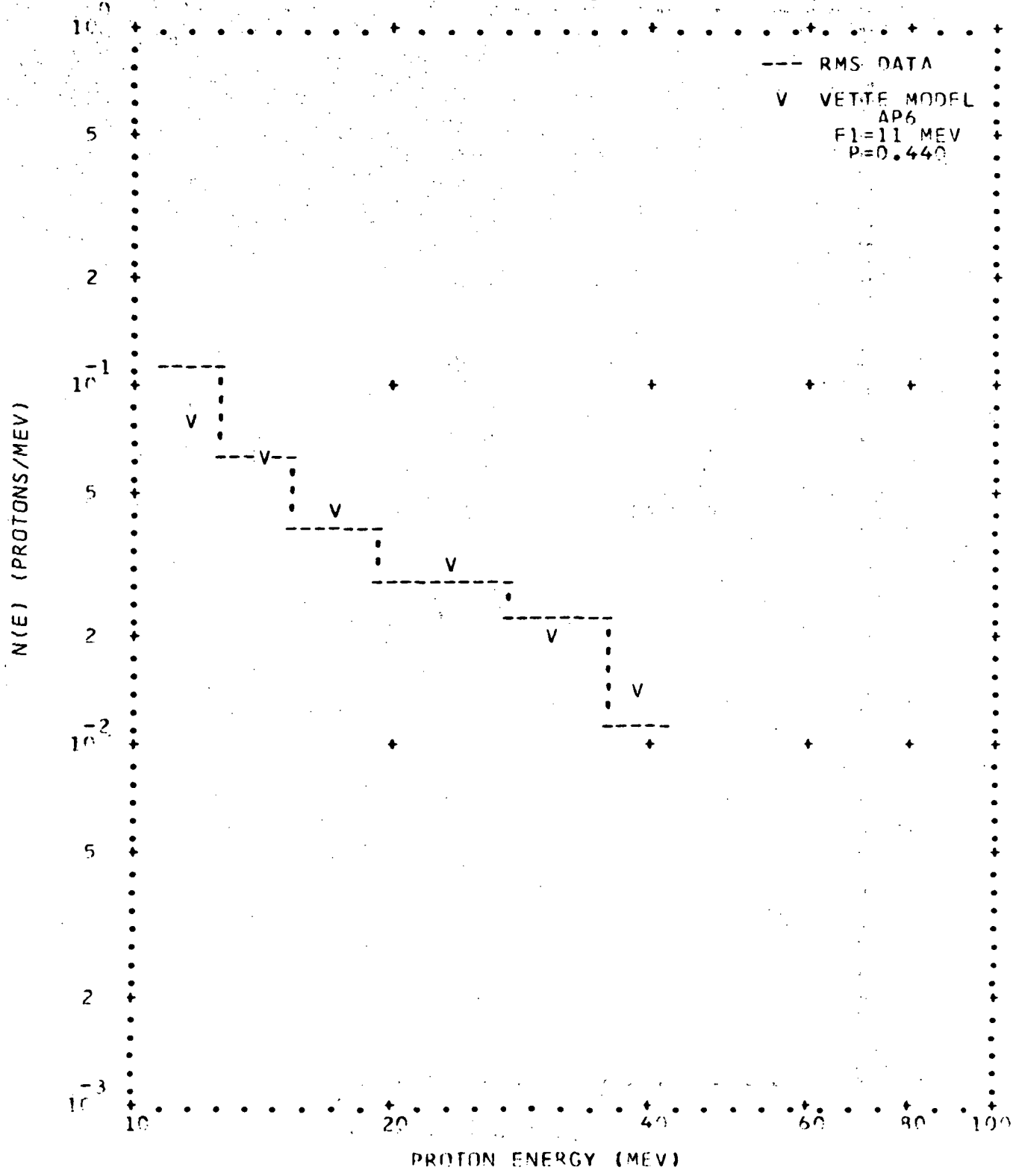

FIG. 4-18. RMS PROTON SPECTRA (CONT.)

(HEAD 1 ENABLED)

** L = 1.40 **

** B = .220 **

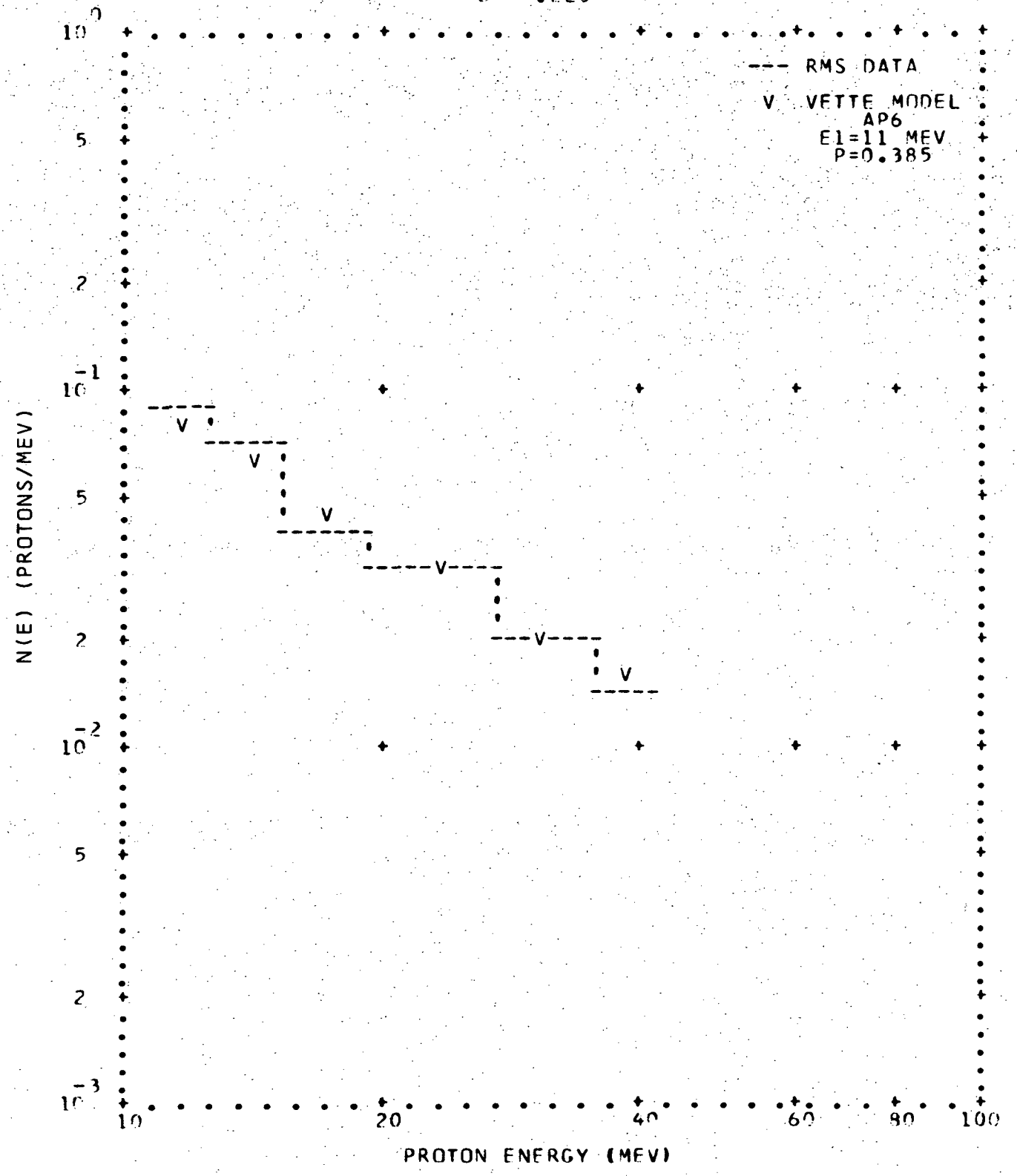

FIG. 4-18. RMS PROTON SPECTRA (CONT.)

(HEAD 1 ENABLED)

** L = 1.40 **

** B = .225 **

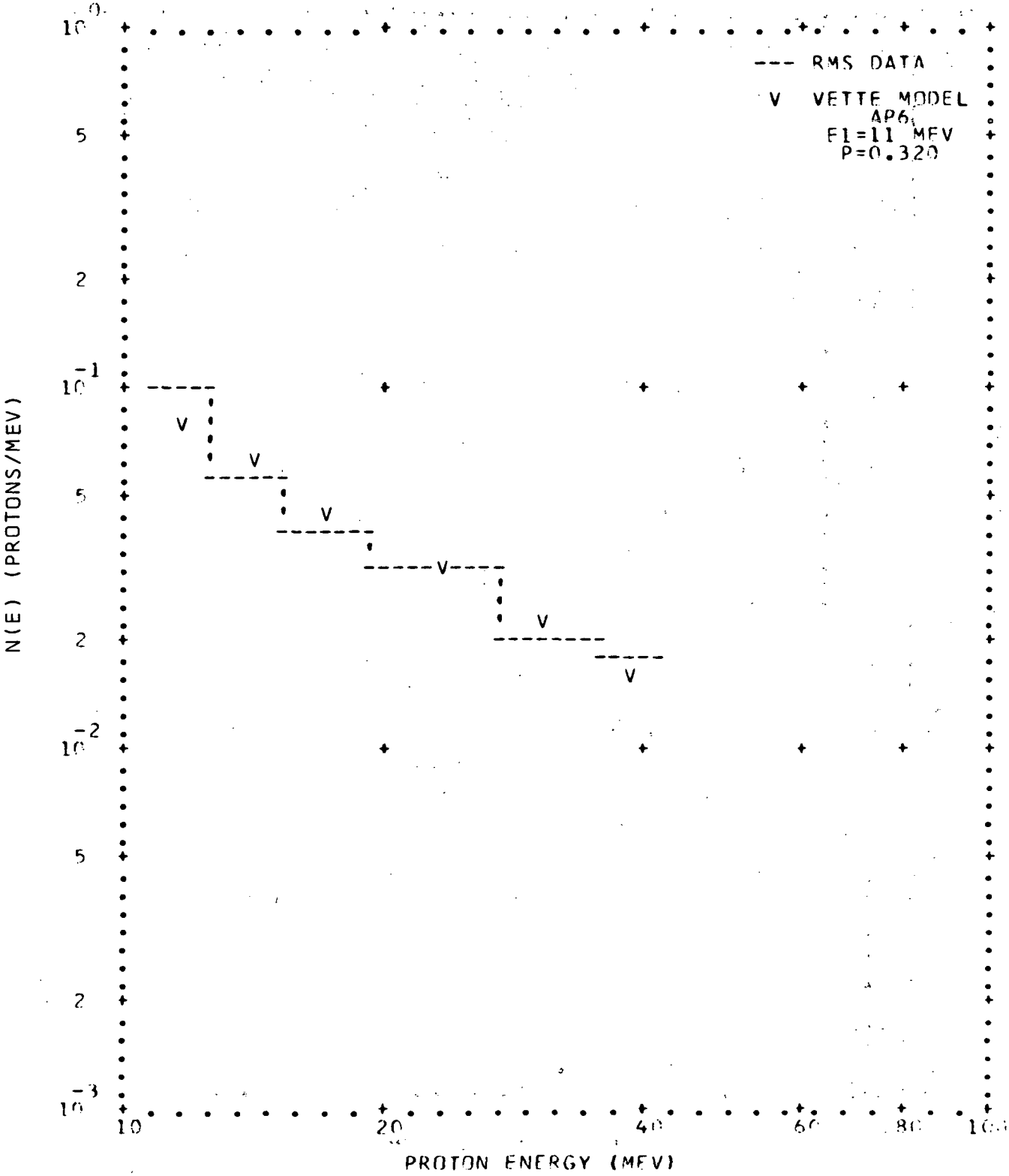

FIG. 4-18. RMS PROTON SPECTRA (CONT.)

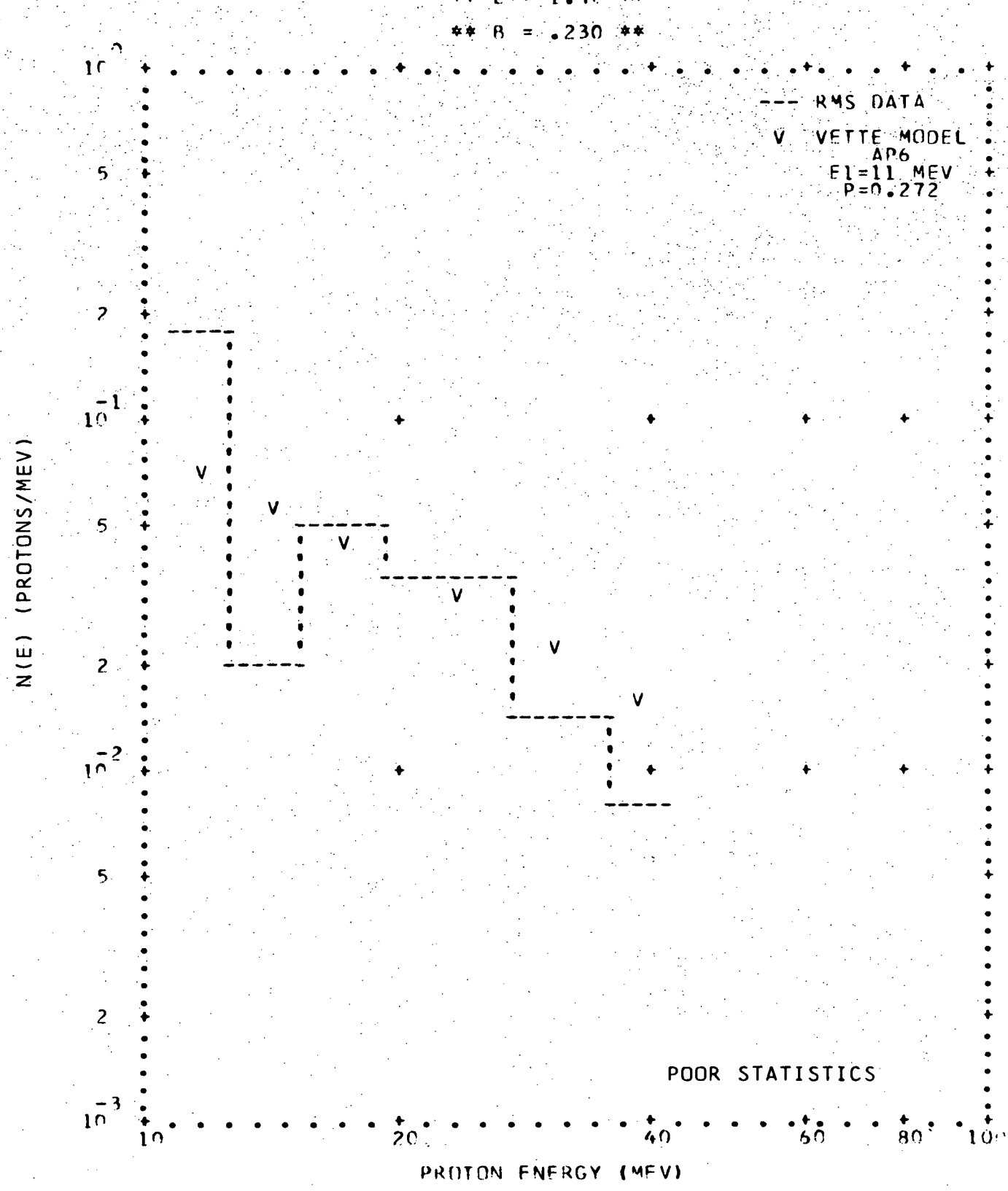

FIG. 4-18. RMS PROTON SPECTRA (CONT.)

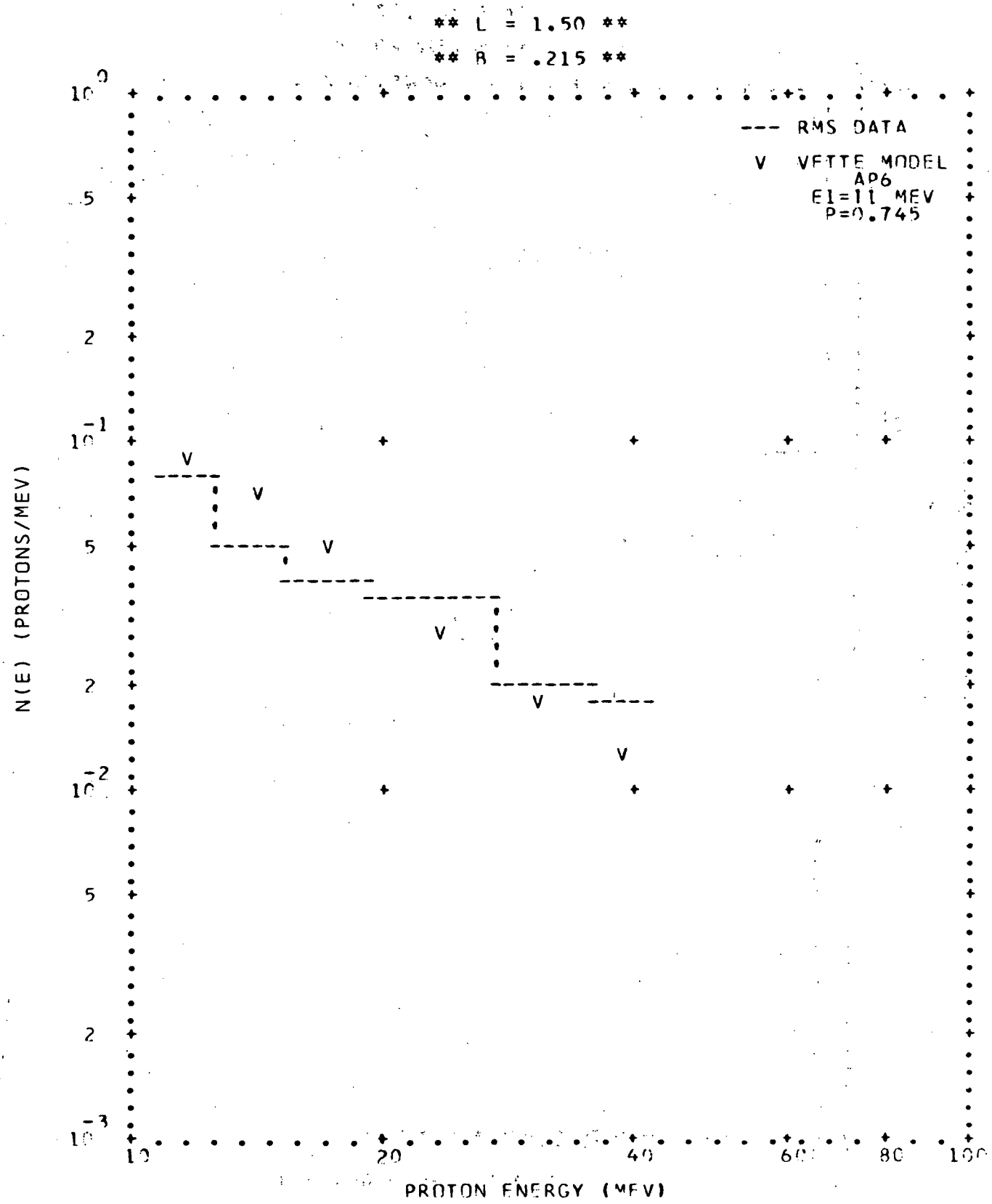

FIG. 4-18. RMS PROTON SPECTRA (CONT.)

(HEAD 1 ENABLED)

** L = 1.50 **

** B = .220 **

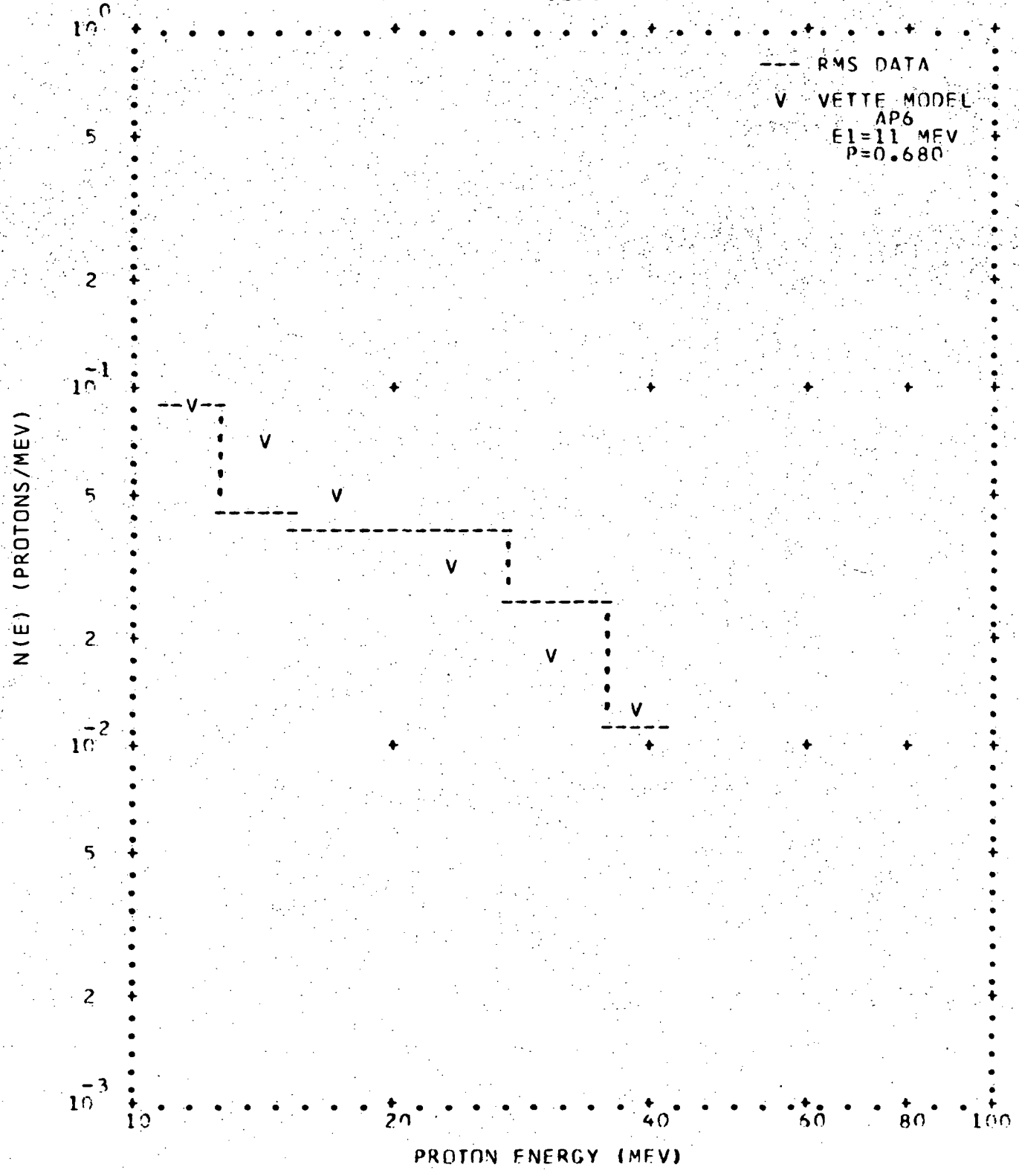

FIG. 4-18. RMS PROTON SPECTRA (CONT.)

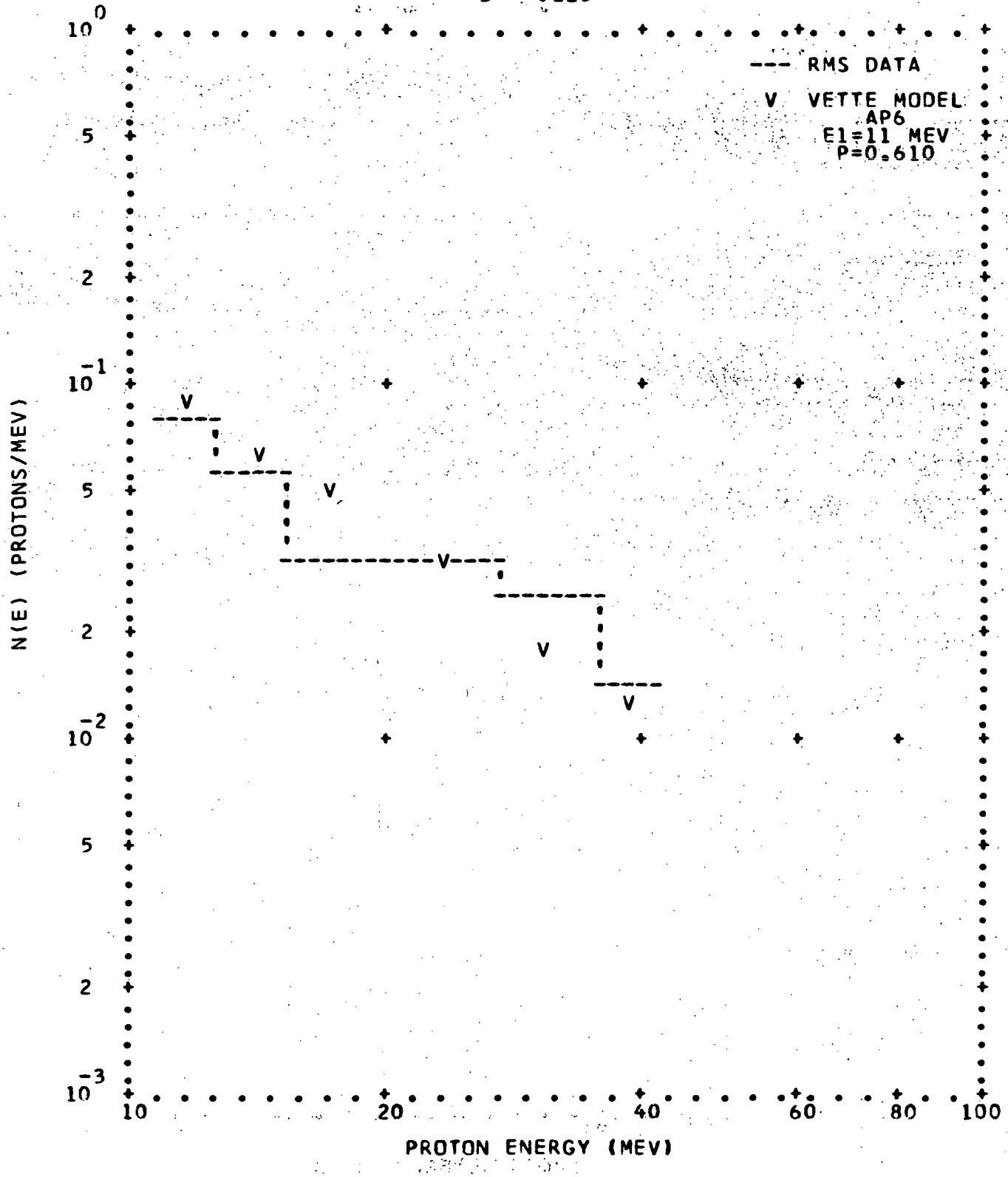

FIG. 4-18. RMS PROTON SPECTRA (CONT.)

(HEAD 1 ENABLED)

** L = 1.50 **

** B = .230 **

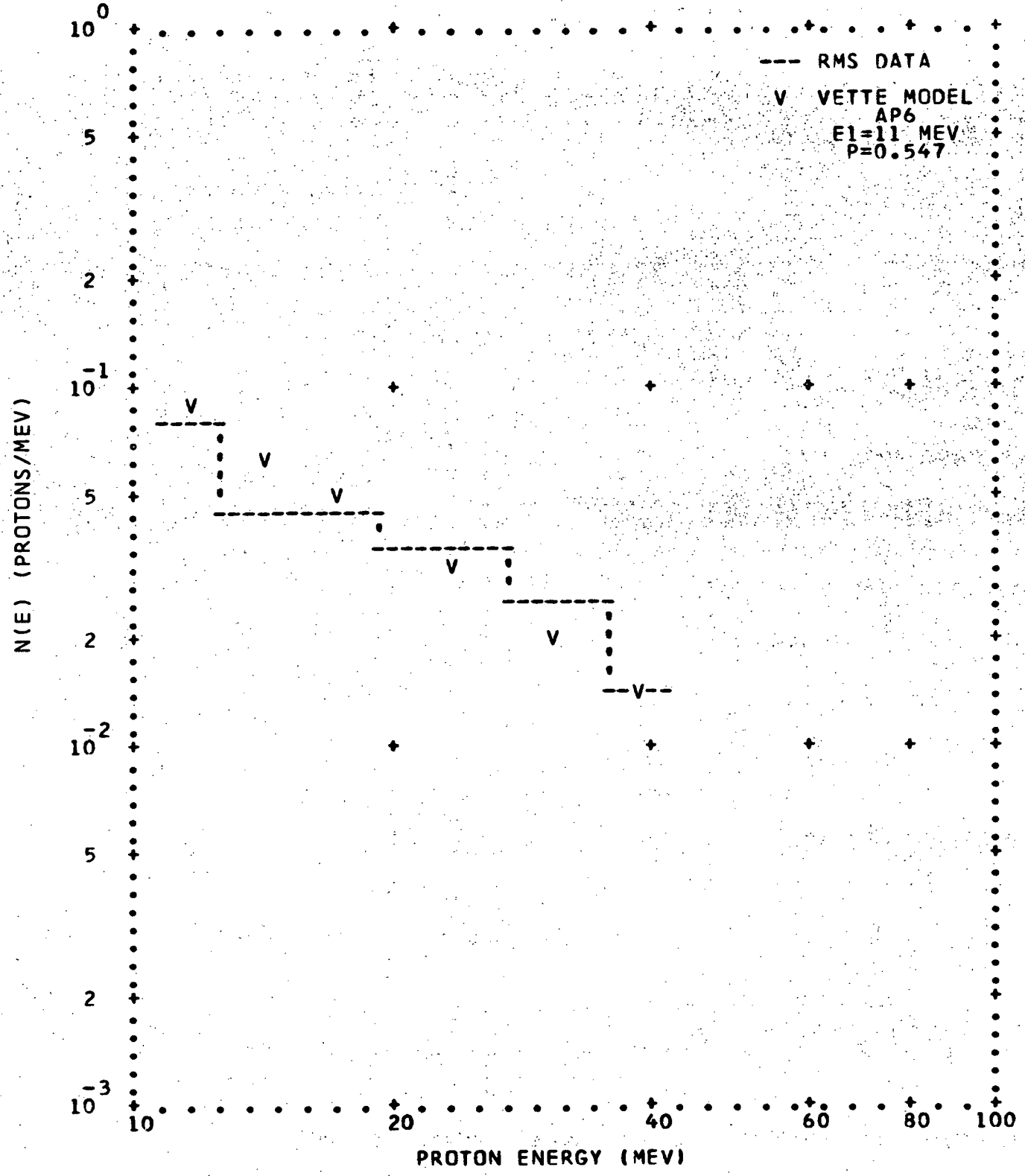

FIG. 4-18. RMS PROTON SPECTRA (CONT.)

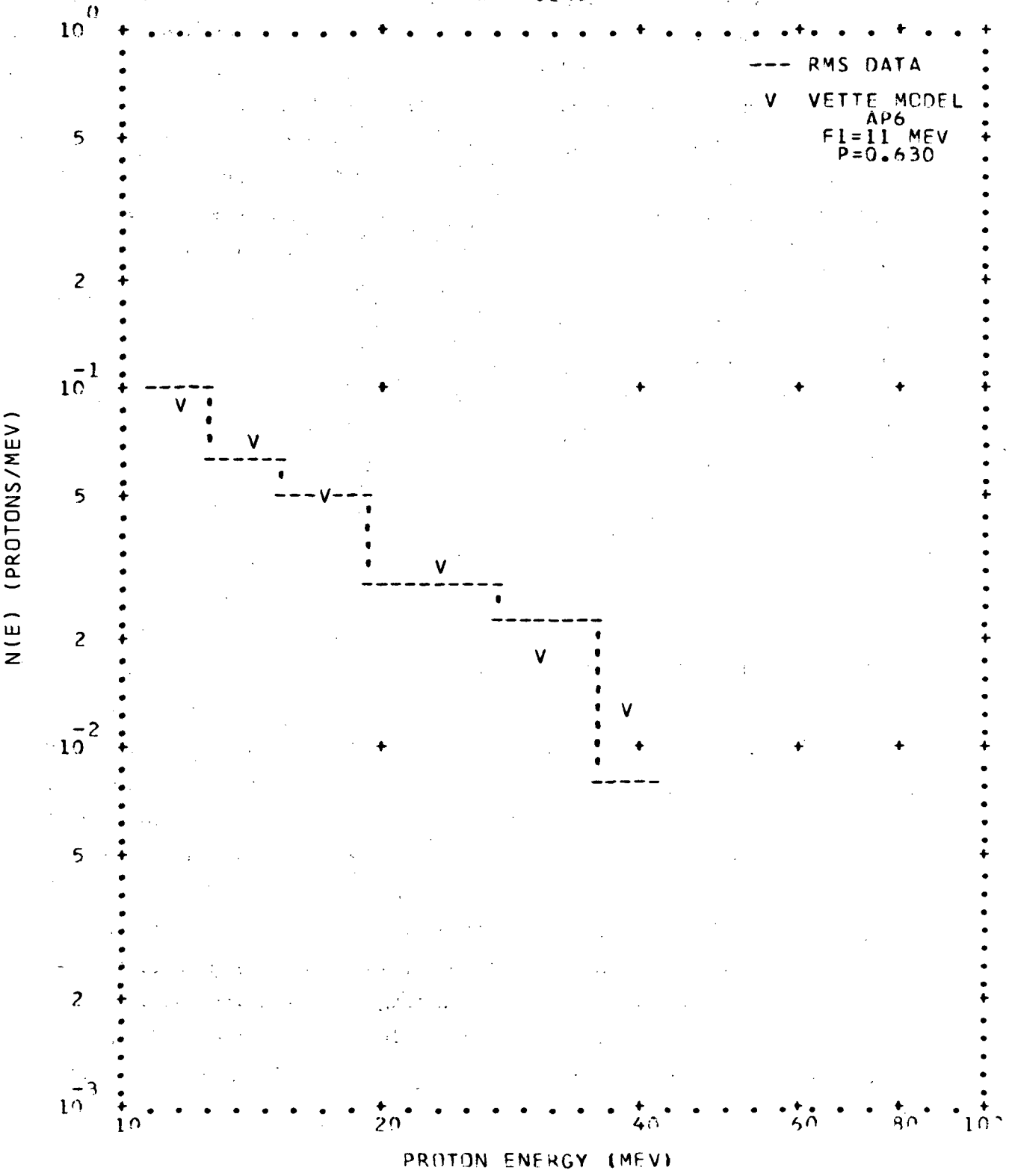

The dose maps, as presented in Table 4-5 were taken from the G-II tape with the B and L coordinates correlated. The table includes those entries taken only in November 1970. The B and L grid is that of the Vette AE2 projected 68 electron maps. The Vette electron flux values are presented for reference only. The data is the average of all readings taken within the grid spaces and the number of entries included in each location is shown in the last column. The standard deviation is that computed in the normal way and results primarily from the time variations in the data. These time variations were taken from separate printouts of each pass through the anomaly. A detailed analysis of the data in this manner was beyond the scope of this program; however, a brief review of the data indicated a standard deviation of about 20% would be expected. This is consistent with the dose tables. Entries shown as 0.0 refer to readings below 0.01 REM/HR, the lower limits of calibration of the ionization chambers.

4.3.3 Dose Comparisons

In order to establish the most accurate comparisons between the doses as computed from the spectrometer readings to those measured with the ionization chambers, the readings from a single pass through the anomaly were compared directly, as though in real-time. The data from the pass through the South Atlantic magnetic anomaly for RMS orbit 52 (dumped during orbit 53) were used. These are presented in Table 4-6. The run number refers to the data acquisition periods for a particular radiation sequence. These could be programmed by ground command to be one of the four sequences shown in Fig. 4-19. The one used for the data sequence presented here was the 25% duty cycle with an 8 second spectrum data period. For these comparisons the B and L coordinates were correlated at the center of each of the 8-second runs and the dose readings are averaged for a comparison, whereas for the dose maps, each of the ionization chamber dose readings at each end of the 8 second period were correlated and included in the maps independently.

TABLE 4-5. IONIZATION CHAMBER DOSE MAPS
NOVEMBER 1970
** L = 1.15 **

B (GAUSS)	VETTE AE2-68 FLUX (CM-2*SEC-1)	*NO SHIELD AVERAGE DOSE (RAD/HR)	*NO SHIELD STANDARD DEVIATION (RAD/HR)	THIN SHIELD AVERAGE DOSE (RAD/HR)	THIN SHIELD STANDARD DEVIATION (RAD/HR)	THICK SHIELD AVERAGE DOSE (RAD/HR)	THICK SHIELD STANDARD DEVIATION (RAD/HR)	NO. OF ENTRIES
0.196	7.800E 03	0.0	0.0	0.0	0.0	0.0	0.0	0
0.198	5.200E 03	1.236E-01	0.0	1.210E-01	0.0	9.333E-02	0.0	1
0.200	2.760E 03	9.834E-02	1.682E-02	9.584E-02	1.195E-02	6.684E-02	1.175E-02	16
0.202	2.080E 03	6.574E-02	1.181E-02	6.664E-02	8.980E-03	4.150E-02	8.515E-03	25
0.204	1.580E 03	4.545E-02	1.434E-02	4.886E-02	1.117E-02	2.760E-02	7.082E-03	14
0.205	1.400E 03	3.232E-02	1.086E-02	3.897E-02	8.748E-03	1.989E-02	6.964E-03	20
0.206	1.200E 03	0.0	0.0	2.807E-02	4.486E-03	0.0	0.0	19
0.208	9.200E 02	0.0	0.0	2.069E-02	3.587E-03	0.0	0.0	23
0.210	6.840E 02	0.0	0.0	1.668E-02	3.077E-03	0.0	0.0	29
0.212	4.920E 02	0.0	0.0	0.0	0.0	0.0	0.0	21
0.214	3.200E 02	0.0	0.0	0.0	0.0	0.0	0.0	25
0.216	2.080E 02	0.0	0.0	0.0	0.0	0.0	0.0	25
0.218	1.340E 02	0.0	0.0	0.0	0.0	0.0	0.0	19
0.220	8.280E 01	0.0	0.0	0.0	0.0	0.0	0.0	14
0.222	4.840E 01	0.0	0.0	0.0	0.0	0.0	0.0	5
0.224	2.880E 01	0.0	0.0	0.0	0.0	0.0	0.0	33
0.230	4.720E 00	0.0	0.0	0.0	0.0	0.0	0.0	16
0.235	1.000E 00	0.0	0.0	0.0	0.0	0.0	0.0	13
0.240	1.000E 00	0.0	0.0	0.0	0.0	0.0	0.0	6
0.245	1.000E 00	0.0	0.0	0.0	0.0	0.0	0.0	12

*THE NO SHIELD DATA IS IN ERROR AND IS INCLUDED HERE FOR REFERENCE ONLY

TABLE 4-5. IONIZATION CHAMBER DOSE MAPS (CONT.)
NOVEMBER 1970
** L = 1.18 **

B (GAUSS)	VETTE AE2-68 FLUX (CM-2*SEC-1)	*NO SHIELD AVERAGE DOSE (RAD/HR)	*NO SHIELD STANDARD DEVIATION (RAD/HR)	THIN SHIELD AVERAGE DOSE (RAD/HR)	THIN SHIELD STANDARD DEVIATION (RAD/HR)	THICK SHIELD AVERAGE DOSE (RAD/HR)	THICK SHIELD STANDARD DEVIATION (RAD/HR)	NO. OF ENTRIES
0.196	2.400E 04	2.460E-01	3.348E-02	2.424E-01	3.533E-02	1.822E-01	1.964E-02	8
0.198	1.760E 04	1.852E-01	3.120E-02	1.609E-01	2.132E-02	1.233E-01	1.508E-02	21
0.200	1.260E 04	1.642E-01	3.957E-02	1.393E-01	2.918E-02	1.077E-01	2.347E-02	28
0.202	8.900E 03	1.285E-01	3.107E-02	1.188E-01	2.616E-02	8.786E-02	1.755E-02	13
0.204	6.200E 03	8.243E-02	1.707E-02	7.943E-02	1.720E-02	5.812E-02	1.146E-02	6
0.206	4.200E 03	5.681E-02	1.660E-02	6.054E-02	1.475E-02	3.382E-02	1.117E-02	7
0.208	2.800E 03	3.125E-02	6.973E-03	3.653E-02	8.369E-03	1.648E-02	4.013E-03	5
0.210	1.940E 03	2.412E-02	1.499E-02	2.966E-02	1.428E-02	0.0	0.0	4
0.212	1.370E 03	0.0	0.0	1.776E-02	5.176E-03	0.0	0.0	9
0.214	9.600E 02	0.0	0.0	0.0	0.0	0.0	0.0	9
0.216	6.400E 02	0.0	0.0	0.0	0.0	0.0	0.0	3
0.218	4.100E 02	0.0	0.0	0.0	0.0	0.0	0.0	6
0.220	2.780E 02	0.0	0.0	0.0	0.0	0.0	0.0	9
0.222	1.800E 02	0.0	0.0	0.0	0.0	0.0	0.0	5
0.224	1.100E 02	0.0	0.0	0.0	0.0	0.0	0.0	4
0.226	6.800E 01	0.0	0.0	0.0	0.0	0.0	0.0	2
0.228	4.000E 01	0.0	0.0	0.0	0.0	0.0	0.0	8
0.230	2.280E 01	0.0	0.0	0.0	0.0	0.0	0.0	3
0.235	4.600E 00	0.0	0.0	0.0	0.0	0.0	0.0	6
0.240	1.000E 00	0.0	0.0	0.0	0.0	0.0	0.0	1
0.245	1.000E 00	0.0	0.0	0.0	0.0	0.0	0.0	5
0.250	1.000E 00	0.0	0.0	0.0	0.0	0.0	0.0	1

*THE NO SHIELD DATA IS IN ERROR AND IS INCLUDED HERE FOR REFERENCE ONLY

TABLE 4-5. IONIZATION CHAMBER DOSE MAPS (CONT.)
NOVEMBER 1970
** L = 1.20 **

B (GAUSS)	VETTE AE2-68 FLUX (CM-2*SEC-1)	*NO SHIELD AVERAGE DOSE (RAD/HR)	*NO SHIELD STANDARD DEVIATION (RAD/HR)	THIN SHIELD AVERAGE DOSE (RAD/HR)	THIN SHIELD STANDARD DEVIATION (RAD/HR)	THICK SHIELD AVERAGE DOSE (RAD/HR)	THICK SHIELD STANDARD DEVIATION (RAD/HR)	NO. OF ENTRIES
0.196	9.400E 04	3.025E-01	0.0	3.070E-01	0.0	2.154E-01	0.0	1
0.198	6.960E 04	3.740E-01	8.266E-02	3.276E-01	4.821E-02	2.510E-01	4.023E-02	16
0.200	5.200E 04	2.562E-01	3.577E-02	2.135E-01	3.156E-02	1.654E-01	2.033E-02	11
0.202	3.720E 04	1.877E-01	3.508E-02	1.568E-01	2.851E-02	1.194E-01	1.914E-02	11
0.204	2.640E 04	1.393E-01	3.153E-02	1.283E-01	2.202E-02	9.226E-02	1.772E-02	13
0.206	1.840E 04	1.089E-01	1.480E-02	9.863E-02	7.641E-03	6.380E-02	6.286E-03	6
0.208	1.260E 04	7.648E-02	1.964E-02	7.668E-02	1.442E-02	4.757E-02	1.040E-02	8
0.210	8.600E 03	4.305E-02	1.518E-02	4.543E-02	1.282E-02	3.165E-02	1.949E-02	8
0.212	5.840E 03	0.0	0.0	2.822E-02	9.211E-03	0.0	0.0	11
0.214	3.920E 03	0.0	0.0	2.241E-02	7.255E-03	0.0	0.0	9
0.216	2.580E 03	0.0	0.0	1.459E-02	3.699E-03	0.0	0.0	9
0.218	1.700E 03	0.0	0.0	0.0	0.0	0.0	0.0	6
0.220	1.120E 03	0.0	0.0	0.0	0.0	0.0	0.0	7
0.222	7.120E 02	0.0	0.0	0.0	0.0	0.0	0.0	6
0.224	4.720E 02	0.0	0.0	0.0	0.0	0.0	0.0	3
0.226	3.030E 02	0.0	0.0	0.0	0.0	0.0	0.0	0
0.228	1.920E 02	0.0	0.0	0.0	0.0	0.0	0.0	7
0.230	1.200E 02	0.0	0.0	0.0	0.0	0.0	0.0	6
0.232	7.200E 01	0.0	0.0	0.0	0.0	0.0	0.0	3
0.235	2.360E 01	0.0	0.0	0.0	0.0	0.0	0.0	7
0.240	2.600E 00	0.0	0.0	0.0	0.0	0.0	0.0	8
0.250	1.000E 00	0.0	0.0	0.0	0.0	0.0	0.0	5

*THE NO SHIELD DATA IS IN ERROR AND IS INCLUDED HERE FOR REFERENCE ONLY

TABLE 4-5. IONIZATION CHAMBER DOSE MAPS (CONT.)
NOVEMBER 1970
** L = 1.25 **

B (GAUSS)	VETTE AE2-68 FLUX (CM-2*SEC-1)	*NO SHIELD AVERAGE DOSE (RAD/HR)	*NO SHIELD STANDARD DEVIATION (RAD/HR)	THIN SHIELD AVERAGE DOSE (RAD/HR)	THIN SHIELD STANDARD DEVIATION (RAD/HR)	THICK SHIELD AVERAGE DOSE (RAD/HR)	THICK SHIELD STANDARD DEVIATION (RAD/HR)	NO. OF ENTRIES
0.200	3.100E 05	5.401E-01	1.525E-01	4.221E-01	8.684E-02	3.365E-01	8.331E-02	41
0.202	2.330E 05	3.453E-01	1.186E-01	2.945E-01	8.024E-02	2.192E-01	6.238E-02	18
0.204	1.720E 05	3.305E-01	9.646E-02	2.867E-01	7.404E-02	2.070E-01	5.696E-02	19
0.206	1.270E 05	2.178E-01	6.547E-02	1.896E-01	6.528E-02	1.343E-01	4.225E-02	16
0.208	9.500E 04	1.913E-01	5.365E-02	1.533E-01	4.492E-02	1.095E-01	3.140E-02	9
0.210	6.870E 04	1.031E-01	2.660E-02	9.009E-02	1.710E-02	5.978E-02	1.703E-02	9
0.212	4.860E 04	6.770E-02	1.910E-02	5.775E-02	1.012E-02	3.557E-02	6.810E-03	3
0.214	3.340E 04	4.332E-02	2.810E-02	4.694E-02	2.292E-02	2.515E-02	1.344E-02	8
0.216	2.200E 04	0.0	0.0	3.158E-02	1.496E-02	0.0	0.0	9
0.218	1.410E 04	0.0	0.0	2.109E-02	6.973E-03	0.0	0.0	4
0.220	9.000E 03	2.405E-02	5.117E-03	2.404E-02	2.292E-03	0.0	0.0	2
0.222	5.700E 03	0.0	0.0	0.0	0.0	0.0	0.0	5
0.224	3.480E 03	0.0	0.0	0.0	0.0	0.0	0.0	2
0.226	2.100E 03	0.0	0.0	0.0	0.0	0.0	0.0	3
0.228	1.260E 03	0.0	0.0	0.0	0.0	0.0	0.0	4
0.230	7.540E 02	0.0	0.0	0.0	0.0	0.0	0.0	6
0.232	4.860E 02	0.0	0.0	0.0	0.0	0.0	0.0	11
0.234	2.810E 02	0.0	0.0	0.0	0.0	0.0	0.0	6
0.236	1.560E 02	0.0	0.0	0.0	0.0	0.0	0.0	3
0.238	8.400E 01	0.0	0.0	0.0	0.0	0.0	0.0	2
0.240	4.110E 01	0.0	0.0	0.0	0.0	0.0	0.0	6
0.250	1.000E 00	0.0	0.0	0.0	0.0	0.0	0.0	8
0.255	1.000E 00	0.0	0.0	0.0	0.0	0.0	0.0	1

*THE NO SHIELD DATA IS IN ERROR AND IS INCLUDED HERE FOR REFERENCE ONLY

TABLE 4-5. IONIZATION CHAMBER DOSE MAPS (CONT.)
NOVEMBER 1970
** L = 1.30 **

B (GAUSS)	VETTE AE2-68 FLUX (CM-2*SEC-1)	*NO SHIELD AVERAGE DOSE (RAD/HR)	*NO SHIELD STANDARD DEVIATION (RAD/HR)	THIN SHIELD AVERAGE DOSE (RAD/HR)	THIN SHIELD STANDARD DEVIATION (RAD/HR)	THICK SHIELD AVERAGE DOSE (RAD/HR)	THICK SHIELD STANDARD DEVIATION (RAD/HR)	NO. OF ENTRIES
0.200	5.410E 05	6.233E-01	1.819E-01	4.747E-01	1.037E-01	3.830E-01	9.336E-02	26
0.205	3.180E 05	4.967E-01	1.131E-01	3.977E-01	7.474E-02	3.032E-01	6.188E-02	9
0.210	1.760E 05	3.184E-01	5.774E-02	2.593E-01	4.766E-02	1.882E-01	4.227E-02	15
0.212	1.360E 05	2.477E-01	4.499E-02	1.867E-01	3.891E-02	1.381E-01	3.269E-02	9
0.214	1.030E 05	1.901E-01	3.619E-02	1.472E-01	3.952E-02	1.034E-01	1.996E-02	7
0.216	7.800E 04	1.097E-01	5.384E-02	9.110E-02	2.718E-02	6.228E-02	3.193E-02	9
0.218	5.800E 04	7.710E-02	2.451E-02	6.623E-02	1.488E-02	4.312E-02	1.699E-02	12
0.220	4.390E 04	0.0	0.0	4.649E-02	1.335E-02	0.0	0.0	18
0.222	3.140E 04	0.0	0.0	2.850E-02	8.146E-03	0.0	0.0	15
0.224	2.160E 04	0.0	0.0	0.0	0.0	0.0	0.0	17
0.226	1.370E 04	0.0	0.0	0.0	0.0	0.0	0.0	14
0.228	8.500E 03	0.0	0.0	0.0	0.0	0.0	0.0	4
0.230	5.020E 03	0.0	0.0	0.0	0.0	0.0	0.0	8
0.232	3.020E 03	0.0	0.0	0.0	0.0	0.0	0.0	7
0.234	1.730E 03	0.0	0.0	0.0	0.0	0.0	0.0	2
0.236	9.600E 02	0.0	0.0	0.0	0.0	0.0	0.0	1
0.238	5.490E 02	0.0	0.0	0.0	0.0	0.0	0.0	3
0.240	3.130E 02	0.0	0.0	0.0	0.0	0.0	0.0	2
0.242	1.820E 02	0.0	0.0	0.0	0.0	0.0	0.0	2
0.244	1.020E 02	0.0	0.0	0.0	0.0	0.0	0.0	2
0.246	5.020E 01	0.0	0.0	0.0	0.0	0.0	0.0	4
0.250	8.900E 00	0.0	0.0	0.0	0.0	0.0	0.0	5
0.260	1.000E 00	0.0	0.0	0.0	0.0	0.0	0.0	8
0.265	1.000E 00	0.0	0.0	0.0	0.0	0.0	0.0	6

*THE NO SHIELD DATA IS IN ERROR AND IS INCLUDED HERE FOR REFERENCE ONLY

TABLE 4-5. IONIZATION CHAMBER DOSE MAPS (CONT.)
NOVEMBER 1970
** L = 1.35 **

B (GAUSS)	VETTE AE2-68 FLUX (CM-2*SEC-1)	*NO SHIELD AVERAGE DOSE (RAD/HR)	*NO SHIELD STANDARD DEVIATION (RAD/HR)	THIN SHIELD AVERAGE DOSE (RAD/HR)	THIN SHIELD STANDARD DEVIATION (RAD/HR)	THICK SHIELD AVERAGE DOSE (RAD/HR)	THICK SHIELD STANDARD DEVIATION (RAD/HR)	NO. OF ENTRIES
0.200	9.990E 05	0.0	0.0	0.0	0.0	0.0	0.0	0
0.205	6.840E 05	6.888E-01	7.430E-02	4.793E-01	3.372E-02	3.714E-01	3.020E-02	14
0.210	4.450E 05	4.670E-01	1.166E-01	3.542E-01	7.410E-02	2.584E-01	5.677E-02	38
0.215	2.810E 05	2.606E-01	7.141E-02	2.039E-01	6.260E-02	1.368E-01	3.760E-02	65
0.220	1.630E 05	1.196E-01	3.327E-02	9.892E-02	2.258E-02	5.547E-02	1.905E-02	59
0.222	1.290E 05	0.0	0.0	6.125E-02	1.945E-02	0.0	0.0	14
0.224	9.990E 04	3.175E-02	6.501E-03	3.322E-02	6.839E-03	1.397E-02	3.687E-03	6
0.226	7.430E 04	2.663E-02	7.700E-03	2.112E-02	3.375E-03	0.0	0.0	2
0.228	5.340E 04	0.0	0.0	1.259E-02	1.991E-03	0.0	0.0	4
0.230	3.550E 04	0.0	0.0	0.0	0.0	0.0	0.0	4
0.232	2.400E 04	0.0	0.0	0.0	0.0	0.0	0.0	4
0.234	1.550E 04	0.0	0.0	0.0	0.0	0.0	0.0	6
0.236	9.580E 03	0.0	0.0	0.0	0.0	0.0	0.0	2
0.238	6.020E 03	0.0	0.0	0.0	0.0	0.0	0.0	1
0.240	3.420E 03	0.0	0.0	0.0	0.0	0.0	0.0	2
0.242	1.920E 03	0.0	0.0	0.0	0.0	0.0	0.0	3
0.244	1.100E 03	0.0	0.0	0.0	0.0	0.0	0.0	2
0.246	6.500E 02	0.0	0.0	0.0	0.0	0.0	0.0	2
0.248	3.630E 02	0.0	0.0	0.0	0.0	0.0	0.0	2
0.250	1.900E 02	0.0	0.0	0.0	0.0	0.0	0.0	3
0.252	9.990E 01	0.0	0.0	0.0	0.0	0.0	0.0	1
0.254	5.200E 01	0.0	0.0	0.0	0.0	0.0	0.0	0
0.256	2.530E 01	0.0	0.0	0.0	0.0	0.0	0.0	3
0.258	1.160E 01	0.0	0.0	0.0	0.0	0.0	0.0	5
0.260	4.450E 00	0.0	0.0	0.0	0.0	0.0	0.0	1
0.265	1.000E 00	0.0	0.0	0.0	0.0	0.0	0.0	6
0.270	1.000E 00	0.0	0.0	0.0	0.0	0.0	0.0	4

* THE NO SHIELD DATA IS IN ERROR AND IS INCLUDED HERE FOR REFERENCE ONLY

TABLE 4-5. IONIZATION CHAMBER DOSE MAPS (CONT.)
NOVEMBER 1970
** L = 1.40 **

B (GAUSS)	VETTE AE2-68 FLUX (CM-2*SEC-1)	* NO SHIELD AVERAGE DOSE (RAD/HR)	NO SHIELD STANDARD DEVIATION (RAD/HR)	THIN SHIELD AVERAGE DOSE (RAD/HR)	THIN SHIELD STANDARD DEVIATION (RAD/HR)	THICK SHIELD AVERAGE DOSE (RAD/HR)	THICK SHIELD STANDARD DEVIATION (RAD/HR)	NO. OF ENTRIES
0.200	2.090E 06	0.0	0.0	0.0	0.0	0.0	0.0	0
0.205	1.530E 06	0.0	0.0	0.0	0.0	0.0	0.0	0
0.210	1.080E 06	6.843E-01	1.006E-01	4.438E-01	4.394E-02	3.337E-01	4.205E-02	23
0.215	7.190E 05	4.545E-01	1.154E-01	3.246E-01	5.514E-02	2.244E-01	3.848E-02	62
0.220	4.500E 05	2.220E-01	4.986E-02	1.570E-01	3.742E-02	9.898E-02	2.773E-02	70
0.225	2.590E 05	1.426E-01	5.972E-02	9.926E-02	2.881E-02	5.695E-02	2.093E-02	25
0.230	1.360E 05	3.779E-02	1.140E-02	3.762E-02	8.848E-03	1.726E-02	4.293E-03	6
0.232	1.090E 05	0.0	0.0	1.478E-02	2.704E-04	0.0	0.0	4
0.234	7.440E 04	0.0	0.0	0.0	0.0	0.0	0.0	9
0.236	5.250E 04	0.0	0.0	0.0	0.0	0.0	0.0	22
0.238	3.660E 04	0.0	0.0	0.0	0.0	0.0	0.0	17
0.240	2.470E 04	0.0	0.0	0.0	0.0	0.0	0.0	6
0.242	1.630E 04	0.0	0.0	0.0	0.0	0.0	0.0	1
0.244	1.050E 04	0.0	0.0	0.0	0.0	0.0	0.0	4
0.246	6.380E 03	0.0	0.0	0.0	0.0	0.0	0.0	7
0.248	3.970E 03	0.0	0.0	0.0	0.0	0.0	0.0	3
0.250	2.340E 03	0.0	0.0	0.0	0.0	0.0	0.0	2
0.252	1.330E 03	0.0	0.0	0.0	0.0	0.0	0.0	4
0.254	7.060E 02	0.0	0.0	0.0	0.0	0.0	0.0	2
0.256	3.630E 02	0.0	0.0	0.0	0.0	0.0	0.0	0
0.258	1.560E 02	0.0	0.0	0.0	0.0	0.0	0.0	0
0.260	6.250E 01	0.0	0.0	0.0	0.0	0.0	0.0	9
0.265	6.560E 00	0.0	0.0	0.0	0.0	0.0	0.0	8
0.270	1.000E 00	0.0	0.0	0.0	0.0	0.0	0.0	0
0.275	1.000E 00	0.0	0.0	0.0	0.0	0.0	0.0	9

*THE NO SHIELD DATA IS IN ERROR AND IS INCLUDED HERE FOR REFERENCE ONLY

TABLE 4-5. IONIZATION CHAMBER DOSE MAPS (CONT.)
NOVEMBER 1970
** L = 1.50 **

B (GAUSS)	VETTE AE2-68 FLUX (CM-2*SEC-1)	*NO SHIELD AVERAGE DOSE (RAD/HR)	*NO SHIELD STANDARD DEVIATION (RAD/HR)	THIN SHIELD AVERAGE DOSE (RAD/HR)	THIN SHIELD STANDARD DEVIATION (RAD/HR)	THICK SHIELD AVERAGE DOSE (RAD/HR)	THICK SHIELD STANDARD DEVIATION (RAD/HR)	NO. OF ENTRIES
0.200	3.100E 06	0.0	0.0	0.0	0.0	0.0	0.0	0
0.210	1.850E 06	6.180E-01	5.036E-02	3.586E-01	2.284E-02	2.519E-01	1.138E-02	4
0.220	9.800E 05	4.057E-01	1.025E-01	2.590E-01	5.294E-02	1.632E-01	3.819E-02	55
0.225	6.600E 05	2.558E-01	4.449E-02	1.505E-01	2.958E-02	8.730E-02	1.942E-02	58
0.230	4.160E 05	1.393E-01	5.586E-02	8.892E-02	2.449E-02	4.595E-02	1.672E-02	41
0.235	2.500E 05	0.0	0.0	5.116E-02	1.553E-02	0.0	0.0	28
0.240	1.440E 05	0.0	0.0	0.0	0.0	0.0	0.0	35
0.245	8.400E 04	0.0	0.0	0.0	0.0	0.0	0.0	31
0.250	4.650E 04	0.0	0.0	0.0	0.0	0.0	0.0	11
0.252	3.680E 04	0.0	0.0	0.0	0.0	0.0	0.0	0
0.254	2.880E 04	0.0	0.0	0.0	0.0	0.0	0.0	4
0.256	2.160E 04	0.0	0.0	0.0	0.0	0.0	0.0	7
0.258	1.600E 04	0.0	0.0	0.0	0.0	0.0	0.0	4
0.260	1.070E 04	0.0	0.0	0.0	0.0	0.0	0.0	3
0.262	5.800E 03	0.0	0.0	0.0	0.0	0.0	0.0	6
0.264	2.500E 03	0.0	0.0	0.0	0.0	0.0	0.0	2
0.266	9.800E 02	0.0	0.0	0.0	0.0	0.0	0.0	4
0.268	3.700E 02	0.0	0.0	0.0	0.0	0.0	0.0	6
0.270	1.500E 02	0.0	0.0	0.0	0.0	0.0	0.0	0
0.275	1.500E 01	0.0	0.0	0.0	0.0	0.0	0.0	12
0.280	1.580E 00	0.0	0.0	0.0	0.0	0.0	0.0	0
0.285	1.000E 00	0.0	0.0	0.0	0.0	0.0	0.0	12

*THE NO SHIELD DATA IS IN ERROR AND IS INCLUDED HERE FOR REFERENCE ONLY

TABLE 4-5. IONIZATION CHAMBER DOSE MAPS (CONT.)
NOVEMBER 1970
** L = 1.60 **

B (GAUSS)	VETTE AE2-68 FLUX (CM-2*SEC-1)	*NO SHIELD AVERAGE DOSE (RAD/HR)	*NO SHIELD STANDARD DEVIATION (RAD/HR)	THIN SHIELD AVERAGE DOSE (RAD/HR)	THIN SHIELD STANDARD DEVIATION (RAD/HR)	THICK SHIELD AVERAGE DOSE (RAD/HR)	THICK SHIELD STANDARD DEVIATION (RAD/HR)	NO. OF ENTRIES
0.200	4.930E 05	0.0	0.0	0.0	0.0	0.0	0.0	0
0.210	3.440E 05	0.0	0.0	0.0	0.0	0.0	0.0	0
0.220	2.130E 05	3.410E-01	3.849E-02	1.876E-01	1.175E-02	1.090E-01	6.000E-03	2
0.230	1.160E 05	2.320E-01	5.541E-02	1.255E-01	2.938E-02	6.276E-02	2.098E-02	19
0.240	5.840E 04	9.766E-02	2.670E-02	5.895E-02	1.503E-02	0.0	0.0	40
0.250	2.710E 04	0.0	0.0	0.0	0.0	0.0	0.0	11
0.255	1.790E 04	0.0	0.0	0.0	0.0	0.0	0.0	17
0.260	1.150E 04	0.0	0.0	0.0	0.0	0.0	0.0	8
0.265	7.330E 03	0.0	0.0	0.0	0.0	0.0	0.0	6
0.270	4.250E 03	0.0	0.0	0.0	0.0	0.0	0.0	10
0.272	1.670E 03	0.0	0.0	0.0	0.0	0.0	0.0	2
0.274	5.880E 02	0.0	0.0	0.0	0.0	0.0	0.0	3
0.276	2.040E 02	0.0	0.0	0.0	0.0	0.0	0.0	4
0.278	7.240E 01	0.0	0.0	0.0	0.0	0.0	0.0	0
0.280	2.810E 01	0.0	0.0	0.0	0.0	0.0	0.0	0
0.285	2.310E 00	0.0	0.0	0.0	0.0	0.0	0.0	3
0.290	1.000E 00	0.0	0.0	0.0	0.0	0.0	0.0	6

*THE NO SHIELD DATA IS IN ERROR AND IS INCLUDED HERE FOR REFERENCE ONLY

TABLE 4-5. IONIZATION CHAMBER DOSE MAPS (CONT.)
NOVEMBER 1970
** L = 1.70 **

B (GAUSS)	VETTE AE2-68 FLUX (CM-2*SEC-1)	*NO SHIELD AVERAGE DOSE (RAD/HR)	*NO SHIELD STANDARD DEVIATION (RAD/HR)	THIN SHIELD AVERAGE DOSE (RAD/HR)	THIN SHIELD STANDARD DEVIATION (RAD/HR)	THICK SHIELD AVERAGE DOSE (RAD/HR)	THICK SHIELD STANDARD DEVIATION (RAD/HR)	NO. OF ENTRIES
0.200	8.120E 04	0.0	0.0	0.0	0.0	0.0	0.0	0
0.210	5.950E 04	0.0	0.0	0.0	0.0	0.0	0.0	0
0.220	4.210E 04	0.0	0.0	0.0	0.0	0.0	0.0	0
0.230	2.780E 04	0.0	0.0	0.0	0.0	0.0	0.0	0
0.240	1.740E 04	9.757E-02	2.321E-02	5.211E-02	1.041E-02	0.0	0.0	42
0.250	1.060E 04	0.0	0.0	0.0	0.0	0.0	0.0	37
0.260	6.380E 03	0.0	0.0	0.0	0.0	0.0	0.0	27
0.270	3.230E 03	0.0	0.0	0.0	0.0	0.0	0.0	11
0.272	2.760E 03	0.0	0.0	0.0	0.0	0.0	0.0	0
0.274	2.230E 03	0.0	0.0	0.0	0.0	0.0	0.0	1
0.276	1.590E 03	0.0	0.0	0.0	0.0	0.0	0.0	3
0.278	8.080E 02	0.0	0.0	0.0	0.0	0.0	0.0	6
0.280	3.190E 02	0.0	0.0	0.0	0.0	0.0	0.0	1
0.282	1.400E 02	0.0	0.0	0.0	0.0	0.0	0.0	0
0.284	6.380E 01	0.0	0.0	0.0	0.0	0.0	0.0	0
0.286	3.120E 01	0.0	0.0	0.0	0.0	0.0	0.0	0
0.288	1.490E 01	0.0	0.0	0.0	0.0	0.0	0.0	0
0.290	7.010E 00	0.0	0.0	0.0	0.0	0.0	0.0	1
0.295	1.080E 00	0.0	0.0	0.0	0.0	0.0	0.0	2
0.300	1.000E 00	0.0	0.0	0.0	0.0	0.0	0.0	2

*THE NO SHIELD DATA IS IN ERROR AND IS INCLUDED HERE FOR REFERENCE ONLY

TABLE 4-5. IONIZATION CHAMBER DOSE MAPS (CONT.)
NOVEMBER 1970
** L = 1.80 **

B (GAUSS)	VETTE AE2-68 FLUX (CM-2*SEC-1)	*NO SHIELD AVERAGE DOSE (RAD/HR)	*NO SHIELD STANDARD DEVIATION (RAD/HR)	THIN SHIELD AVERAGE DOSE (RAD/HR)	THIN SHIELD STANDARD DEVIATION (RAD/HR)	THICK SHIELD AVERAGE DOSE (RAD/HR)	THICK SHIELD STANDARD DEVIATION (RAD/HR)	NO. OF ENTRIES
0.200	2.620E 04	0.0	0.0	0.0	0.0	0.0	0.0	0
0.210	1.980E 04	0.0	0.0	0.0	0.0	0.0	0.0	0
0.220	1.480E 04	0.0	0.0	0.0	0.0	0.0	0.0	0
0.230	1.100E 04	0.0	0.0	0.0	0.0	0.0	0.0	0
0.240	8.090E 03	1.043E-01	1.674E-02	4.629E-02	5.750E-03	0.0	0.0	7
0.250	5.840E 03	7.984E-02	1.525E-02	3.797E-02	6.204E-03	0.0	0.0	24
0.260	4.010E 03	0.0	0.0	0.0	0.0	0.0	0.0	26
0.270	2.360E 03	0.0	0.0	0.0	0.0	0.0	0.0	6
0.272	2.050E 03	0.0	0.0	0.0	0.0	0.0	0.0	6
0.274	1.760E 03	0.0	0.0	0.0	0.0	0.0	0.0	1
0.276	1.380E 03	0.0	0.0	0.0	0.0	0.0	0.0	0
0.278	1.030E 03	0.0	0.0	0.0	0.0	0.0	0.0	2
0.280	6.890E 02	0.0	0.0	0.0	0.0	0.0	0.0	3
0.282	4.480E 02	0.0	0.0	0.0	0.0	0.0	0.0	2
0.284	2.450E 02	0.0	0.0	0.0	0.0	0.0	0.0	1
0.286	1.210E 02	0.0	0.0	0.0	0.0	0.0	0.0	1
0.288	5.420E 01	0.0	0.0	0.0	0.0	0.0	0.0	1
0.290	2.240E 01	0.0	0.0	0.0	0.0	0.0	0.0	2
0.295	2.410E 00	0.0	0.0	0.0	0.0	0.0	0.0	0
0.300	1.000E 00	0.0	0.0	0.0	0.0	0.0	0.0	0
0.305	1.000E 00	0.0	0.0	0.0	0.0	0.0	0.0	2

*THE NO SHIELD DATA IS IN ERROR AND IS INCLUDED HERE FOR REFERENCE ONLY

TABLE 4-5. IONIZATION CHAMBER DOSE MAPS (CONT.)
NOVEMBER 1970
** L = 1.90 **

B (GAUSS)	VETTE AE2-68 FLUX (CM-2*SEC-1)	*NO SHIELD AVERAGE DOSE (RAD/HR)	*NO SHIELD STANDARD DEVIATION (RAD/HR)	THIN SHIELD AVERAGE DOSE (RAD/HR)	THIN SHIELD STANDARD DEVIATION (RAD/HR)	THICK SHIELD AVERAGE DOSE (RAD/HR)	THICK SHIELD STANDARD DEVIATION (RAD/HR)	NO. OF ENTRIES
0.200	1.790E 04	0.0	0.0	0.0	0.0	0.0	0.0	0
0.210	1.410E 04	0.0	0.0	0.0	0.0	0.0	0.0	0
0.220	1.070E 04	0.0	0.0	0.0	0.0	0.0	0.0	0
0.230	7.820E 03	0.0	0.0	0.0	0.0	0.0	0.0	0
0.240	5.640E 03	0.0	0.0	0.0	0.0	0.0	0.0	0
0.250	3.930E 03	5.974E-02	1.218E-02	2.425E-02	3.890E-03	0.0	0.0	11
0.260	2.690E 03	0.0	0.0	0.0	0.0	0.0	0.0	20
0.270	1.530E 03	0.0	0.0	0.0	0.0	0.0	0.0	12
0.275	1.030E 03	0.0	0.0	0.0	0.0	0.0	0.0	9
0.280	6.490E 02	0.0	0.0	0.0	0.0	0.0	0.0	2
0.285	3.580E 02	0.0	0.0	0.0	0.0	0.0	0.0	3
0.290	1.640E 02	0.0	0.0	0.0	0.0	0.0	0.0	2
0.295	2.400E 01	0.0	0.0	0.0	0.0	0.0	0.0	1
0.300	2.840E 00	0.0	0.0	0.0	0.0	0.0	0.0	2
0.305	1.000E 00	0.0	0.0	0.0	0.0	0.0	0.0	1
0.310	1.000E 00	0.0	0.0	0.0	0.0	0.0	0.0	0

*THE NO SHIELD DATA IS IN ERROR AND IS INCLUDED HERE FOR REFERENCE ONLY

TABLE 4-5. IONIZATION CHAMBER DOSE MAPS (CONT.)
NOVEMBER 1970
** L = 2.00 **

B (GAUSS)	VETTE AE2-68 FLUX (CM-2*SEC-1)	*NO SHIELD AVERAGE DOSE (RAD/HR)	*NO SHIELD STANDARD DEVIATION (RAD/HR)	THIN SHIELD AVERAGE DOSE (RAD/HR)	THIN SHIELD STANDARD DEVIATION (RAD/HR)	THICK SHIELD AVERAGE DOSE (RAD/HR)	THICK SHIELD STANDARD DEVIATION (RAD/HR)	NO. OF ENTRIES
0.200	1.290E 04	0.0	0.0	0.0	0.0	0.0	0.0	0
0.210	9.910E 03	0.0	0.0	0.0	0.0	0.0	0.0	0
0.220	7.490E 03	0.0	0.0	0.0	0.0	0.0	0.0	0
0.230	5.660E 03	0.0	0.0	0.0	0.0	0.0	0.0	0
0.240	4.200E 03	0.0	0.0	0.0	0.0	0.0	0.0	0
0.250	3.110E 03	4.754E-02	6.937E-03	1.674E-02	2.168E-03	0.0	0.0	9
0.260	2.160E 03	0.0	0.0	0.0	0.0	0.0	0.0	10
0.270	1.430E 03	0.0	0.0	0.0	0.0	0.0	0.0	19
0.280	8.510E 02	0.0	0.0	0.0	0.0	0.0	0.0	10
0.290	3.420E 02	0.0	0.0	0.0	0.0	0.0	0.0	3
0.295	8.450E 01	0.0	0.0	0.0	0.0	0.0	0.0	2
0.300	1.490E 01	0.0	0.0	0.0	0.0	0.0	0.0	2
0.310	1.000E 00	0.0	0.0	0.0	0.0	0.0	0.0	2
0.315	1.000E 00	0.0	0.0	0.0	0.0	0.0	0.0	1

*THE NO SHIELD DATA IS IN ERROR AND IS INCLUDED HERE FOR REFERENCE ONLY

RUN NO.	B (GAUSS)	L (E.R.)	UNSHIELDED CHAMBER DOSES (RAD/HR)					
				SPECTRUM-TO-DOSE			VETTE MODEL	
			IONIZATION CHAMBER AVERAGE	ELECTRON RMS SPECTROMETER	PROTON RMS SPECTROMETER	PROTON RMS E 42<MEV AP7 E 42>MEV	ELECTRON AE2-68	PROTON AP1, AP6, AP7
1	.219	1.34	1.1(-1)	2.6(-1)	2.2	1.1	3.7(-1)	7.2
2	.217	1.34	1.7(-1)	4.2(-1)	3.6	2.1	5.0(-1)	2.5
3	.215	1.35	2.9(-1)	6.5(-1)	5.6	2.3	8.5(-1)	1.2
4	.214	1.37	4.0(-1)	6.7(-1)	7.2	3.7	1.0	1.5
5	.213	1.37	4.9(-1)	8.2(-1)	8.1	3.7	1.4	1.8
6	.211	1.38	5.0(-1)	1.1	9.4	5.1	2.1	2.3
7	.211	1.39	6.0(-1)	1.2	1.1(1)	6.3	2.3	2.4
8	.210	1.40	7.4(-1)	1.1	1.1(1)	5.4	2.4	2.7
9	.210	1.41	8.0(-1)	1.1	1.1(1)	5.4	2.6	2.9
10	.210	1.41	7.8(-1)	1.3	1.3(1)	6.8	2.7	3.1
11	.210	1.42	7.2(-1)	1.3	1.2(1)	6.0	2.7	3.1
12	.211	1.43	7.1(-1)	1.3	1.4(1)	6.8	2.6	2.9
13	.211	1.43	8.0(-1)	1.1	1.2(1)	5.9	2.7	3.1
14	.212	1.44	7.2(-1)	1.1	1.1(1)	5.6	2.4	2.8
15	.213	1.45	7.2(-1)	1.1	1.0(1)	5.6	2.4	2.8
16	.214	1.45	5.8(-1)	1.0	9.4	4.8	2.3	2.8
17	.215	1.45	5.6(-1)	1.0	6.7	3.4	2.1	2.6
18	.216	1.45	5.1(-1)	7.9(-1)	4.9	2.8	1.9	2.3
19	.217	1.45	4.4(-1)	6.7(-1)	5.7	3.4	1.8	2.2
20	.218	1.45	3.3(-1)	5.3(-1)	5.6	2.9	1.7	2.1
21	.220	1.45	2.8(-1)	5.5(-1)	4.9	3.0	1.3	1.7
22	.221	1.45	2.4(-1)	4.5(-1)	3.7	2.0	1.3	1.6
23	.223	1.45	2.0(-1)	2.9(-1)	2.3	1.2	1.1	1.3
24	.225	1.44	1.5(-1)	2.7(-1)	2.2	1.3	9.2(-1)	1.0
25	.226	1.43	8.6(-1)	1.1(-1)	1.5	1.0	8.0(-1)	8.4(-1)
26	.228	1.42	5.0(-2)	8.5(-2)	6.6(-1)	2.9(-1)	6.4(-1)	6.0(-1)
27	.230	1.41	2.4(-2)	3.0(-2)	4.4(-1)	3.7(-1)	5.0(-1)	3.7(-1)
28	.232	1.40	7.0(-3)	1.8(-2)	2.6(-1)	1.1(-1)	2.6(-1)	2.5(-1)
29	.234	1.38	3.0(-3)	2.5(-2)	2.7(-2)		3.0(-2)	1.4(-1)
30	.236	1.37	2.5(-3)	1.6(-2)	2.9(-2)		1.2(-2)	7.2(-2)

TABLE 4-6. COMPARISONS OF IONIZATION CHAMBER DOSE READINGS TO THE REAL-TIME SPECTRUM-TO-DOSE VALUES, THE SPECTRUM-TO-DOSE VALUES USING VETTE MODEL FOR HIGH ENERGY PROTONS, AND DOSE VALUES COMPUTED FROM VETTE MODEL USING IONIZATION CHAMBER RESPONSE FUNCTIONS. DATA FROM RMS ORBIT 52.

RUN NO.	THIN SHIELD DOSES (RAD/HR)			THICK SHIELD DOSES (RAD/HR)		
	IONIZATION CHAMBER	S-TO-DOSE PROTONS	VETTE MODEL AP1,AP7	IONIZATION CHAMBER	S-TO-DOSE PROTONS	VETTE MODEL AP7
1	1.0(-1)	9.4(-1)	2.4(-1)	5.8(-2)	7.4(-1)	1.5(-1)
2	1.4(-1)	1.6	2.7(-1)	9.2(-2)	1.3	2.1(-1)
3	1.9(-1)	2.7	3.8(-1)	1.3(-1)	1.9	2.7(-1)
4	2.8(-1)	3.1	4.8(-1)	1.9(-1)	2.4	3.4(-1)
5	3.5(-1)	4.1	5.5(-1)	2.5(-1)	3.0	3.9(-1)
6	4.0(-1)	4.6	6.2(-1)	2.8(-1)	3.6	4.4(-1)
7	4.1(-1)	5.4	6.4(-1)	3.0(-1)	3.8	4.6(-1)
8	4.5(-1)	5.7	6.7(-1)	3.6(-1)	4.1	5.2(-1)
9	4.9(-1)	5.3	7.3(-1)	3.8(-1)	3.9	5.6(-1)
10	5.1(-1)	6.5	7.3(-1)	3.8(-1)	4.8	5.6(-1)
11	4.9(-1)	6.0	7.3(-1)	3.7(-1)	4.4	5.6(-1)
12	4.7(-1)	7.0	6.9(-1)	3.6(-1)	4.7	5.2(-1)
13	4.6(-1)	5.8	6.9(-1)	3.5(-1)	4.3	5.1(-1)
14	4.5(-1)	6.1	6.5(-1)	3.3(-1)	4.4	4.8(-1)
15	4.4(-1)	5.3	6.4(-1)	3.0(-1)	3.9	3.1(-1)
16	3.8(-1)	5.3	5.9(-1)	2.6(-1)	3.9	3.1(-1)
17	3.4(-1)	4.2	5.4(-1)	2.5(-1)	3.2	2.2(-1)
18	3.3(-1)	2.7	5.1(-1)	2.2(-1)	2.2	3.6(-1)
19	3.1(-1)	3.0	4.8(-1)	2.0(-1)	2.2	3.4(-1)
20	2.6(-1)	3.2	4.5(-1)	1.6(-1)	2.4	3.1(-1)
21	2.0(-1)	2.8	3.9(-1)	1.4(-1)	2.1	2.6(-1)
22	1.7(-1)	2.2	3.7(-1)	1.2(-1)	1.6	2.4(-1)
23	1.3(-1)	1.7	3.1(-1)	9.3(-2)	1.2	2.0(-1)
24	1.0(-1)	1.3	2.6(-1)	6.4(-2)	1.0	1.6(-1)
25	7.0(-2)	9.4(-1)	2.2(-1)	3.8(-2)	6.1(-1)	1.4(-1)
26	4.4(-2)	3.8(-1)	1.6(-1)	2.2(-2)	3.2(-1)	1.0(-1)
27	2.6(-2)	2.6(-1)	1.0(-1)	1.4(-2)	2.3(-1)	5.8(-1)
28	1.5(-2)	7.4(-2)	6.4(-2)	5.4(-3)	8.7(-2)	3.6(-2)
29	8.9(-3)	3.1(-2)	2.5(-2)		3.7(-2)	1.8(-2)
30	4.9(-3)	3.1(-2)	1.4(-2)		5.0(-4)	1.3(-2)

TABLE 4-6. (Continued)

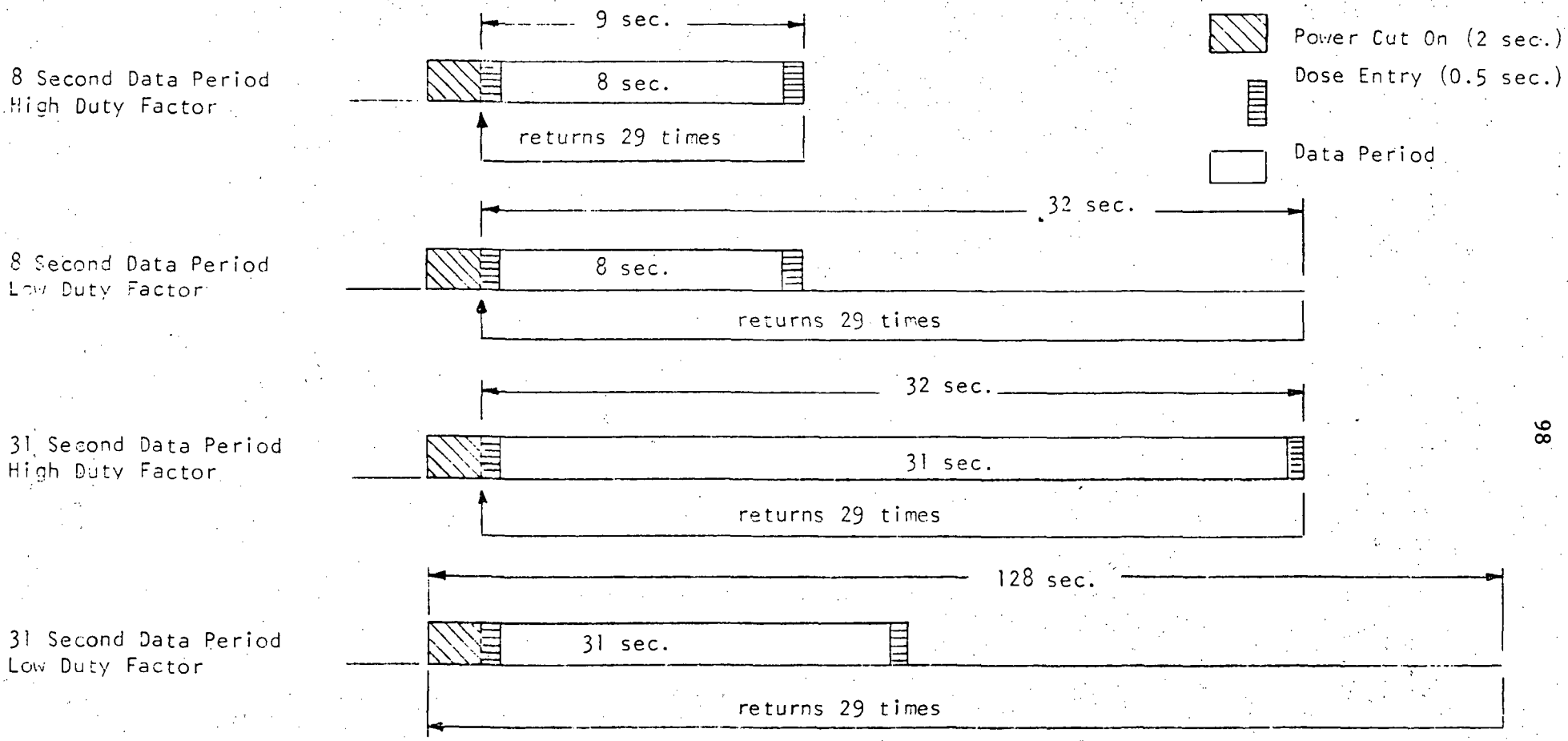

Fig. 4-19. Radiation Data Run Sequences

The correlated B and L coordinates are shown so that comparisons can be made directly to other data. Four types of information are given for the three chambers, where possible. First the ionization chamber readings given are the average of the readings taken before and after each spectral measurement. Second the dose is shown as computed on RMS from the spectrum-to-dose conversion. Next the dose is computed for the RMS data, where possible, and filled in with the Vette models in the regions where the RMS data is known to be bad (protons > 42 MeV). Finally the last entry is the dose computed from the overlap integral of the ionization chamber response functions and the Vette model. The comparisons show several features which should be discussed briefly.

In all cases the non-shielded ionization chamber readings are significantly lower than the computations from the RMS spectra or the Vette model. This problem was discussed in Section 4.3.3 and is believed to result from a loss of sensitivity of the bare ionization chamber. The second feature of importance is that the real-time dose computations corresponding to the shielded chambers are significantly higher than the chamber readings. These should be compared, also, to the doses as computed with the Vette models. The latter comparison shows the effect of the high energy spectral distortion of the spectrometer data as discussed in Section 4.2.2.1.

The real-time dose computations which are believed to be accurate are those corresponding to the electron dose in the bare chamber. These data are verified by computations directly from the spectrum. Unfortunately the ionization chamber data is in error and, thus, not available for direct comparison.

With the exception of the electron pulse-height spectrum-to-dose values, which were corrected by a factor of four error found in the original calibration, these data were as computed in real time and indicate that the system did accurately convert the information which it received from the spectrometer.

4.4 Conclusions

In spite of the fact that several disappointing malfunctions occurred, the radiation experiment did demonstrate the relative degree of simplicity by which the spectrum-to-dose conversion system could be applied and it did provide valuable data for the low-energy proton spectra and, with respect to the electrons, it has provided valuable information on the decay of the electron belts produced by the Starfish high-altitude nuclear test.

The application of pulse-height spectrum-to-dose conversion was demonstrated with a relatively simple system which employed both analog and digital techniques, and it was shown that such a system could be made to function in a remote location. Such a system is not required for current space programs such as Apollo and Skylab, since almost continuous contact is maintained between the vehicle monitoring systems and large ground-based computing facilities. The system could, however, be employed, with a large savings in computational requirements, in permanent lunar base operations and in the future, long-duration space voyages throughout the solar system.

The data actually obtained by the radiation instruments are a valuable addition to the models of the radiation environments in the South Atlantic anomaly zone. The RMS proton spectra between 11 and 42 MeV are in almost perfect agreement with the power law of the AP7 model, as seen in Fig. 4-18. Subtle differences may be noted, especially at low energies, which indicate that the power laws are not an adequate representation. However, the vast increase in the entries necessary to incorporate these divergencies into the model is not warranted in most applications. Where theories are being studied, these differences can be of great importance and the data should prove useful.

Also, in the case of the electron data, new information was obtained with respect to the remanent electrons injected into the geomagnetic field by the Starfish high-altitude nuclear detonation in 1962. The RMS data clearly shows that the spectra above 2 MeV are still dominated by the effects of the test.

We see that, although much desired information was lost, the RMS radiation experiment did provide a significant amount of valuable information.

V. ANALYSIS OF METEOROID DATA

5.1 Introduction

The objectives of the meteoroid experiment on RMS were two-fold, the primary one being of an engineering nature, to evaluate the thin-film type meteoroid sensor for future large areas, long duration meteoroid experiments. The secondary objective was of a basic nature, in which an attempt was to be made to measure meteoroid flux and velocity, realizing that the total time-area product of the experiment would be low. The analysis conducted in this program then logically fell into two parts:

(a) meteoroid flux determination

(b) evaluation of sensor reliabilities

5.2 Meteoroid Flux Determination

The interpretation of the meteoroid flux data was accomplished in a series of steps, each of which involved a sequence of identical calculations on each real-time data frame or series of data frames terminating with a satellite memory dump. In each step the results of the calculations were stored on a data tape with the original meteoroid data contained on the G-2 tape.

5.2.1 Determination of Experiment Package Conditions

In order to determine the accumulated time-area product, it was necessary to know the time when each meteoroid box and the memory were turned on and off. The "status" of each of these packages is given in each real-time frame; however, it was necessary to know some information about the previous or subsequent real-time run to determine the "condition" of each package. We define our terminology in this way: "Status" refers to that which is given in the command status word of the real-time run and tells simply that at the time of the run the particular packages was on or off. "Condition" refers to one of four states: off, being turned on, on, or being turned off. To determine the condition from the information on the tape it was necessary to determine whether a particular

real-time routine was run before or after the sending of commands which could change the status of any meteoroid related package. This was done by referring to the pass summaries and assigning a notation by hand to each real-time run. If a run was prior to commands or there were no commands it was called "A" in place of "RT" in the frame leader. If it followed commands it was called "B". With this information and the status from the command status word it was possible to determine the appropriate condition for each package. The procedure may be followed by reference to the generalized flow diagram in Figure 5-1. The results were stored on a new tape in the data portions of the relevant real-time frames.

5.2.2 Area Calculations

The areas for meteoroid detection actually refer to an area-solid angle product. The resulting units are cm^2 or m^2 and actually refer to the equivalent cross-sectional area of a sphere in an omnidirectional flux of particles. For each real-time frame a set of six areas (defined in the above manner) was calculated. These were areas for velocity, top plane, and bottom plane fluxes on each meteoroid package calculated individually for "good" sensors.

The term "good" refers to those sensors which are believed to be capable of sensing the passage of a particle. The determination of "good" sensors is not absolute and the uncertainties give one of the largest errors involved in the measurements. All the information available was used to make the assessment "good" or "bad". This information included the shorts as measured from the column leakage currents and those sensors showing excessive counts in the memory. Four counts or greater in a particular sensor was selected as being excessive, since a preliminary Poisson analysis indicated that a trivial number of sensors with four counts or above should be observed.

The determination of the location of a shorted sensor was made in the following rather complex manner. First all sensors which had four

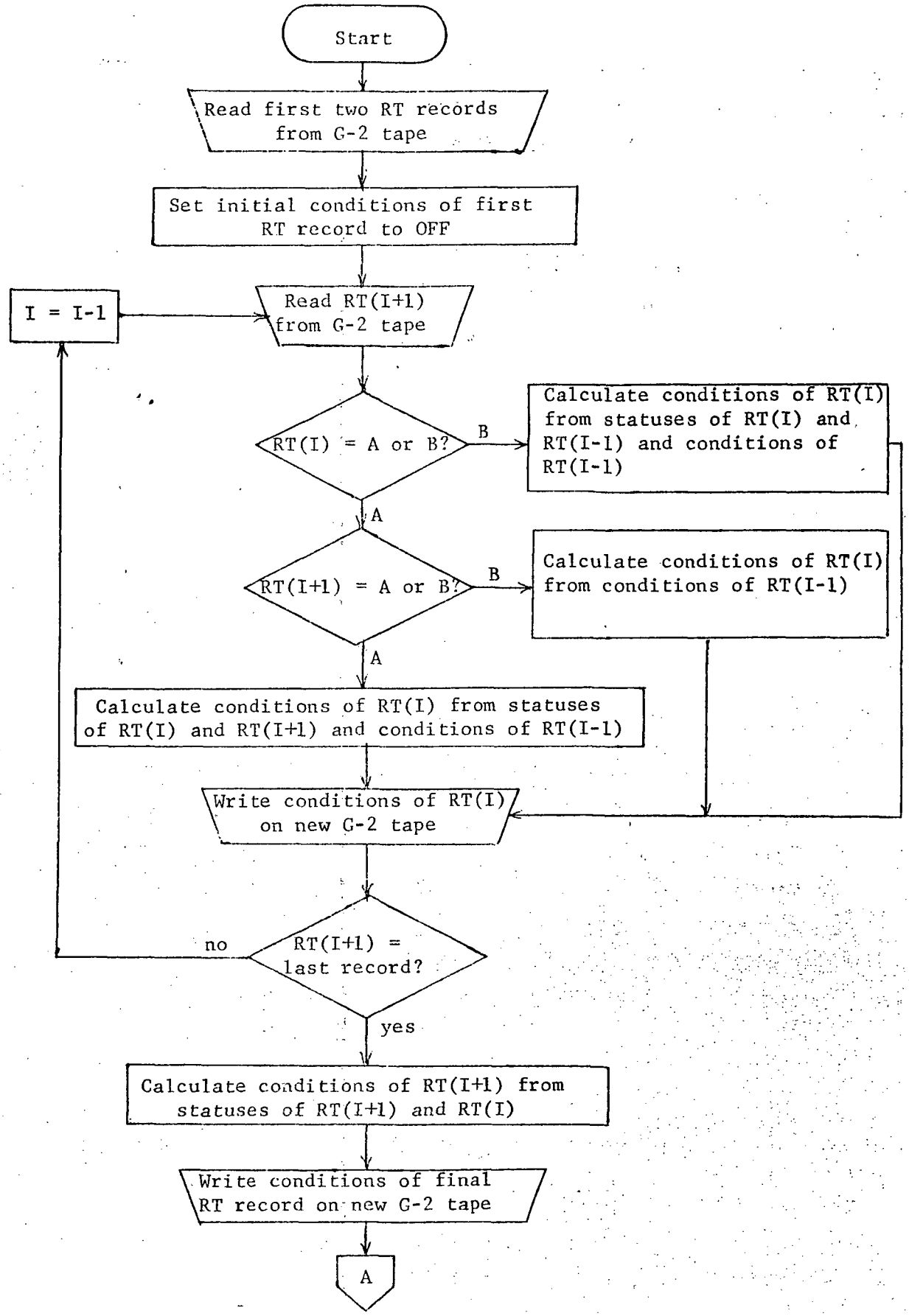

Fig. 5-1. Generalized Flow Diagram of Meteoroid Data Analysis

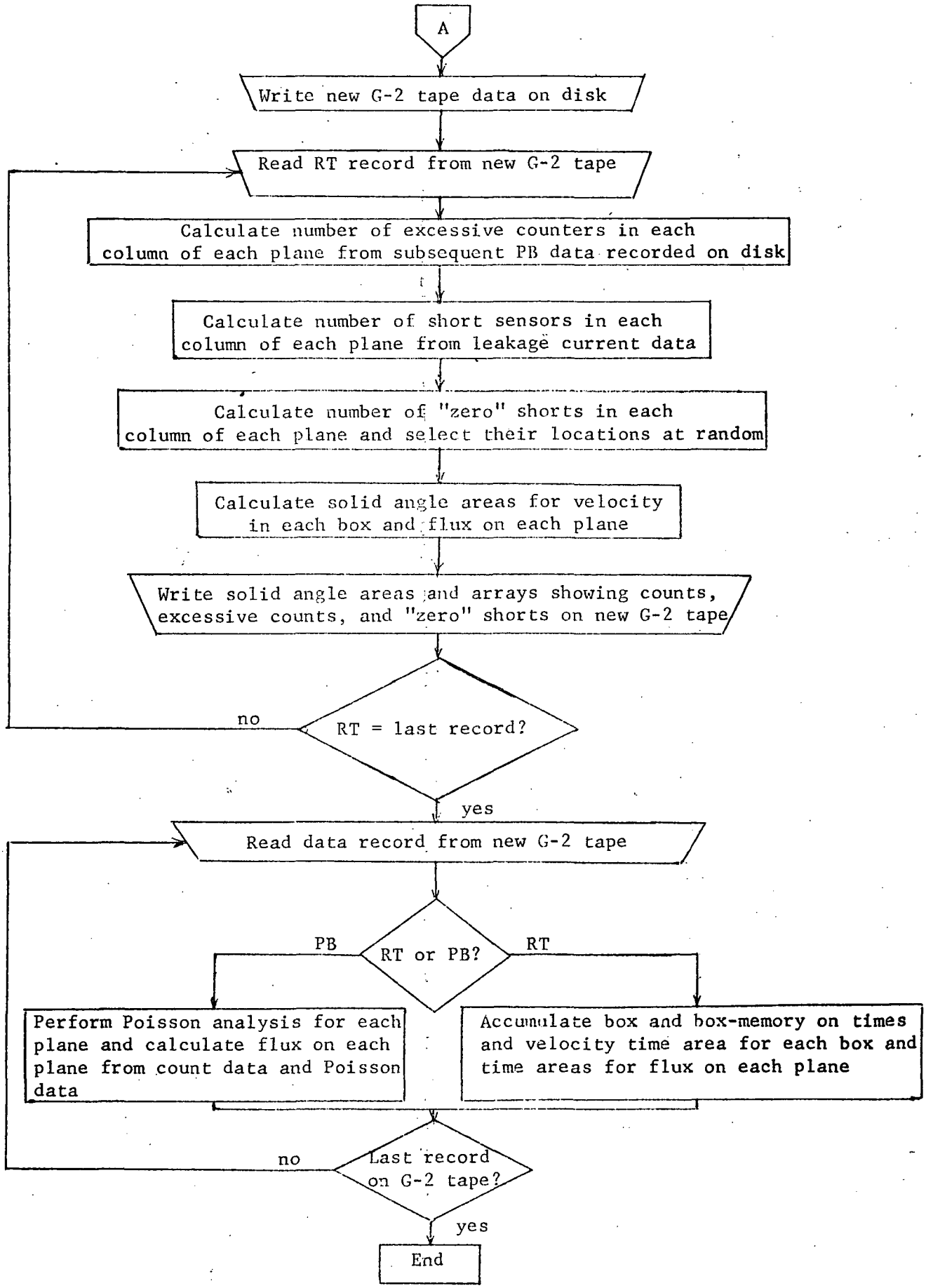

Fig. 5-1. Continued

or more discharges for the entire life of the experiment were marked at the beginning of the analyses by adding the number 100,000 to each count. Sensors so marked were considered to be "bad" and their time-area product was not accumulated. The number of shorted sensors in each column was calculated from the leakage current of that column. The shorts were then assigned to those sensors which had excessive counts, the assumption being that these were likely broken sensors which periodically pulsed due to movement of the film caused by solar heating. If there were more shorts on a given column than sensors with excessive counts, a random selection routine was used to assign the short to a sensor with zero counts. The assumption here is that a sensor could have been broken and shorted at launch and, thus, would never have counted. These are termed "zero shorts" and were marked on the printout by replacing the zero with the number 1000. For the case of less shorts than those with excessive counts, the excessive counts were still called "bad". The computer printouts showing this information for most of the RMS data dumps are given in Table 5-1. In going through the entries in the table one may observe the accumulation of data and the increase in the number of bad sensors as a function of orbit number or time (GMT). A summary of the information is given at the bottom of each page of the table. The term "hard shorts" refers to the number of shorts obtained for the leakage currents and "fast shorts" refers to the number of excessive counters which are considered to be shorted as described in paragraph 5.1.2 above.

With the definitions of "good" and "bad" sensors as given above we can describe the three types of areas which were calculated:

(a) Velocity Area - This refers to the total area-solid angle (as defined above) which was available at the time of any real-time data dump to accept velocity words. Since the four standby storage words were used, this area was available for a reading any time a meteoroid package was on. The area was calculated individually for each "good" top plane sensor and each "good" bottom plane sensor except for those paths which were subtended by the wind shields at the

TABLE 5-1. LISTINGS OF RMS MEMORY DUMPS OF METEOROID SENSOR DISCHARGES

ORBIT NO. 15, STATION FTMYRS, TYPE B, GMT = 314 5 11 23 (8467837 CENTISECONDS)

ROW	0	1	2	3	4	5	6	7
			FLUX COUNTS, BOX 1, PLANE 1					
COLUMN 0	100000	0	100003	100000	0	0	100000	0
COLUMN 1	0	0	0	100000	0	100000	0	100000
COLUMN 2	100000	0	0	100000	100000	100000	100000	0
COLUMN 3	0	100000	0	0	100000	0	0	100000
COLUMN 4	0	0	100000	0	0	0	0	0
COLUMN 5	100000	0	100000	100000	100009	100000	100000	0
COLUMN 6	0	100000	0	100000	0	0	0	0
COLUMN 7	0	0	100000	0	100000	100000	0	100000
			FLUX COUNTS, BOX 1, PLANE 2					
COLUMN 0	0	100000	0	0	0	0	0	100001
COLUMN 1	0	0	0	0	100000	0	100000	0
COLUMN 2	0	0	100000	0	0	0	0	0
COLUMN 3	0	100000	0	0	0	0	0	0
COLUMN 4	0	0	0	0	0	0	0	100000
COLUMN 5	0	0	0	0	0	0	0	0
COLUMN 6	0	0	0	0	0	0	0	0
COLUMN 7	0	0	0	0	0	0	0	100000
			FLUX COUNTS, BOX 2, PLANE 1					
COLUMN 0	100000	100000	100000	0	0	0	100000	0
COLUMN 1	100001	100000	0	0	0	1	0	100000
COLUMN 2	0	100000	0	0	100000	100000	0	0
COLUMN 3	100000	2	100000	0	100000	2	0	100000
COLUMN 4	1	1	100000	100000	100000	0	0	100516
COLUMN 5	0	0	100000	100000	0	0	0	100000
COLUMN 6	0	0	1000	100000	0	1000	0	0
COLUMN 7	100007	100002	0	0	107325	0	0	100000
			FLUX COUNTS, BOX 2, PLANE 2					
COLUMN 0	0	0	0	0	0	0	0	2
COLUMN 1	0	0	0	0	0	0	0	0
COLUMN 2	0	100000	0	0	0	0	0	0
COLUMN 3	0	0	0	0	0	0	0	0
COLUMN 4	100000	0	0	0	0	0	0	100000
COLUMN 5	0	0	0	0	100009	0	0	0
COLUMN 6	0	0	0	0	0	0	0	0
COLUMN 7	0	1	0	0	0	0	0	0

	BOX 1	BOX 2		BOX 1 PLANE 1	BOX 1 PLANE 2	BOX 2 PLANE 1	BOX 2 PLANE 2
STATUS	1	1	NO. OF HARD SHORTS	7	2	15	0
CONDITION	2	2	NO. OF ZERO SHORTS	0	0	2	0
MEMORY-BOX CONDITION	1	1	NO. OF FAST SHORTS	28	8	26	4
VEL AREA(10-3 CM+2)	7751	6760	FLUX AREA(10-3 CM+2)	31960	6567	27801	5250

MEMORY STATUS = 0, MEMORY CONDITION = 1

NOTES: ZERO SHORTS ARE MARKED BY 1000. EXCESSIVE COUNTERS ARE MARKED BY HAVING 100000 ADDED TO THE COUNTS.

TABLE 5-1. (CONTINUED)

ORBIT NO. 88, STATION ORORAL, TYPE A, GMT = 318 22 41 47 (49330229 CENTISECONDS)

ROW	0	1	2	3	4	5	6	7
				FLUX COUNTS, BOX 1, PLANE 1				
COLUMN 0	100000	1000	100216	100001	0	0	100000	1
COLUMN 1	0	2	0	100003	0	100009	0	100000
COLUMN 2	100038	0	0	100004	100004	100310	100000	0
COLUMN 3	0	100000	0	0	100001	0	0	100004
COLUMN 4	1	0	100023	0	0	0	1	0
COLUMN 5	100074	0	100004	100000	100150	100008	100055	0
COLUMN 6	1	100000	0	100003	0	0	0	0
COLUMN 7	0	0	100004	1	100008	100002	0	100000
				FLUX COUNTS, BOX 1, PLANE 2				
COLUMN 0	0	100031	1	0	0	0	0	100007
COLUMN 1	2	0	0	2	100006	0	100004	1
COLUMN 2	0	1	100000	1	0	0	0	1
COLUMN 3	0	100001	0	0	0	0	0	0
COLUMN 4	0	0	0	0	0	0	0	100001
COLUMN 5	0	2	0	1	0	0	0	0
COLUMN 6	0	0	0	0	0	0	0	0
COLUMN 7	0	1	0	0	0	0	0	100000
				FLUX COUNTS, BOX 2, PLANE 1				
COLUMN 0	100000	100000	100001	0	0	0	100007	0
COLUMN 1	100008	100001	0	0	0	1	0	100069
COLUMN 2	0	100000	0	0	100004	100000	0	0
COLUMN 3	100000	2	100000	0	100000	2	0	100000
COLUMN 4	2	1	100000	100000	100000	0	0	100932
COLUMN 5	0	0	100000	100000	1	0	1	100000
COLUMN 6	0	0	0	100001	0	0	0	0
COLUMN 7	100018	100017	0	0	134684	0	0	100000
				FLUX COUNTS, BOX 2, PLANE 2				
COLUMN 0	0	0	0	0	0	0	0	2
COLUMN 1	0	0	0	0	0	0	0	0
COLUMN 2	0	100000	0	0	0	0	0	0
COLUMN 3	0	0	0	0	0	0	0	0
COLUMN 4	100000	0	0	0	0	0	0	100000
COLUMN 5	0	0	0	0	100009	0	0	0
COLUMN 6	0	0	0	0	0	0	0	0
COLUMN 7	0	1	0	0	0	0	0	0

	BOX 1	BOX 2		BOX 1		BOX 2	
				PLANE 1	PLANE 2	PLANE 1	PLANE 2
STATUS	1	0	NO. OF HARD SHORTS	18	2	0	0
CONDITION	3	1	NO. OF ZERO SHORTS	1	0	0	0
MEMORY-BOX CONDITION	3	1	NO. OF FAST SHORTS	29	8	26	4
VEL AREA(10-3 CM+2)	7638	0	FLUX AREA(10-3 CM+2)	31157	6680	0	0

MEMORY STATUS = 1, MEMORY CONDITION = 3

NOTES: ZERO SHORTS ARE MARKED BY 1000. EXCESSIVE COUNTERS ARE MARKED BY HAVING 100000 ADDED TO THE COUNTS.

TABLE 5-1. (CONTINUED)

ORBIT NO. 88, STATION ORORAL, TYPE B, GMT = 318 22 44 42 (49347705 CENTISECONDS)

ROW	0	1	2	3	4	5	6	7
			FLUX COUNTS, BOX 1, PLANE 1					
COLUMN 0	100000	0	100216	100001	1000	0	100000	1
COLUMN 1	0	2	0	100003	0	100009	0	100000
COLUMN 2	100038	0	0	100004	100004	100310	100000	0
COLUMN 3	0	100000	0	1	100001	0	0	100005
COLUMN 4	1	0	100029	0	0	0	1	0
COLUMN 5	100074	0	100004	100000	100171	100008	100055	0
COLUMN 6	1	100000	0	100006	0	0	0	0
COLUMN 7	0	0	100004	1	100008	100003	0	100000
			FLUX COUNTS, BOX 1, PLANE 2					
COLUMN 0	0	100031	1	0	0	0	0	100007
COLUMN 1	2	0	0	2	100006	0	100004	1
COLUMN 2	0	1	100000	1	0	0	0	1
COLUMN 3	0	100001	0	0	0	0	0	0
COLUMN 4	0	0	0	0	0	0	0	100001
COLUMN 5	0	2	0	1	0	0	0	0
COLUMN 6	0	0	0	0	0	0	0	0
COLUMN 7	0	1	0	0	0	0	0	100000
			FLUX COUNTS, BOX 2, PLANE 1					
COLUMN 0	100000	100033	100015	0	0	0	100032	0
COLUMN 1	100020	100001	0	0	0	2	0	100104
COLUMN 2	0	100003	0	0	100004	100011	1	0
COLUMN 3	100000	2	100000	0	100000	2	0	100005
COLUMN 4	2	1	100000	100002	100001	0	0	101109
COLUMN 5	1	0	100006	100000	1	0	1	100004
COLUMN 6	1000	0	1000	100003	0	1	0	1000
COLUMN 7	100041	100017	0	0	134989	0	0	100033
			FLUX COUNTS, BOX 2, PLANE 2					
COLUMN 0	0	0	0	0	0	0	0	3
COLUMN 1	0	0	0	0	0	1000	0	0
COLUMN 2	0	100000	0	0	0	0	0	0
COLUMN 3	0	0	0	0	0	0	0	0
COLUMN 4	100000	0	0	2	0	0	2	100009
COLUMN 5	0	0	0	0	100009	0	0	0
COLUMN 6	0	0	0	0	0	0	0	0
COLUMN 7	0	2	0	0	0	1	0	0

	BOX 1	BOX 2		BOX 1		BOX 2	
				PLANE 1	PLANE 2	PLANE 1	PLANE 2
STATUS	1	1	NO. OF HARD SHORTS	19	2	24	1
CONDITION	3	2	NO. OF ZERO SHORTS	1	0	3	1
MEMORY-BOX CONDITION	3	2	NO. OF FAST SHORTS	28	8	26	4
VEL AREA(10-3 CM*2)	7516	6492	FLUX AREA(10-3 CM*2)	31003	6902	26808	5282

MEMORY STATUS = 1, MEMORY CONDITION = 3

NOTES: ZERO SHORTS ARE MARKED BY 1000. EXCESSIVE COUNTERS ARE MARKED BY HAVING 100000 ADDED TO THE COUNTS.

TABLE 5-1. (CONTINUED)

ORBIT NO. 97, STATION SNTAGO, TYPE 8, GMT = 319 12 35 3 (54329800 CENTISECONDS)

ROW	0	1	2	3	4	5	6	7
				FLUX COUNTS, BOX 1, PLANE 1				
COLUMN 0	100000	1000	100216	100001	0	0	100000	1
COLUMN 1	0	2	0	100003	0	100009	0	100000
COLUMN 2	100885	1000	1000	100004	100004	100310	100000	1000
COLUMN 3	0	100000	0	1	100001	0	0	100007
COLUMN 4	1	1000	100030	0	1000	0	1	0
COLUMN 5	100074	0	100004	100000	100199	100008	100055	0
COLUMN 6	1	100000	0	100006	0	0	0	0
COLUMN 7	0	0	100004	1	100008	100003	0	100000
				FLUX COUNTS, BOX 1, PLANE 2				
COLUMN 0	0	100031	1	0	0	0	0	100007
COLUMN 1	2	0	0	2	100006	0	100004	1
COLUMN 2	0	1	100000	1	0	0	0	1
COLUMN 3	0	100001	0	1	0	0	0	0
COLUMN 4	0	0	0	0	0	0	0	100001
COLUMN 5	0	2	0	1	0	0	0	0
COLUMN 6	0	0	0	0	0	0	0	0
COLUMN 7	0	1	0	0	0	0	0	100000
				FLUX COUNTS, BOX 2, PLANE 1				
COLUMN 0	100000	100034	100015	0	0	0	100032	0
COLUMN 1	100020	100001	0	0	0	2	0	100104
COLUMN 2	0	100003	0	0	100004	100011	1	0
COLUMN 3	100000	2	100000	0	100000	2	0	100005
COLUMN 4	2	1	100000	100002	100001	0	0	101109
COLUMN 5	1	0	100006	100000	1	0	1	100004
COLUMN 6	1000	1000	0	100003	1000	1	0	0
COLUMN 7	100041	100017	0	0	134989	0	0	100033
				FLUX COUNTS, BOX 2, PLANE 2				
COLUMN 0	0	0	0	0	0	0	0	3
COLUMN 1	0	0	0	0	0	0	0	1000
COLUMN 2	0	100000	0	0	0	0	0	0
COLUMN 3	0	0	0	0	0	0	0	0
COLUMN 4	100000	0	0	2	0	0	2	100009
COLUMN 5	0	0	0	0	100009	0	0	0
COLUMN 6	0	0	0	0	0	0	0	0
COLUMN 7	0	2	0	0	0	1	0	0

	BOX 1	BOX 2
STATUS	1	0
CONDITION	3	1
MEMORY-BOX CONDITION	2	1
VEL AREA(10-3 CM+2)	6561	0

	BOX 1		BOX 2	
	PLANE 1	PLANE 2	PLANE 1	PLANE 2
NO. OF HARD SHORTS	27	2	24	1
NO. OF ZERO SHORTS	8	0	3	1
NO. OF FAST SHORTS	28	8	26	4
FLUX AREA(10-3 CM+2)	26793	7757	0	0

MEMORY STATUS = 1, MEMORY CONDITION = 2

NOTES: ZERO SHORTS ARE MARKED BY 1000. EXCESSIVE COUNTERS ARE MARKED BY HAVING 100000 ADDED TO THE COUNTS.

TABLE 5-1. (CONTINUED)

ORBIT NO. 206, STATION SNTAGO, TYPE A, GMT = 325 13 51 36 (106629077 CENTISECONDS)

ROW	0	1	2	3	4	5	6	7
				FLUX COUNTS, BOX 1, PLANE 1				
COLUMN 0	100005	1000	100216	100053	1000	0	100450	1
COLUMN 1	0	2	0	100003	3	100010	0	100004
COLUMN 2	101045	1	0	100023	100256	100354	100032	0
COLUMN 3	1000	100046	0	1	100004	0	0	100010
COLUMN 4	1	1	100043	0	1000	1000	1	2
COLUMN 5	100074	0	100006	100009	100392	100008	100055	0
COLUMN 6	1	100030	0	100018	0	0	0	2
COLUMN 7	0	0	100007	3	100009	100007	0	100196
				FLUX COUNTS, BOX 1, PLANE 2				
COLUMN 0	0	100031	1	0	0	0	0	100011
COLUMN 1	3	0	0	2	100007	0	100005	1
COLUMN 2	0	3	100000	1	0	0	0	1
COLUMN 3	0	100004	0	1	0	0	0	0
COLUMN 4	0	0	0	0	0	0	0	100006
COLUMN 5	0	3	0	1	0	0	0	0
COLUMN 6	0	0	0	1	0	0	0	0
COLUMN 7	0	1	0	0	0	0	0	100008
				FLUX COUNTS, BOX 2, PLANE 1				
COLUMN 0	100036	100052	100870	0	0	0	100072	0
COLUMN 1	100035	100010	0	1000	0	2	0	100158
COLUMN 2	0	100013	0	1000	100020	100011	1	0
COLUMN 3	100296	2	100010	0	100000	2	0	100008
COLUMN 4	3	1	100011	100004	100001	0	0	101519
COLUMN 5	2	0	100051	100019	1	0	1	100013
COLUMN 6	1000	1000	0	100004	0	2	0	1000
COLUMN 7	100400	100017	0	0	144377	0	0	100073
				FLUX COUNTS, BOX 2, PLANE 2				
COLUMN 0	0	1000	0	0	0	0	0	3
COLUMN 1	1	0	1000	0	0	0	0	0
COLUMN 2	0	100000	0	0	0	0	0	1
COLUMN 3	0	1	1000	0	0	0	2	0
COLUMN 4	100003	0	1	2	0	0	3	100010
COLUMN 5	0	0	0	0	100009	0	0	0
COLUMN 6	0	0	0	0	0	0	1000	0
COLUMN 7	0	2	0	1	2	2	0	0

	BOX 1	BOX 2		BOX 1		BOX 2	
				PLANE 1	PLANE 2	PLANE 1	PLANE 2
STATUS	1	1	NO. OF HARD SHORTS	25	2	29	4
CONDITION	3	3	NO. OF ZERO SHORTS	5	0	5	4
MEMORY-BOX CONDITION	1	1	NO. OF FAST SHORTS	28	9	26	4
VEL AREA(10-3 CM+2)	6668	5789	FLUX AREA(10-3 CM+2)	27611	7650	25582	5467

MEMORY STATUS = 0, MEMORY CONDITION = 1

NOTES: ZERO SHORTS ARE MARKED BY 1000. EXCESSIVE COUNTERS ARE MARKED BY HAVING 100000 ADDED TO THE COUNTS.

TABLE 5-1. (CONTINUED)

ORBIT NO. 332, STATION ORORAL, TYPE B, GMT = 334 14 53 1 (184757610 CENTISECONDS)

ROW	0	1	2	3	4	5	6	7
				FLUX COUNTS, BOX 1, PLANE 1				
COLUMN 0	100005	0	100216	100054	0	1000	100450	1
COLUMN 1	0	2	0	100025	3	100010	0	100004
COLUMN 2	101045	1	1	100023	100257	100354	100032	0
COLUMN 3	0	100046	0	1	100004	0	0	100010
COLUMN 4	1	1	100043	0	1000	1000	1	2
COLUMN 5	100074	0	100006	100009	100392	100008	100055	0
COLUMN 6	2	100030	0	100018	0	0	1000	2
COLUMN 7	0	0	100007	3	100009	100007	0	100196
				FLUX COUNTS, BOX 1, PLANE 2				
COLUMN 0	0	100031	1	0	0	0	0	100011
COLUMN 1	3	0	0	3	100007	0	100006	1
COLUMN 2	0	3	100038	1	0	0	0	1
COLUMN 3	0	100004	0	1	0	0	0	0
COLUMN 4	0	0	0	0	0	0	0	100006
COLUMN 5	0	3	0	1	0	0	0	0
COLUMN 6	0	0	0	1	0	0	0	0
COLUMN 7	0	1	0	0	0	0	0	100008
				FLUX COUNTS, BOX 2, PLANE 1				
COLUMN 0	100036	100052	100870	0	0	0	100072	0
COLUMN 1	100035	100010	1000	1	0	2	0	100158
COLUMN 2	0	100013	0	0	100020	100011	2	0
COLUMN 3	100296	2	100010	0	100047	2	0	100008
COLUMN 4	3	1	100011	100004	101120	0	0	101519
COLUMN 5	2	0	100051	100019	1	0	1	100013
COLUMN 6	0	0	0	100004	1000	2	1000	0
COLUMN 7	100405	100017	0	0	144417	0	0	100073
				FLUX COUNTS, BOX 2, PLANE 2				
COLUMN 0	0	1000	0	0	0	0	0	3
COLUMN 1	1	0	0	1000	0	0	1000	0
COLUMN 2	0	100024	0	0	0	0	0	1
COLUMN 3	0	1	0	0	0	0	2	1000
COLUMN 4	100006	0	1	2	0	0	3	100010
COLUMN 5	0	0	0	0	100009	0	0	0
COLUMN 6	0	0	0	1000	0	0	0	0
COLUMN 7	1000	2	0	1	2	3	0	0

	BOX 1	BOX 2		BOX 1 PLANE 1	BOX 1 PLANE 2	BOX 2 PLANE 1	BOX 2 PLANE 2
STATUS	1	1	NO. OF HARD SHORTS	26	2	26	6
CONDITION	3	3	NO. OF ZERO SHORTS	4	0	3	6
MEMORY-BOX CONDITION	2	2	NO. OF FAST SHORTS	28	8	26	4
VEL AREA(10-3 CM+2)	6604	6003	FLUX AREA(10-3 CM+2)	28080	7714	27387	4885

MEMORY STATUS = 1, MEMORY CONDITION = 2

NOTES: ZERO SHORTS ARE MARKED BY 1000. EXCESSIVE COUNTERS ARE MARKED BY HAVING 100000 ADDED TO THE COUNTS.

TABLE 5-1. (CONTINUED)

ORBIT NO. 617, STATION SNTA60, TYPE 8, GMT = 352 20 21 28 (342248269 CENTISECONDS)

ROW	0	1	2	3	4	5	6	7
			FLUX COUNTS, BOX 1, PLANE 1					
COLUMN 0	100005	1000	100216	100054	1000	1000	100450	1
COLUMN 1	0	2	0	100026	3	100010	0	100004
COLUMN 2	101045	1	1	100023	100257	100354	100032	0
COLUMN 3	0	100046	0	1	100004	0	0	100010
COLUMN 4	1	1	100043	0	1000	1000	1	2
COLUMN 5	100074	0	100006	100009	100392	100008	100055	0
COLUMN 6	2	100030	0	100018	0	0	0	2
COLUMN 7	0	0	100007	3	100009	100007	0	100196
			FLUX COUNTS, BOX 1, PLANE 2					
COLUMN 0	0	100031	1	0	0	0	0	100011
COLUMN 1	3	0	0	3	100007	0	100006	1
COLUMN 2	1000	3	100038	1	1000	0	0	1
COLUMN 3	0	100004	0	1	0	0	0	0
COLUMN 4	0	0	0	0	0	0	0	100006
COLUMN 5	0	3	0	1	0	0	0	0
COLUMN 6	0	0	0	1	0	0	0	0
COLUMN 7	0	1	0	0	0	0	0	100008
			FLUX COUNTS, BOX 2, PLANE 1					
COLUMN 0	100036	100052	100870	0	0	0	100072	0
COLUMN 1	100035	100010	0	1	0	2	1000	100158
COLUMN 2	0	100013	0	0	100020	100011	2	0
COLUMN 3	100296	2	100010	0	100047	2	0	100008
COLUMN 4	3	1	100011	100004	101121	0	0	101519
COLUMN 5	2	0	100051	100019	1	0	1	100013
COLUMN 6	1000	1000	0	100004	0	2	0	0
COLUMN 7	100405	100017	0	0	144417	0	0	100073
			FLUX COUNTS, BOX 2, PLANE 2					
COLUMN 0	1000	1000	0	0	0	0	1000	3
COLUMN 1	1	1000	0	0	0	0	0	1000
COLUMN 2	0	100024	0	0	0	0	0	1
COLUMN 3	0	1	0	0	0	1000	2	0
COLUMN 4	100006	0	1	2	0	0	3	100010
COLUMN 5	0	0	0	0	100009	0	0	0
COLUMN 6	0	0	1000	0	0	0	0	0
COLUMN 7	0	2	0	1	2	3	1000	0

	BOX 1	BOX 2		BOX 1		BOX 2	
				PLANE 1	PLANE 2	PLANE 1	PLANE 2
STATUS	1	0	NO. OF HARD SHORTS	28	4	24	9
CONDITION	3	1	NO. OF ZERO SHORTS	5	2	3	8
MEMORY-BOX CONDITION	4	1	NO. OF FAST SHORTS	29	9	26	4
VEL AREA(10-3 CM+2)	6274	0	FLUX AREA(10-3 CM+2)	27309	7447	0	0

MEMORY STATUS = 0, MEMORY CONDITION = 4

NOTES: ZERO SHORTS ARE MARKED BY 1000. EXCESSIVE COUNTERS ARE MARKED BY HAVING 100000 ADDED TO THE COUNTS.

TABLE 5-1. (CONTINUED)

ORBIT NO. 770, STATION MADGAR, TYPE A, GMT = 362 14 30 32 (426542690 CENTISECONDS)

ROW	0	1	2	3	4	5	6	7
			FLUX COUNTS, BOX 1, PLANE 1					
COLUMN 0	100005	1000	100216	100054	1000	1000	100450	1
COLUMN 1	1000	2	0	100026	3	100010	0	100004
COLUMN 2	101045	1	1	100023	100257	100354	100032	1000
COLUMN 3	0	100046	0	1	100004	0	0	100010
COLUMN 4	1	1	100043	1000	1000	1000	1	2
COLUMN 5	100074	0	100006	100009	100392	100008	100055	0
COLUMN 6	2	100030	0	100018	0	1000	1000	2
COLUMN 7	0	0	100007	3	100009	100007	0	100196
			FLUX COUNTS, BOX 1, PLANE 2					
COLUMN 0	0	100031	1	0	0	0	0	100011
COLUMN 1	3	0	0	3	100007	0	100006	1
COLUMN 2	0	3	100038	1	1000	0	1000	1
COLUMN 3	0	100004	0	1	0	0	0	1000
COLUMN 4	0	0	0	0	0	0	0	100006
COLUMN 5	0	3	0	1	0	0	0	0
COLUMN 6	0	0	0	1	0	1000	0	0
COLUMN 7	0	1	0	0	0	0	0	100008
			FLUX COUNTS, BOX 2, PLANE 1					
COLUMN 0	100036	100052	100870	0	0	0	100072	0
COLUMN 1	100035	100010	1000	1	0	2	0	100158
COLUMN 2	0	100013	0	0	100020	100011	2	0
COLUMN 3	100296	2	100010	0	100047	2	0	100008
COLUMN 4	3	1	100011	100004	101121	0	0	101519
COLUMN 5	2	0	100051	100019	1	0	1	100013
COLUMN 6	0	1000	0	100004	1000	2	0	0
COLUMN 7	100405	100017	0	0	144417	0	0	100073
			FLUX COUNTS, BOX 2, PLANE 2					
COLUMN 0	0	0	0	1000	1000	1000	0	3
COLUMN 1	1	1000	1000	0	0	0	0	0
COLUMN 2	0	100024	0	0	0	0	0	1
COLUMN 3	0	1	0	0	0	0	2	1000
COLUMN 4	100006	0	1	2	0	0	3	100010
COLUMN 5	0	0	0	0	100009	0	0	0
COLUMN 6	0	0	0	0	1000	0	0	0
COLUMN 7	1000	2	0	1	2	3	0	0

	BOX 1	BOX 2		BOX 1		BOX 2	
				PLANE 1	PLANE 2	PLANE 1	PLANE 2
STATUS	1	0	NO. OF HARD SHORTS	38	6	24	9
CONDITION	3	1	NO. OF ZERO SHORTS	11	4	3	8
MEMORY-BOX CONDITION	1	1	NO. OF FAST SHORTS	28	8	26	4
VEL AREA(10-3 CM+2)	5014	0	FLUX AREA(10-3 CM+2)	22759	8263	0	0

MEMORY STATUS = 0, MEMORY CONDITION = 1

NOTES: ZERO SHORTS ARE MARKED BY 1000. EXCESSIVE COUNTERS ARE MARKED BY HAVING 100000 ADDED TO THE COUNTS.

TABLE 5-1. (CONTINUED)

ORBIT NO. 1001, STATION MADGAR, TYPE A, GMT = 12 6 8 42 (553131664 CENTISECONDS)

ROW	0	1	2	3	4	5	6	7
				FLUX COUNTS, BOX 1, PLANE 1				
COLUMN 0	100006	1000	100216	100054	1000	1000	100450	1
COLUMN 1	0	2	1000	100041	3	100010	0	100004
COLUMN 2	101045	1	1	100023	100257	100354	100032	1000
COLUMN 3	0	100046	0	1	100004	0	0	100010
COLUMN 4	1	1	100043	1000	1000	1000	1	2
COLUMN 5	100074	0	100006	100009	100392	100008	100058	0
COLUMN 6	2	100040	1000	100019	0	1000	0	2
COLUMN 7	0	1	100007	3	100009	100007	0	100196
				FLUX COUNTS, BOX 1, PLANE 2				
COLUMN 0	0	100035	1	0	0	0	0	100012
COLUMN 1	3	0	0	3	100010	0	100006	1
COLUMN 2	1000	3	100038	1	0	1000	0	1
COLUMN 3	0	100004	0	1	0	0	0	1000
COLUMN 4	0	1000	0	1000	1000	1000	1000	100006
COLUMN 5	0	3	0	1	0	0	0	0
COLUMN 6	1000	0	0	1	0	0	0	0
COLUMN 7	0	1	0	0	0	0	0	100008
				FLUX COUNTS, BOX 2, PLANE 1				
COLUMN 0	100036	100052	100870	0	0	0	100072	0
COLUMN 1	100035	100010	0	1	1000	2	0	100158
COLUMN 2	0	100013	0	0	100020	100011	2	0
COLUMN 3	100296	2	100010	0	100047	2	0	100008
COLUMN 4	3	1	100011	100004	101121	0	0	101519
COLUMN 5	2	0	100051	100019	1	0	1	100013
COLUMN 6	0	0	0	100004	1000	2	0	1000
COLUMN 7	100405	100017	0	0	144417	0	0	100073
				FLUX COUNTS, BOX 2, PLANE 2				
COLUMN 0	0	0	1000	0	0	1000	1000	3
COLUMN 1	1	0	1000	1000	0	0	0	0
COLUMN 2	0	100024	0	0	0	0	0	1
COLUMN 3	0	1	1000	0	0	0	2	0
COLUMN 4	100006	0	1	2	0	0	3	100010
COLUMN 5	0	0	0	0	100009	0	0	0
COLUMN 6	0	0	0	0	0	1000	0	0
COLUMN 7	0	2	1000	1	2	3	0	0

	BOX 1	BOX 2		BOX 1		BOX 2	
				PLANE 1	PLANE 2	PLANE 1	PLANE 2
STATUS	0	0	NO. OF HARD SHORTS	37	12	24	9
CONDITION	1	1	NO. OF ZERO SHORTS	10	9	3	8
MEMORY-BOX CONDITION	1	1	NO. OF FAST SHORTS	28	8	26	4
VEL AREA(10-3 CM*2)	0	0	FLUX AREA(10-3 CM*2)	0	0	0	0

MEMORY STATUS = 0, MEMORY CONDITION = 1

NOTES: ZERO SHORTS ARE MARKED BY 1000. EXCESSIVE COUNTERS ARE MARKED BY HAVING 100000 ADDED TO THE COUNTS.

TABLE 5-1. (CONTINUED)

ORBIT NO. 1042, STATION ARORAL, TYPE B, GMT = 14 20 7 46 (575446085 CENTISECONDS)

ROW	0	1	2	3	4	5	6	7
				FLUX COUNTS, BOX 1, PLANE 1				
COLUMN 0	100006	0	100215	100054	1000	0	100450	1
COLUMN 1	0	2	0	100041	3	100010	0	100004
COLUMN 2	101045	1	1	100023	100257	100354	100032	0
COLUMN 3	0	100046	0	1	100004	0	0	100010
COLUMN 4	1	1	100043	1000	0	1000	1	2
COLUMN 5	100074	0	100006	100009	100392	100008	100058	0
COLUMN 6	2	100040	0	100018	1000	0	0	2
COLUMN 7	0	1	100007	3	100009	100007	0	100196
				FLUX COUNTS, BOX 1, PLANE 2				
COLUMN 0	0	100035	1	0	0	0	0	100012
COLUMN 1	3	0	0	3	100010	0	100006	1
COLUMN 2	0	3	100038	1	0	1000	0	1
COLUMN 3	0	100004	0	1	0	0	0	0
COLUMN 4	0	0	0	0	0	0	0	100006
COLUMN 5	0	3	0	1	0	0	0	0
COLUMN 6	0	1000	0	1	0	0	0	0
COLUMN 7	0	1	0	0	0	0	0	100008
				FLUX COUNTS, BOX 2, PLANE 1				
COLUMN 0	100036	100052	100870	0	0	0	100072	0
COLUMN 1	100035	100010	0	1	0	2	0	100158
COLUMN 2	0	100013	0	0	100020	100011	2	0
COLUMN 3	100296	2	100010	0	100047	2	0	100008
COLUMN 4	3	1	100011	100004	101121	0	0	101519
COLUMN 5	2	0	100051	100019	1	0	1	100013
COLUMN 6	0	0	0	100004	1000	2	0	1000
COLUMN 7	100405	100017	0	0	144417	0	0	100073
				FLUX COUNTS, BOX 2, PLANE 2				
COLUMN 0	0	0	1000	0	0	1000	0	3
COLUMN 1	1	0	0	1000	1000	0	0	0
COLUMN 2	0	100024	0	0	0	0	0	1
COLUMN 3	0	1	0	0	0	0	2	1000
COLUMN 4	100006	0	1	2	0	0	3	100010
COLUMN 5	0	0	0	0	100009	0	0	0
COLUMN 6	0	0	0	0	0	0	1000	0
COLUMN 7	0	2	0	1	2	2	0	0

	BOX 1	BOX 2		BOX 1		BOX 2	
				PLANE 1	PLANE 2	PLANE 1	PLANE 2
STATUS	1	1	NO. OF HARD SHORTS	26	5	19	9
CONDITION	2	2	NO. OF ZERO SHORTS	4	2	2	6
MEMORY-BOX CONDITION	1	1	NO. OF FAST SHORTS	23	8	26	4
VEL AREA(10-3 CM+2)	6346	6125	FLUX AREA(10-3 CM+2)	28175	7440	27931	4582

MEMORY STATUS = 0, MEMORY CONDITION = 1

NOTES: ZERO SHORTS ARE MARKED BY 1000. EXCESSIVE COUNTERS ARE MARKED BY HAVING 100000 ADDED TO THE COUNTS.

end of each meteoroid box. The area formula used was

$$A_v = \frac{a^2 \cos^2\theta}{4\pi d^2}$$

where a is the individual sensor area, θ the angle between the normal to the sensors and the ray through the centers of the sensors and d is the distance between the centers. The individual areas A_v were then summed for each box and at each real-time run the boxes were on.

(b) Top Plane Area - This refers to the total area-solid angle viewed by each "good" sensor on the top planes of the meteoroid packages. The area A_t for each sensor individually is

$$A_t = a/4$$

less that area subtended by the wind shields. These were calculated and summed over all "good" sensors on each top plane at each real-time run only when the boxes and the memory were on together, since the counts were stored in memory.

(c) Bottom Plane Area - This area-solid angle was calculated for the combination of a "good" sensor on the bottom plane and a "bad" sensor on the top plane. This criterion was used, since the passage of a particle through a "good" top sensor would have resulted in a velocity word. The formula for the individual area A_b is the same as that used for velocity area, i.e.

$$A_b = \frac{a^2 \cos^2\theta}{4\pi d^2}$$

where the top sensor used is "bad" and the bottom one is "good".

After the areas were calculated they were used to generate a new tape in which the area values were stored in the data portion of each real-time frame.

5.2.3 Time-Area Accumulation

For the final analysis the last tape was processed using the previously determined conditions and the areas. The result was a running accumulation of "on" times for the individual meteoroid packages and the combination box-memory "on" time. For each "on" period the average area over that period was multiplied by the time and summed at each real-time run. This information was used in conjunction with the count information to determine the flux at each memory dump.

5.2.4 Poisson Analysis of Counts

A very superficial examination of the count data, which was accumulated in the memory, showed that most of the counts resulted from spurious breakdowns in the sensors. These most probably occurred in sensors which had been damaged at launch and were periodically shorting out, due to thermal stresses. A Binomial analysis would have been exact for this problem but for simplicity a Poisson analysis was used which introduced only a trivial uncertainty. The expression for the probability P_x of a sensor's receiving x counts is

$$P_x = \frac{m^x}{x!} e^{-m} \qquad (1)$$

where m is the mean number of counts per sensor. For our situation m is equal to the total number of counts divided by the number of "good" sensors (as defined above). A simple analysis was first made using the ratio of P_1 to P_0. One sees from Eq. (1) that

$$\frac{P_1}{P_0} = m$$

or

$$\frac{P_1}{P_0} = \frac{C}{N_g}$$

Since the number of sensors N_x with x counts is given by

$$N_x = P_x N_g$$

we have

$$\frac{N_1}{N_0} = \frac{C}{N_g}$$

or

$$C = \frac{N_1 N_g}{N_0} \qquad (2)$$

Using Eqs. (1) and (2) the values of N_x and C were calculated and the effective fluxes were determined. An output of the form shown in Table 5-2 was obtained. The top portion of the table shows the time and time-area accumulation for the real-time dumps and the bottom portion gives a summary which was made at each memory dump. The ease with which each data segment could be studied made it possible to locate the remaining anomalies in the data. First, four bad data accumulation periods were found. These all registered a large number of counts in the first observation period immediately after a particular box was turned on. This phenomenon is not unexpected and may result from a "shock" of the capacitors when the voltage was first applied or may actually be the "burn-out" resulting from meteoroids which struck the capacitor while the voltage was off. The time-area was not accumulated during these four periods and the counts were deleted.

The second type of anomaly became evident when the Poisson distribution was compared to the count distribution. This may be seen in Table 5-2. It is seen in all but one instance that the number of sensors with 2 and 3 counts is significantly greater than the number

TABLE 5-2. SAMPLE PRINTOUT FROM FIRST POISSON ANALYSIS USING ONLY RATIO N_1/N_0. THE DATA IN THIS TABLE IS SUPERSEDED BY TABLE 5-3, BUT IT INDICATES THE NUMBER OF EXCESSIVE COUNTS WHICH WERE ELIMINATED AS DISCUSSED IN THE TEXT.

ORB. NO.	GMT (.01 SEC)	TYPE	BOX	BOX COND.	TOTAL TIME ON	M-B COND.	TOTAL TIME ON	PLANE 1 (CM+2 SEC)	PLANE 2 (CM+2 SEC)	VELOCITY (CM+2 SEC)
1013	559303959	B	1	OFF	4831823	OFF	798235	0.2324E 08	0.5775E 07	0.2997E 08
			2	OFF	1698173	OFF	125164	0.3348E 07	0.6614E 06	0.9720E 07
1028	567464934	A	1	OFF	4831823	OFF	798235	0.2324E 08	0.5775E 07	0.2997E 08
			2	OFF	1698173	OFF	125164	0.3348E 07	0.6614E 06	0.9720E 07
1042	575426565	B	1	OFF	4831823	OFF	798235	0.2324E 08	0.5775E 07	0.2997E 08
			2	OFF	1698173	OFF	125164	0.3348E 07	0.6614E 06	0.9720E 07
1042	575446085	B	1	SWON	4831823	OFF	798235	0.2324E 08	0.5775E 07	0.2997E 08
			2	SWON	1698173	OFF	125164	0.3348E 07	0.6614E 06	0.9720E 07
1043	575849062	CRD	1	SWOF	4835852	OFF	798235	0.2324E 08	0.5775E 07	0.3000E 08
			2	SWOF	1702202	OFF	125164	0.3348E 07	0.6614E 06	0.9744E 07
1048	575983684	A	1	OFF	4835852	OFF	798235	0.2324E 08	0.5775E 07	0.3000E 08
			2	OFF	1702202	OFF	125164	0.3348E 07	0.6614E 06	0.9744E 07
1047	577979616	A	1	OFF	4835852	OFF	798235	0.2324E 08	0.5775E 07	0.3000E 08
			2	OFF	1702202	OFF	125164	0.3348E 07	0.6614E 06	0.9744E 07
1073	591977062	CRD	1	OFF	4835852	OFF	798235	0.2324E 08	0.5775E 07	0.3000E 08
			2	OFF	1702202	OFF	125164	0.3348E 07	0.6614E 06	0.9744E 07
1083	597802591	A	1	OFF	4835852	OFF	798235	0.2324E 08	0.5775E 07	0.3000E 08
			2	OFF	1702202	OFF	125164	0.3348E 07	0.6614E 06	0.9744E 07
1107	610578662	CRD	1	OFF	4835852	OFF	798235	0.2324E 08	0.5775E 07	0.3000E 08
			2	OFF	1702202	OFF	125164	0.3348E 07	0.6614E 06	0.9744E 07

ORB. NO.	GMT (.01 SEC)	TYPE	BOX	PLANE	GOOD SENS	RATIO 1S/0S		NO. 0'S	NO. 1'S	NO. 2'S	NO. 3'S	NO. X'S	NO. COUNTS	FLUX (COUNTS/ CM+2 SEC)
1123	619298301	PB	1	1	32	0.556	DATA	18	8	4	2	28	22	0.9465E-06
							POISSON	18.4	10.2	2.8	0.5	0.1	17.8	0.7649E-06
			1	2	54	0.286	DATA	42	8	0	4	8	20	0.3463E-05
							POISSON	40.6	11.6	1.7	0.2	0.0	15.4	0.2672E-05
			2	1	36	0.185	DATA	27	4	4	1	26	15	0.4481E-05
							POISSON	29.9	5.5	0.5	0.0	0.0	6.7	0.1991E-05
			2	2	54	0.186	DATA	43	5	3	3	4	20	0.3024E-04
							POISSON	44.8	8.3	0.8	0.0	0.0	10.0	0.1519E-04

the Poisson analysis predicted. In other words the probability of a second and third discharge in a sensor is much larger than would be expected from real meteoroid events. The impliciation is that the sensor is damaged by a meteoroid and the probability is high that the sensor will spontaneously breakdown at a later time. To eliminate the error caused by these discharges it was necessary to use a slightly different relationship which is based on the following supposition: the total number of sensors with one, two, and three counts is known accurately; however, the distribution of counts in these sensors has been modified by the spurious breakdowns. We may obtain an expression using this information from Eq. (1) by summing the probabilities of obtaining one, two, and three counts and dividing by the probability of obtaining zero counts. The results are as follows:

$$\frac{P_1 + P_2 + P_3}{P_0} = m + \frac{m^2}{2} + \frac{m^3}{6}$$

Since

$$P_x = \frac{N_x}{N_g}$$

then

$$\frac{N_1 + N_2 + N_3}{N_0} = m + \frac{m^2}{2} + \frac{m^3}{6}$$

Using the solution for a cubic equation m was determined for each memory dump and the solution was found for C and the Poisson distribution was calculated and compared with the count data. The results of this analysis are given at various points in the mission in Table 5-3. This table gives a nearly complete history of the time-area and data accumulation during the entire RMS mission.

5.2.5 Flux Calculation

The last calculation made was to compute the flux at the time of

TABLE 5-3. PRINTOUTS OF TIME-AREA ACCUMULATIONS, POISSON ANALYSES, AND OTHER RELEVANT INFORMATION AS INDICATED IN THE TABLE

ORB. NO.	GMT DAY	HR	MN	TYPE	BOX	BOX COND.	TOTAL TIME ON	M-B COND.	TOTAL TIME ON	PLANE 1 (CM+2 SEC)	PLANE 2 (CM+2 SEC)	VELOCITY (CM+2 SEC)	ZERO P1	ZERO P2	SHORTS P1	SHORTS P2
3	313	11	37	A	1	OFF	0	OFF	0	0.0	0.0	0.0	0	0		
					2	OFF	0	OFF	0	0.0	0.0	0.0	0	0		
12	314	1	19	B	1	OFF	0	OFF	0	0.0	0.0	0.0	0	0		
					2	OFF	0	OFF	0	0.0	0.0	0.0	0	0		
13	314	1	54	A	1	OFF	0	OFF	0	0.0	0.0	0.0	0	0		
					2	OFF	0	OFF	0	0.0	0.0	0.0	0	0		
14	314	3	34	A	1	OFF	0	OFF	0	0.0	0.0	0.0	0	0		
					2	OFF	0	OFF	0	0.0	0.0	0.0	0	0		
15	314	5	11	B	1	SWON	0	OFF	0	0.0	0.0	0.0	0	0		
					2	SWON	0	OFF	0	0.0	0.0	0.0	0	0		
17	314	8	26	A	1	ON	11727	OFF	0	0.0	0.0	0.9090E 05	0	0		
					2	ON	11727	OFF	0	0.0	0.0	0.7318E 05	3	1		
18	314	10	5	A	1	ON	17669	OFF	0	0.0	0.0	0.1370E 06	0	0		
					2	ON	17669	OFF	0	0.0	0.0	0.1096E 06	3	1		

					BOX	PLANE	GOOD SENS	RATIO 123S/0S		NO. 0'S	NO. 1'S	NO. 2'S	NO. 3'S	NO. X'S	NO. COUNTS	FLUX (COUNTS/ CM+2 SEC)
23	314	16	48	PB	1	1	36	0.0	DATA	36	0	0	0	28	0	0.0
									POISSON	36.00	-0.00	0.00	-0.00	-0.00	0.0	0.0
					1	2	56	0.0	DATA	56	0	0	0	8	0	0.0
									POISSON	56.00	-0.00	0.00	-0.00	-0.00	0.0	0.0
					2	1	35	0.0	DATA	35	0	0	0	26	0	0.0
									POISSON	35.00	-0.00	0.00	-0.00	-0.00	0.0	0.0
					2	2	59	0.0	DATA	59	0	0	0	4	0	0.0
									POISSON	59.00	-0.00	0.00	-0.00	-0.00	0.0	0.0

ORB. NO.	GMT DAY	HR	MN	TYPE	BOX	BOX COND.	TOTAL TIME ON	M-B COND.	TOTAL TIME ON	PLANE 1 (CM+2 SEC)	PLANE 2 (CM+2 SEC)	VELOCITY (CM+2 SEC)	ZERO P1	ZERO P2	SHORTS P1	SHORTS P2
88	318	22	41	A	1	ON	408598	ON	333276	0.1040E 08	0.2244E 07	0.3107E 07	1	0		
					2	OFF	95315	OFF	19993	0.5030E 06	0.1067E 06	0.5826E 06	0	0		

					BOX	PLANE	GOOD SENS	RATIO 123S/0S		NO. 0'S	NO. 1'S	NO. 2'S	NO. 3'S	NO. X'S	NO. COUNTS	FLUX (COUNTS/ CM+2 SEC)
88	318	22	43	PB	1	1	35	0.207	DATA	29	5	1	0	28	7	0.6732E-06
									POISSON	29.00	5.45	0.51	0.03	0.00	6.58	0.6331E-06
					1	2	56	0.217	DATA	46	7	3	0	8	13	0.5793E-05
									POISSON	46.00	9.05	0.89	0.06	0.00	11.02	0.4910E-05
					2	1	38	0.086	DATA	35	3	0	0	26	3	0.5964E-05
									POISSON	35.00	2.88	0.12	0.00	0.00	3.13	0.6213E-05
					2	2	60	0.0	DATA	60	0	0	0	4	0	0.0
									POISSON	60.00	-0.00	0.00	-0.00	-0.00	0.0	0.0

ORB. NO.	GMT DAY	HR	MN	TYPE	BOX	BOX COND.	TOTAL TIME ON	M-B COND.	TOTAL TIME ON	PLANE 1 (CM+2 SEC)	PLANE 2 (CM+2 SEC)	VELOCITY (CM+2 SEC)	ZERO P1	ZERO P2	SHORTS P1	SHORTS P2
88	318	22	44	B	1	ON	408772	ON	333450	0.1040E 08	0.2245E 07	0.3109E 07	1	0		
					2	SWON	95315	OFF	19993	0.5030E 06	0.1067E 06	0.5826E 06	3	1		
90	319	0	57	A	1	ON	416755	ON	341433	0.1064E 08	0.2301E 07	0.3167E 07	3	0		
					2	ON	103298	OFF	19993	0.5030E 06	0.1067E 06	0.6310E 06	3	1		

					BOX	PLANE	GOOD SENS	RATIO 123S/0S		NO. 0'S	NO. 1'S	NO. 2'S	NO. 3'S	NO. X'S	NO. COUNTS	FLUX (COUNTS/ CM+2 SEC)
91	319	2	35	PB	1	1	33	0.269	DATA	26	6	1	0	28	8	0.7515E-06
									POISSON	26.00	6.20	0.74	0.06	0.00	7.87	0.7394E-06
					1	2	56	0.217	DATA	46	7	3	0	8	13	0.5650E-05
									POISSON	46.00	9.05	0.89	0.06	0.00	11.02	0.4788E-05
					2	1	35	0.094	DATA	32	3	0	0	26	3	0.5964E-05
									POISSON	32.00	2.87	0.13	0.00	0.00	3.14	0.6236E-05
					2	2	59	0.0	DATA	59	0	0	0	4	0	0.0
									POISSON	59.00	-0.00	0.00	-0.00	-0.00	0.0	0.0

TABLE 5-3. (CONTINUED)

ORB. NO.	GMT DAY	HR	MN	TYPE	BOX	BOX COND.	TOTAL TIME ON	M-B COND.	TOTAL TIME ON	PLANE 1 (CM+2 SEC)	PLANE 2 (CM+2 SEC)	VELOCITY (CM+2 SEC)	ZERO SHORTS P1	P2
93	319	5	51	A	1	ON	434381	ON	359059	0.1115E 08	0.2431E 07	0.3290E 07	5	0
					2	OFF	109327	OFF	19993	0.5030E 06	0.1067E 06	0.6675E 06	3	1
94	319	7	32	B	1	ON	440408	SWOF	365086	0.1131E 08	0.2477E 07	0.3329E 07	6	0
					2	OFF	109327	OFF	19993	0.5030E 06	0.1067E 06	0.6675E 06	3	1
97	319	12	35	B	1	ON	458589	SWON	365086	0.1131E 08	0.2477E 07	0.3448E 07	6	0
					2	OFF	109327	OFF	19993	0.5030E 06	0.1067E 06	0.6675E 06	3	1

		BOX	PLANE	GOOD SENS	RATIO 123S/OS		NO. 0'S	NO. 1'S	NO. 2'S	NO. 3'S	NO. X'S	NO. COUNTS	FLUX (COUNTS/ CM+2 SEC)
97	319 12 36	PB	1	1	30	0.304	DATA	23	6	1	0	28	8	0.7072E-06
							POISSON	23.00	6.11	0.81	0.07	0.01	7.98	0.7051E-06
			1	2	56	0.244	DATA	45	8	3	0	8	14	0.5651E-05
							POISSON	45.00	9.84	1.08	0.08	0.00	12.25	0.4945E-05
			2	1	35	0.094	DATA	32	3	0	0	26	3	0.5964E-05
							POISSON	32.00	2.87	0.13	0.00	0.00	3.14	0.6236E-05
			2	2	59	0.0	DATA	59	0	0	0	4	0	0.0
							POISSON	59.00	-0.00	0.00	-0.00	-0.00	0.0	0.0

ORB. NO.	GMT DAY	HR	MN	TYPE	BOX	BOX COND.	TOTAL TIME ON	M-B COND.	TOTAL TIME ON	PLANE 1 (CM+2 SEC)	PLANE 2 (CM+2 SEC)	VELOCITY (CM+2 SEC)	ZERO SHORTS P1	P2
145	322	14	54	B	1	ON	726118	SWOF	632615	0.1908E 08	0.4445E 07	0.5310E 07	4	0
					2	SWON	133003	OFF	19993	0.5030E 06	0.1067E 06	0.8129E 06	3	1
160	323	13	59	A	1	ON	809257	OFF	632615	0.1908E 08	0.4445E 07	0.5874E 07	4	0
					2	ON	216142	OFF	19993	0.5030E 06	0.1067E 06	0.1304E 07	4	2
168	324	1	30	A	1	ON	850730	OFF	632615	0.1908E 08	0.4445E 07	0.6151E 07	5	1
					2	ON	257615	OFF	19993	0.5030E 06	0.1067E 06	0.1542E 07	4	2
168	324	1	31	B	1	ON	850786	SWON	632615	0.1908E 08	0.4445E 07	0.6151E 07	5	0
					2	ON	257671	SWON	19993	0.5030E 06	0.1067E 06	0.1542E 07	4	2
175	324	13	8	B	1	ON	892604	SWOF	674433	0.2023E 08	0.4767E 07	0.6428E 07	5	0
					2	ON	299439	SWOF	61811	0.1529E 07	0.3369E 06	0.1783E 07	4	2
206	325	13	51	A	1	ON	981568	OFF	674433	0.2023E 08	0.4767E 07	0.7021E 07	5	0
					2	ON	388453	OFF	61811	0.1529E 07	0.3369E 06	0.2283E 07	5	4
226	327	18	40	A	1	ON	1171711	OFF	674433	0.2023E 08	0.4767E 07	0.8308E 07	3	0
					2	ON	578596	OFF	61811	0.1529E 07	0.3369E 06	0.3322E 07	5	5
230	328	1	10	A	1	ON	1195111	OFF	674433	0.2023E 08	0.4767E 07	0.8468E 07	4	0
					2	ON	601996	OFF	61811	0.1529E 07	0.3369E 06	0.3449E 07	6	5
230	328	1	13	B	1	SWOF	1195278	OFF	674433	0.2023E 08	0.4767E 07	0.8469E 07	4	0
					2	SWOF	602163	OFF	61811	0.1529E 07	0.3369E 06	0.3450E 07	6	5
231	328	2	49	A	1	OFF	1195278	OFF	674433	0.2023E 08	0.4767E 07	0.8469E 07	4	0
					2	OFF	602163	OFF	61811	0.1529E 07	0.3369E 06	0.3450E 07	6	5

		BOX	PLANE	GOOD SENS	RATIO 123S/OS		NO. 0'S	NO. 1'S	NO. 2'S	NO. 3'S	NO. X'S	NO. COUNTS	FLUX (COUNTS/ CM+2 SEC)
231	328 2 52	PB	1	1	32	0.600	DATA	20	7	3	2	28	19	0.9393E-06
							POISSON	19.97	9.42	2.22	0.35	0.05	15.09	0.7458E-06
			1	2	56	0.273	DATA	44	8	1	3	8	19	0.3986E-05
							POISSON	43.99	10.61	1.28	0.10	0.01	13.51	0.2834E-05
			2	1	32	0.143	DATA	23	4	0	0	26	4	0.2617E-05
							POISSON	28.00	3.74	0.25	0.01	0.00	4.27	0.2796E-05
			2	2	55	0.019	DATA	54	0	1	0	4	2	0.5937E-05
							POISSON	54.00	0.99	0.01	0.00	0.00	1.01	0.2995E-05

TABLE 5-3. (CONTINUED)

ORB. NO.	GMT DAY	HR	MN	TYPE	BOX	BOX COND.	TOTAL TIME ON	M-B COND.	TOTAL TIME ON	PLANE 1 (CM+2 SEC)	PLANE 2 (CM+2 SEC)	VELOCITY (CM+2 SEC)	ZERO P1	SHORTS P2
279	331	5	31	A	1	ON	1297795	OFF	674433	0.2023E 08	0.4767E 07	0.9146E 07	4	0
					2	ON	704696	OFF	61827	0.1529E 07	0.3369E 06	0.4021E 07	4	6
305	331	5	32	A	1	ON	1297837	OFF	674433	0.2023E 08	0.4767E 07	0.9146E 07	4	0
					2	ON	704738	OFF	61827	0.1529E 07	0.3369E 06	0.4022E 07	4	6
308	332	20	34	A	1	ON	1438359	OFF	674433	0.2023E 08	0.4767E 07	0.1009E 08	3	1
					2	ON	845260	OFF	61827	0.1529E 07	0.3369E 06	0.4734E 07	6	6
332	334	14	51	A	1	ON	1590587	OFF	674433	0.2023E 08	0.4767E 07	0.1110E 08	4	0
					2	ON	997488	OFF	61827	0.1529E 07	0.3369E 06	0.5529E 07	3	6
332	334	14	53	B	1	ON	1590664	SWON	674433	0.2023E 08	0.4767E 07	0.1110E 08	4	0
					2	ON	997565	SWON	61827	0.1529E 07	0.3369E 06	0.5529E 07	3	6

					BOX	PLANE	GOOD SENS	RATIO 123S/0S		NO. 0'S	NO. 1'S	NO. 2'S	NO. 3'S	NO. X'S	NO. COUNTS	FLUX (COUNTS/ CM+2 SEC)
337	334	21	58	PB	1	1	32	0.600	DATA	20	7	3	2	28	19	0.9393E-06
									POISSON	19.97	9.42	2.22	0.35	0.05	15.09	0.7458E-06
					1	2	56	0.273	DATA	44	8	1	3	8	19	0.3986E-05
									POISSON	43.99	10.61	1.28	0.10	0.01	13.51	0.2834E-05
					2	1	35	0.129	DATA	31	4	0	0	26	4	0.2616E-05
									POISSON	31.00	3.76	0.23	0.01	0.00	4.25	0.2778E-05
					2	2	54	0.019	DATA	53	0	1	0	4	2	0.5936E-05
									POISSON	53.00	0.99	0.01	0.00	0.00	1.01	0.2995E-05

TABLE 5-3. (CONTINUED)

ORB. NO.	GMT DAY	HR	MN	TYPE	BOX	BOX COND.	TOTAL TIME ON	M-B COND.	TOTAL TIME ON	PLANE 1 (CM+2 SEC)	PLANE 2 (CM+2 SEC)	VELOCITY (CM+2 SEC)	ZERO SHORTS P1	P2
337	334	22	0	B	1	ON	1616313	SWOF	700082	0.2095E 08	0.4965E 07	0.1127E 08	4	1
					2	ON	1023214	SWOF	87476	0.2188E 07	0.4623E 06	0.5674E 07	3	6
339	335	1	18	A	1	ON	1628200	OFF	700082	0.2095E 08	0.4965E 07	0.1135E 08	4	0
					2	ON	1035101	OFF	87476	0.2188E 07	0.4623E 06	0.5741E 07	3	6
351	335	19	23	A	1	ON	1693313	OFF	700082	0.2095E 08	0.4965E 07	0.1178E 08	4	1
					2	ON	1100214	OFF	87476	0.2188E 07	0.4623E 06	0.6114E 07	3	7
359	336	8	37	A	1	ON	1740901	OFF	700082	0.2095E 08	0.4965E 07	0.1209E 08	4	1
					2	ON	1147802	OFF	87476	0.2188E 07	0.4623E 06	0.6380E 07	3	7
362	336	12	59	A	1	SWOF	1756622	OFF	700082	0.2095E 08	0.4965E 07	0.1220E 08	2	1
					2	ON	1163523	OFF	87476	0.2188E 07	0.4623E 06	0.6469E 07	3	5
381	337	17	29	A	1	SWON	1756622	OFF	700082	0.2095E 08	0.4965E 07	0.1220E 08	2	1
					2	ON	1266163	OFF	87476	0.2188E 07	0.4623E 06	0.6856E 07	18	33
396	338	16	33	A	1	ON	1839620	OFF	700082	0.2095E 08	0.4965E 07	0.1276E 08	4	1
					2	ON	1349161	OFF	87476	0.2188E 07	0.4623E 06	0.7164E 07	3	7
411	339	15	35	A	1	ON	1922539	OFF	700082	0.2095E 08	0.4965E 07	0.1330E 08	4	1
					2	ON	1432080	OFF	87476	0.2188E 07	0.4623E 06	0.7644E 07	3	7
429	340	19	30	A	1	ON	2023052	OFF	700082	0.2095E 08	0.4965E 07	0.1396E 08	3	1
					2	ON	1532593	OFF	87476	0.2188E 07	0.4623E 06	0.8215E 07	3	6
443	341	17	25	A	1	ON	2101945	OFF	700082	0.2095E 08	0.4965E 07	0.1451E 08	1	1
					2	ON	1611486	OFF	87476	0.2188E 07	0.4623E 06	0.8646E 07	3	8
459	342	17	29	B	1	ON	2188632	OFF	700082	0.2095E 08	0.4965E 07	0.1510E 08	5	1
					2	SWOF	1698173	OFF	87476	0.2188E 07	0.4623E 06	0.9113E 07	3	8
477	343	21	29	A	1	ON	2289377	OFF	700082	0.2095E 08	0.4965E 07	0.1576E 08	4	1
					2	OFF	1698173	OFF	87476	0.2188E 07	0.4623E 06	0.9113E 07	3	8
489	344	15	31	A	1	ON	2354337	OFF	700082	0.2095E 08	0.4965E 07	0.1619E 08	4	1
					2	OFF	1698173	OFF	87476	0.2188E 07	0.4623E 06	0.9113E 07	3	8
506	345	17	45	A	1	ON	2448738	OFF	700082	0.2095E 08	0.4965E 07	0.1680E 08	4	2
					2	OFF	1698173	OFF	87476	0.2188E 07	0.4623E 06	0.9113E 07	3	8
524	346	22	9	A	1	ON	2550975	OFF	700082	0.2095E 08	0.4965E 07	0.1746E 08	4	2
					2	OFF	1698173	OFF	87476	0.2188E 07	0.4623E 06	0.9113E 07	3	8
531	347	8	35	A	1	ON	2588578	OFF	700082	0.2095E 08	0.4965E 07	0.1771E 08	4	2
					2	OFF	1698173	OFF	87476	0.2188E 07	0.4623E 06	0.9113E 07	3	8
555	348	21	42	A	1	ON	2722195	OFF	700082	0.2095E 08	0.4965E 07	0.1857E 08	4	2
					2	OFF	1698173	OFF	87476	0.2188E 07	0.4623E 06	0.9113E 07	3	8
569	349	19	2	A	1	ON	2798980	OFF	700082	0.2095E 08	0.4965E 07	0.1906E 08	4	2
					2	OFF	1698173	OFF	87476	0.2188E 07	0.4623E 06	0.9113E 07	3	8
587	350	20	49	A	1	ON	2891806	OFF	700082	0.2095E 08	0.4965E 07	0.1966E 08	5	2
					2	OFF	1698173	OFF	87476	0.2188E 07	0.4623E 06	0.9113E 07	3	8
601	351	18	37	A	1	ON	2970289	OFF	700082	0.2095E 08	0.4965E 07	0.2015E 08	5	2
					2	OFF	1698173	OFF	87476	0.2188E 07	0.4623E 06	0.9113E 07	3	8
617	352	19	5	A	1	ON	3058366	OFF	700082	0.2095E 08	0.4965E 07	0.2071E 08	5	2
					2	OFF	1698173	OFF	87476	0.2188E 07	0.4623E 06	0.9113E 07	3	8
617	352	19	6	B	1	ON	3058434	SWON	700082	0.2095E 08	0.4965E 07	0.2071E 08	5	2
					2	OFF	1698173	OFF	87476	0.2188E 07	0.4623E 06	0.9113E 07	3	8

					BOX	PLANE	GOOD SENS	RATIO 123S/OS		NO. 0'S	NO. 1'S	NO. 2'S	NO. 3'S	NO. X'S	NO. COUNTS	FLUX (COUNTS/ CM+2 SEC)
617	352	20	19	PB	1	1	31	0.632	DATA	19	7	3	2	28	19	0.9070E-06
									POISSON	18.97	9.32	2.29	0.37	0.05	15.23	0.7269E-06
					1	2	54	0.286	DATA	42	8	1	3	8	19	0.3827E-05
									POISSON	41.99	10.56	1.33	0.11	0.01	13.58	0.2735E-05
					2	1	35	0.129	DATA	31	4	0	0	26	4	0.1829E-05
									POISSON	31.00	3.76	0.23	0.01	0.00	4.25	0.1942E-05
					2	2	52	0.020	DATA	51	0	1	0	4	2	0.4327E-05
									POISSON	51.00	0.99	0.01	0.00	0.00	1.01	0.2184E-05

TABLE 5-3. (CONTINUED)

ORB. NO.	GMT DAY	HR	MN	TYPE	BOX	BOX COND.	TOTAL TIME ON	M-B COND.	TOTAL TIME ON	PLANE 1 (CM+2 SEC)	PLANE 2 (CM+2 SEC)	VELOCITY (CM+2 SEC)	ZERO P1	SHORTS P2
617	352	20	21	B	1	ON	3062919	SWOF	704567	0.2107E 08	0.4998E 07	0.2074E 08	5	2
					2	OFF	1698173	OFF	87476	0.2188E 07	0.4623E 06	0.9113E 07	3	8
634	353	20	52	A	1	ON	3151183	OFF	704567	0.2107E 08	0.4998E 07	0.2129E 08	5	2
					2	OFF	1698173	OFF	87476	0.2188E 07	0.4623E 06	0.9113E 07	3	8
647	354	17	1	A	1	ON	3223723	OFF	704567	0.2107E 08	0.4998E 07	0.2174E 08	6	2
					2	OFF	1698173	OFF	87476	0.2188E 07	0.4623E 06	0.9113E 07	3	8
664	355	18	42	A	1	ON	3316193	OFF	704567	0.2107E 08	0.4998E 07	0.2231E 08	6	2
					2	OFF	1698173	OFF	87476	0.2188E 07	0.4623E 06	0.9113E 07	3	8
680	356	19	10	B	1	ON	3404283	OFF	704567	0.2107E 08	0.4998E 07	0.2284E 08	6	2
					2	OFF	1698173	OFF	87476	0.2188E 07	0.4623E 06	0.9113E 07	3	8
694	357	18	5	A	1	ON	3486728	OFF	704567	0.2107E 08	0.4998E 07	0.2334E 08	6	3
					2	OFF	1698173	OFF	87476	0.2188E 07	0.4623E 06	0.9113E 07	3	8
710	358	18	34	A	1	ON	3574906	OFF	704567	0.2107E 08	0.4998E 07	0.2382E 08	10	3
					2	OFF	1698173	OFF	87476	0.2188E 07	0.4623E 06	0.9113E 07	3	8
725	359	17	27	A	1	ON	3657278	OFF	704567	0.2107E 08	0.4998E 07	0.2422E 08	10	4
					2	OFF	1698173	OFF	87476	0.2188E 07	0.4623E 06	0.9113E 07	3	8
736	360	9	42	A	1	ON	3715776	OFF	704567	0.2107E 08	0.4998E 07	0.2450E 08	10	4
					2	OFF	1698173	OFF	87476	0.2188E 07	0.4623E 06	0.9113E 07	3	8
756	361	16	48	A	1	ON	3827755	OFF	704567	0.2107E 08	0.4998E 07	0.2505E 08	10	4
					2	OFF	1698173	OFF	87476	0.2188E 07	0.4623E 06	0.9113E 07	3	8
770	362	14	30	A	1	ON	3905858	OFF	704567	0.2107E 08	0.4998E 07	0.2544E 08	10	4
					2	OFF	1698173	OFF	87476	0.2188E 07	0.4623E 06	0.9113E 07	3	8
772	362	17	17	CRD	1	ON	3915881	SWON	704567	0.2107E 08	0.4998E 07	0.2551E 08	0	0
					2	OFF	1698173	OFF	87476	0.2188E 07	0.4623E 06	0.9113E 07	3	8

			BOX	PLANE	GOOD SENS	RATIO 123S/OS		NO. 0'S	NO. 1'S	NO. 2'S	NO. 3'S	NO. X'S	NO. COUNTS	FLUX (COUNTS/ CM+2 SEC)
773	362	18	53	PB	1	1	36	0.500	DATA	24	7	3	2	28	19	0.9017E-06
									POISSON	23.98	9.74	1.98	0.27	0.03	14.63	0.6942E-06
					1	2	56	0.273	DATA	44	8	1	3	8	19	0.3801E-05
									POISSON	43.99	10.61	1.28	0.10	0.01	13.51	0.2703E-05
					2	1	35	0.129	DATA	31	4	0	0	26	4	0.1829E-05
									POISSON	31.00	3.76	0.23	0.01	0.00	4.25	0.1942E-05
					2	2	52	0.020	DATA	51	0	1	0	4	2	0.4327E-05
									POISSON	51.00	0.99	0.01	0.00	0.00	1.01	0.2184E-05

TABLE 5-3. (CONTINUED)

ORB. NO.	GMT DAY	HR	MN	TYPE	BOX	BOX COND.	TOTAL TIME ON	M-B COND.	TOTAL TIME ON	PLANE 1 (CM+2 SEC)	PLANE 2 (CM+2 SEC)	VELOCITY (CM+2 SEC)	ZERO P1	SHORTS P2
773	362	18	55	B	1	ON	3921743	SWOF	710429	0.2126E 08	0.5037E 07	0.2555E 08	10	4
					2	OFF	1698173	OFF	87476	0.2188E 07	0.4623E 06	0.9113E 07	3	8
780	363	4	40	A	1	ON	3956856	OFF	710429	0.2126E 08	0.5037E 07	0.2572E 08	10	4
					2	OFF	1698173	OFF	87476	0.2188E 07	0.4623E 06	0.9113E 07	3	8
796	364	5	7	A	1	ON	4044880	OFF	710429	0.2126E 08	0.5037E 07	0.2614E 08	10	4
					2	OFF	1698173	OFF	87476	0.2188E 07	0.4623E 06	0.9113E 07	3	8
812	365	5	35	A	1	ON	4132962	OFF	710429	0.2126E 08	0.5037E 07	0.2657E 08	10	4
					2	OFF	1698173	OFF	87476	0.2188E 07	0.4623E 06	0.9113E 07	3	8
812	365	5	36	B	1	ON	4132997	SWON	710429	0.2126E 08	0.5037E 07	0.2657E 08	10	4
					2	OFF	1696173	OFF	87476	0.2188E 07	0.4623E 06	0.9113E 07	3	8
813	365	7	10	A	1	ON	4138656	ON	716088	0.2139E 08	0.5084E 07	0.2660E 08	10	4
					2	OFF	1698173	OFF	87476	0.2188E 07	0.4623E 06	0.9113E 07	3	8
819	365	17	1	A	1	ON	4174083	ON	751515	0.2219E 08	0.5381E 07	0.2677E 08	10	4
					2	OFF	1698173	OFF	87476	0.2188E 07	0.4623E 06	0.9113E 07	3	8
828	1	5	59	A	1	SWOF	4220803	SWOF	798235	0.2324E 08	0.5775E 07	0.2699E 08	10	4
					2	OFF	1698173	OFF	87476	0.2188E 07	0.4623E 06	0.9113E 07	3	8
843	2	4	50	A	1	OFF	4220803	OFF	798235	0.2324E 08	0.5775E 07	0.2699E 08	10	4
					2	OFF	1698173	OFF	87476	0.2188E 07	0.4623E 06	0.9113E 07	3	8
859	3	5	14	B	1	SWON	4220803	OFF	798235	0.2324E 08	0.5775E 07	0.2699E 08	10	4
					2	OFF	1698173	OFF	87476	0.2188E 07	0.4623E 06	0.9113E 07	3	8
875	4	5	38	A	1	ON	4308682	OFF	798235	0.2324E 08	0.5775E 07	0.2743E 08	9	4
					2	OFF	1698173	OFF	87476	0.2188E 07	0.4623E 06	0.9113E 07	3	8
885	4	21	24	A	1	ON	4365440	OFF	798235	0.2324E 08	0.5775E 07	0.2771E 08	9	4
					2	OFF	1698173	OFF	87476	0.2188E 07	0.4623E 06	0.9113E 07	3	8
891	5	6	3	A	1	ON	4396576	OFF	798235	0.2324E 08	0.5775E 07	0.2787E 08	9	4
					2	OFF	1698173	OFF	87476	0.2188E 07	0.4623E 06	0.9113E 07	3	8
909	6	10	12	A	1	ON	4497929	OFF	798235	0.2324E 08	0.5775E 07	0.2838E 08	10	4
					2	OFF	1698173	OFF	87476	0.2188E 07	0.4623E 06	0.9113E 07	3	8
924	7	9	4	A	1	ON	4580249	OFF	798235	0.2324E 08	0.5775E 07	0.2877E 08	10	4
					2	OFF	1698173	OFF	87476	0.2188E 07	0.4623E 06	0.9113E 07	3	8
941	8	10	36	A	1	ON	4672153	OFF	798235	0.2324E 08	0.5775E 07	0.2922E 08	10	4
					2	OFF	1698173	OFF	87476	0.2188E 07	0.4623E 06	0.9113E 07	3	8
955	9	8	12	A	1	ON	4749937	OFF	798235	0.2324E 08	0.5775E 07	0.2960E 08	10	4
					2	OFF	1698173	OFF	87476	0.2188E 07	0.4623E 06	0.9113E 07	3	8
970	10	6	57	A	1	SWOF	4831823	OFF	798235	0.2324E 08	0.5775E 07	0.2997E 08	10	9
					2	OFF	1698173	OFF	87476	0.2188E 07	0.4623E 06	0.9113E 07	3	8
987	11	8	26	A	1	OFF	4831823	OFF	798235	0.2324E 08	0.5775E 07	0.2997E 08	10	9
					2	OFF	1698173	OFF	87476	0.2188E 07	0.4623E 06	0.9113E 07	3	8
1001	12	6	8	A	1	OFF	4831823	OFF	798235	0.2324E 08	0.5775E 07	0.2997E 08	10	9
					2	OFF	1698173	OFF	87476	0.2188E 07	0.4623E 06	0.9113E 07	3	8

					BOX	PLANE	GOOD SENS	RATIO 123S/0S		NO. 0'S	NO. 1'S	NO. 2'S	NO. 3'S	NO. X'S	NO. COUNTS	FLUX (COUNTS/ CM+2 SEC)
1013	12	23	16	PB	1	1	26	1.000	DATA	13	3	3	2	28	20	0.8605E-06
									POISSON	12.93	9.03	3.16	0.74	0.15	18.17	0.7818E-06
					1	2	47	0.343	DATA	35	8	1	3	8	19	0.3290E-05
									POISSON	34.99	10.32	1.52	0.15	0.01	13.87	0.2401E-05
					2	1	35	0.129	DATA	31	4	0	0	26	4	0.1829E-05
									POISSON	31.00	3.76	0.23	0.01	0.00	4.25	0.1942E-05
					2	2	52	0.020	DATA	51	0	1	0	4	2	0.4327E-05
									POISSON	51.00	0.99	0.01	0.00	0.00	1.01	0.2184E-05

each memory dump. Both the data counts from the sensors with one, two, and three counts and the Poisson values were used. The calculations were made separately for each plane of each box. The values of flux were computed for each satellite memory dump and for each meteoroid sensor plane individually. These are shown in Table 5-3.

In addition, a value of flux was obtained from the velocity time-area accumulation. Two velocity words were recorded during the mission as discussed in Ref. 1. The total accumulated time-area for both meteoroid packages was 3.91×10^{7} $cm^2 sec$. This gives a flux of 5.1×10^{-8} particles per $cm^2 sec$;* calculated as an omnidirectional flux.

Using the data from the analysis shown in Table 5-3, it was possible to plot the occurrence of meteoroid counts which were obtained from the Poisson analysis as a function of accumulated time-area. The resulting plots are shown for all four detector planes, as well as for the velocity counts, in Figure 5-2. The slope of the resulting curves should correspond to the meteoroid flux.

The accumulated data from Box 1 was too low to be useful. The slopes obtained from the velocity counts and the top plane of Box 1 are in reasonable agreement. The data accumulated on the bottom plane of Box 1 has, however, a curious anomaly. The data rises very smoothly during the first half of the accumulated time-area and then shows no additional counts for the last half. This strongly suggests that the sensor discharges did not result from meteoroid impacts, but instead from spurious discharges.

5.3 Evaluation of Sensor Reliabilities

Since the primary objective of the RMS meteoroid experiment was to gather information on the effects of the launch and space environment on the meteoroid sensors, a relatively extensive analysis was conducted in which failures were correlated with sensor type and location at different times during the mission. The sensor types and their respective locations on the experiment packages are given in Table 5-4. The details of the construction and composition of each

*This value does not include earth shielding or gravitational focusing.

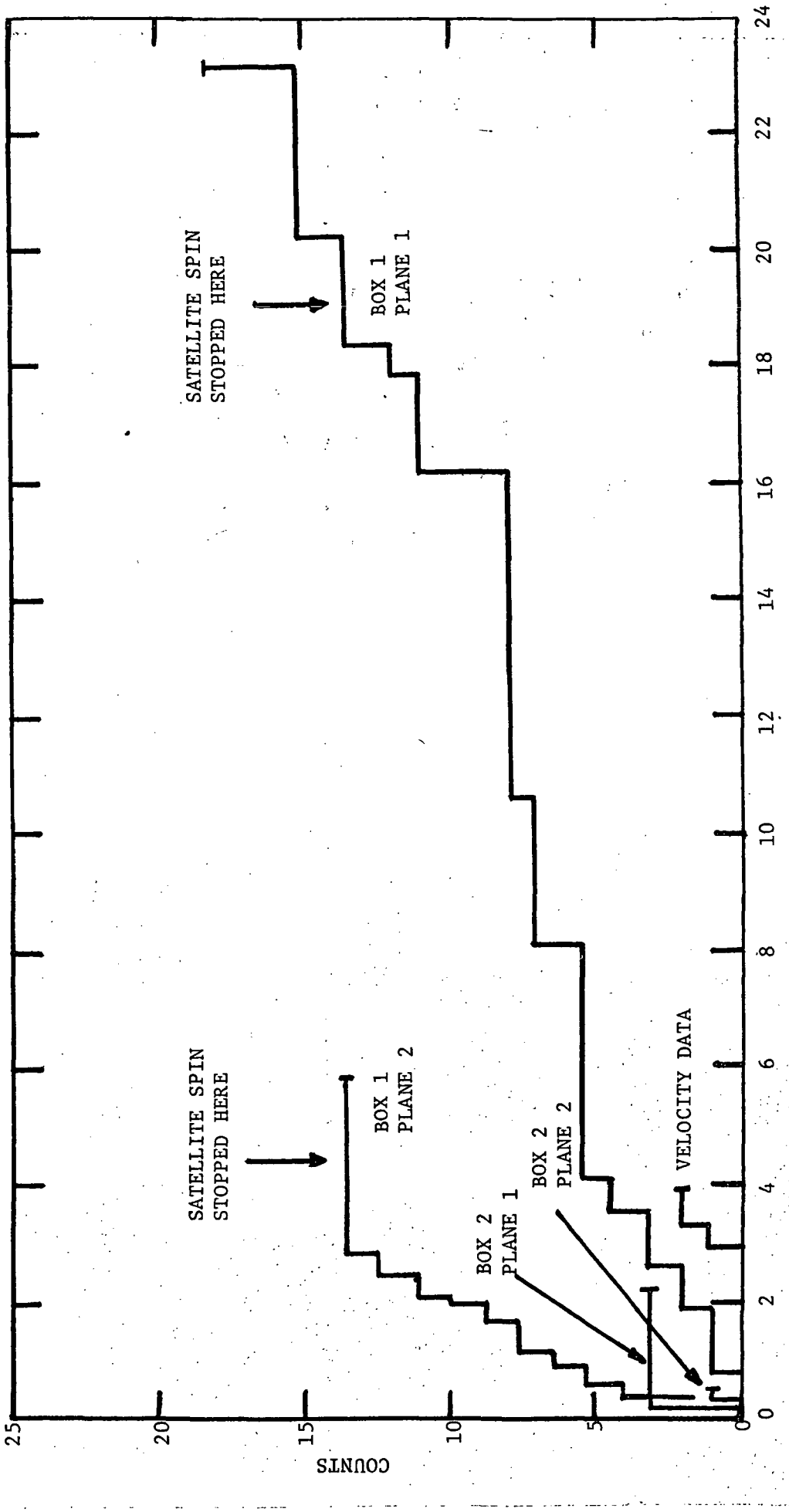

Fig. 5-2. Meteoroid Counts Determined from Poisson Analysis Versus Time-Area Accumulation. Velocity Counts are Included for Comparison.

TABLE 5-4. TYPES OF SENSORS ON RMS METEOROID EXPERIMENT PACKAGES

SENSOR TYPE	LOCATION	SUN SHIELD	SENSOR	TOTAL THICKNESS
1	Box 1 Plane 1 All Columns Box 2 Plane 1 Columns 1-5	Silicon Oxide (6000 A) Aluminum (1000 A) Polycarbonate 4 layers (4000 A)	Aluminum (1000 A) Polysulfone (4000 A) Gold (300 A)	16,300 A or 345 μgm/cm^2
2	Box 2 Plane 1 Column 0	None	Silicon Oxide (6000 A) Aluminum (1000 A) Polysulfone - 4 layers (4000 A) Gold (300 A)	11,300 A or 270 μgm/cm^2
3	Box 2 Plane 1 Column 7	None	Aluminum (1000 A) Polycarbonate - single layer (8000 A) Gold (300 A)	9300 A or 180 μgm/cm^2
4	Box 1 Plane 2 All Columns Box 2 Plane 2 All Columns	Aluminum (1000 A) Polycarbonate - 4 layers (4000 A)	Aluminum (1000 A) Polysulfone - 4 layers (4000 A) Gold (300 A)	10,300 A or 205 μgm/cm^2
Controls	Box 2 Plane 1 Column 6 Rows 0,2,4,6	None	Like type 1 (intentionally shorted)	--
	Box 2 Plane 1 Column 6 Rows 1,3,5,7	Covered with .01 inch iron plate	Like type 1	--

sensor type are given in Ref. 1. The materials and their respective thicknesses are summarized here in Table 5-4. The thickness in angstrom units follows the name of the material making up each layer and the total sensor thickness is given in both angstroms and $\mu gm/cm^2$ in the last column.

The information contained in Tables 5-1, 5-3, and 5-4 were combined in an attempt to determine if environment, time, or sensor location correlations did exist. These results are summarized in Table 5-5.

Most of the items in the table are self-explanatory; however, a brief discussion of some of the entries will avoid confusion. The "total counts exclusive of sucessive counters" refers to all counts obtained in the first analysis as discussed in paragraph 5.1.4 above. Several of these counts were found to occur immediately following the time which a box was turned on. These and their associated time-area products were removed from the data. The remaining counts are referred to as "possible meteoroid counts" in Table 5-5. The counts for the "totals" column for the top plane of Box 2 are different from those shown in Table 5-3, since the controls were not excluded from the analysis. The values have been corrected for Table 5-5.

A number of rather striking (but not too surprising) correlations are apparent in Table 5-5:

(a) Fewer bottom plane sensors were lost during launch than those on the top planes.

(b) The failure rate during the orbital lifetime was greater on the top planes than on the bottom, irrespective of sensor type.

(c) More excessive counters occurred on the top planes than on the bottom planes.

(d) No significant differences were noted in the number of sensor shorts with respect to sensor type.

(e) No significant differences were noted in the number of excessive counters with respect to sensor type.

TABLE 5-5. CORRELATIONS OF SENSOR FAILURES AND METEOROID COUNTS WITH SENSOR TYPE AND LOCATION

METEOROID UNIT		BOX 1 (OPPOSITE SUN AFTER SPIN STOPPED)		BOX 2 (TOWARD SUN AFTER SPIN STOPPED)						
PLANE		TOP PLANE	BOTTOM PLANE	TOP PLANE						BOTTOM PLANE
COLUMN		ALL	ALL	TOTALS (LESS CONTROLS)	0	1-5	6		7	ALL
SENSOR TYPE (REFER TO TABLE 1)		TYPE 1	TYPE 4	-	2	1	CONTROLS COVERED	CONTROLS SHORTED	3	TYPE 4
TOTAL SENSORS		64	64	56	8	40	4	4	8	64
SHORTS: BEFORE LAUNCH	No	1	0	0	0	0	0	4	0	1
SHORTS: ORBIT 15 (FIRST DATA)	No	7	2	12	3	5	0	3	4	0
	%	11%	3%	15%	38%	12%	0%	-	50%	0%
SHORTS: ORBIT 206 (AFTER SPIN STOPPED)	No	25	2	25	4	18	1	3	3	4
	%	40%	3%	44%	50%	45%	25%	-	38%	6%
SHORTS: ORBIT 1042 (LAST REAL TIME BOTH BOXES ON)	No	36	7	24	3	17	1	3	4	13
	%	56%	11%	43%	38%	43%	25%	-	50%	20%
EXCESSIVE COUNTERS	No	28	8	25	4	17	1	0	4	4
	%	44%	13%	45%	50%	43%	25%	-	50%	6%
TOTAL COUNTS EXCLUSIVE OF EXCESSIVE CTRS.		22	20	14	0	14	1	0	0	21
POSSIBLE METEOROID COUNTS		20	19	3	0	3	1	0	0	2
COUNTS FROM POISSON ANALYSIS		18.17	13.87	3.2	-	-	-	-	-	1.01
TOTAL TIME-AREA ACCUMULATION (m^2sec)		23×10^2	5.8×10^2	2.2×10^2	-	-	-	-	-	0.46×10^2
FLUX (POISSON) (PARTICLES/m^2sec)		0.78×10^{-2}	2.4×10^{-2}	1.5×10^{-2}	-	-	-	-	-	2.2×10^{-2}

A number of plots were made from the data in Tables 5-1, 5-3, and 5-5 in an attempt to correlate the loss of sensors with the mission environments. These are shown in Figure 5-3. The parameters associated with sensor loss are the occurrences of shorts and the instances of the occurrence of the first count in a sensor which became an excessive counter. These data were taken from the complete set of data of which Figure 5-1 is a portion. These parameters were plotted individually for each sensor plane as a function of time in orbit. Also shown are the meteoroid box "on", "off" periods. The most striking feature in Figure 5-3 is the contrast in the rate of events (especially on the top planes) before and after the motion of the satellite changed from a spin with precession into an end-over-end tumble.

These correlations suggest that the major cause of sensor failure was the rapid thermal stressing of the thin films due to the rotation of the satellite while it was in sunlight. As can be seen in Figure 5-3, several sensors were shorted when the first observations were made, which indicates they were broken by the lanuch environment. It is believed that others were also broken at launch and that the rapid thermal stressing of the sunlight caused these to short repeatedly and thereby produced the high occurrence of sensor discharges during the time when the satellite was rapidly rotating.

The abrupt increase of seven shorted sensors on the top plane of Box 1, seen in Figure 5-3 at a time in orbit of 45 days, is discussed in the Ref. 1 and is attributed to the dust particles. These were not recorded as flux counts, since, unfortunately, the satellite memory was off during that time period.

In summary it was known that the aerodynamic effects of the upper atmosphere would be present at the time of the Scout heat shield ejection. To remain within the guidelines of the OFO launch and orbital parameters it was not possible to eject the heat shield at

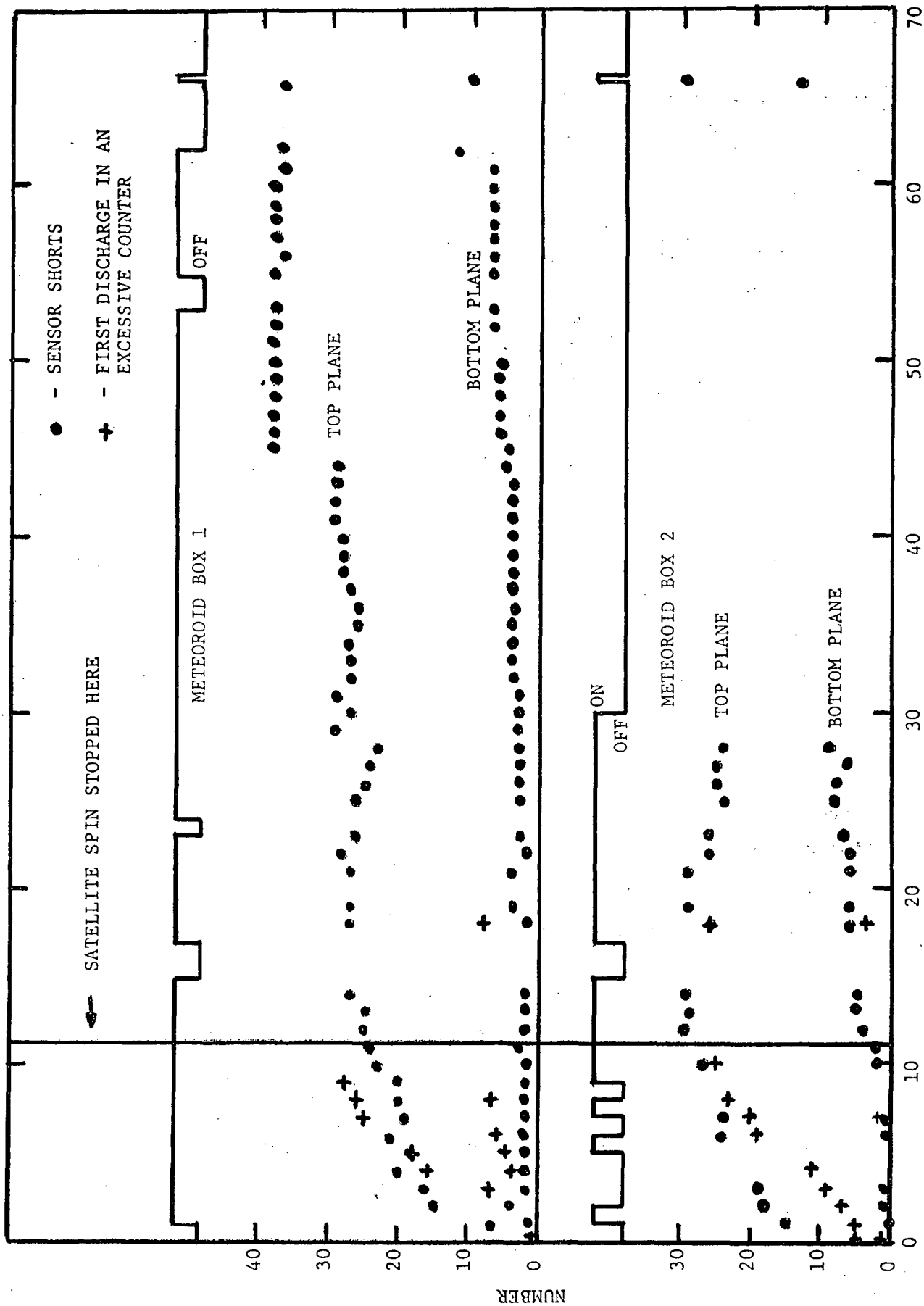

FIG. 5-3. CORRELATION OF SENSOR SHORTS AND FIRST DISCHARGE IN AN EXCESSIVE COUNTER WITH CHANGE IN SATELLITE MOTION FROM SPIN TO TUMBLE

a higher altitude. Wind shields were installed in front of the meteoroid boxes, as discussed in Ref. 1; however, either the aerodynamic flow by the wind shields or the shock at the time of the ejection was apparently responsible for the breakage of some of the top plane sensors. This is evidenced by the shorts recorded in the first real-time run which was taken in Orbit 15 as shown in Table 5-5.

Test data was obtained at Goddard Space Flight Center (Ref. 7) which indicated that the sensors could survive the temperature cycling if they were undamaged. This suggests that the sensors lost were primarily those damaged during launch. The data indicates that the sensors will survive long duration space missions if they are protected to higher altitudes at launch.

5.4 Conclusions

Based on the results of the RMS meteoroid experiments, the thin-film meteoroid sensors have been shown to yield reliable results for velocity-flux measurements; however, their usefulness as simple flux impact detectors is questionable. No actual interpretation of the data or comparisons to existing models was to be a part of this study, but a few brief associations can be made. The threshold for detection of the particles of the velocity measured by RMS (approximately 3 km/sec) is approximately 10^{-12} grams for velocity and bottom plane flux and approximately 10^{-14} grams for top plane flux. These values are discussed in Ref. 1 and were obtained by Van de Graaff measurements. The accepted flux for 10^{-12} gram particles according to Ref. 8 is approximately 4×10^{-5} particles/m^2sec at one astronomical unit. This is to be compared with the RMS velocity-flux of 5.1×10^{-4} particles/m^2sec and the unrealiable Box 1, bottom plane flux of 2.4×10^{-2} particles/m^2sec. As discussed earlier, the bulk of the counts on the bottom plane of Box 1 are considered to be reliable, is nearly an order of magnitude above the expected value.

The flux value obtained from the top plane of Box 2 seems rather reliable, especially when one considers the plot in Figure 5-2. The

flux is 2.4×10^{-2} particles/m^2sec.

The curve in Ref. 8 must be extrapolated to the 10^{-14} gram threshold of the sensors on the top plane. This extrapolated flux value is approximately 10^{-4} particles/m^2 sec. The resulting difference at 10^{-12} grams is a factor of 12 while that at 10^{-14} grams is 240. The velocity-flux error could result from simple statistical uncertainties, in that only two counts were recorded; however, the top plane flux number is based on 20 counts which is statistically significatn; thus, if the extrapolated value from Ref. 8 is in disagreement with the RMS data.

In support of the RMS data, the results of a recent investigation given in a report by Hemmingway et. al (Ref. 9) entitled "Stardust" predicts a high flux of particles from noctlucent cloud studies. The findings in this report are in general agreement with RMS data. The origina of the particles is considered to be the sun and the distribution over the earth suggests that the particles are charged and controlled by the geomagnetic field. A very brief analysis indicates the particles would be given an easterly velocity due to their positive charge which could also explain the low velocities measured in RMS. These results are, of course, very tentative, but they suggest that a more detailed correlation would be of value.

VI. EVALUATION OF MISSION SUCCESS

An actual evaluation in terms of the percent success of a mission is virturally impossible. However, one may list the objectives and relate these to the resulting accomplishments and features associated with the mission. Then the reader may easily draw his own conclusions. This approach is taken here.

6.1 Meteoroid Experiment

Even though the satellite apparently sustained damage during launch, the meteoroid experiment functioned properly. Its primary and secondary objectives (to evaluate thin-film meteoroid sensors and measure meteoroid flux and velocity) were fulfilled. Due to a cell failure in the battery pack, the total time-area accumulations were less than anticipated; however, the objectives were met and the experiment was a full success.

6.2 Radiation Experiment

The malfunctions of the radiation experiment have been attributed to the launch anomaly. This is by no means a proven fact, but the evidence is rather strong. A portion of each objective was accomplished; however, the full intents were not met.

The primary objective of the radiation experiment which was discussed in Ref. 1, was basically to determine the feasibility and accuracy of the spectrum to dose conversion concept and, thus, establish its usefulness in space missions. The proton data at high energies were in error and the unshielded ionization chamber malfunctioned. The failures prevented a direct comparison of the two dose measuring techniques. The accuracy of the spectrum-to-dose conversion concept had been shown earlier, Ref. 4. The more important aspect of this objective was, thus, demonstrated: the design, construction, and operation of a system which could perform the dose conversion function in the space environment.

With respect to the secondary objective, that of obtaining data for

spectral and dose maps, most of the desired data were obtained. However, the very important high energy proton data was lost. An assessment of the value of the experiment must consider the valuable electron spectra which shows clearly the remaining effects of the high altitude nuclear test in 1962 called "Starfish". Also the low energy proton data offers a valuable comparison to the AP6 Vette model.

The information is, thus, presented in a manner which will enable the reader to assign a figure of merit according to any criteria required of him,

REFERENCES

1. Radiation and Meteoroid Satellite, Final Report Contract NAS9-9195, Report No. B-95000/ICR-11, Advanced Technology Center, Inc., Dallas, Texas, March 1971.

2. Support Instrumentation Requirements Document, Goddard Space Flight Center, Greenbelt, Maryland, December 1969.

3. Models of the Trapped Radiation Environment, Vette, James E., et al., NASA SP-3024 (seven volumes), National Aeronautics and Space Administration, Washington, D. C., published 1966 through 1971.

4. Study to Determine the Utility of Spectrum-to-Dose Conversion, Farmer, B. J. and Rainwater, W. J., Report No. 0-71100/9R-5, Advanced Technology Center, Inc., Dallas, Texas, April 1968.

5. OFO - A Mission Performance, Report No. 1333-032, Space General Company, El Monte, California, December 1970.

6. Radiation and Meteoroid Satellite Quality Documentation Logbook No. N105-00000-01, LTV Research Center, Dallas, Texas, June 1970.

7. Solar Vacuum Test Results for Thin-Film Meteoroid Sensors, LEC Document No. OF2013, Lockheed Electronics Co., Houston, Texas, September 1970.

8. Meteoroid Environmental Model, Interplanetary and Planetary, NASA SP-8038, National Aeronautics Space Administration, Washington, D. C., June 1970.

9. Stardust, Hemenway, C. L., Hallgren, D. S., and Schmalberger, D. C., Dudley Observatory and State University of New York at Albany, February 1972.